含圓形邊界拉普拉斯與雙諧和問題之格林函數解析解

Analytical solutions for the Green's functions of Laplace and biharmonic problems with circular boundaries

研 究 生：廖奐禎　　Student：Huan-Zhen Liao

指導教授：陳正宗　　Advisor：Jeng-Tzong Chen

國 立 臺 灣 海 洋 大 學
河 海 工 程 學 系
碩 士 論 文

A Thesis
Submitted to Department of Harbor and River Engineering
College of Engineering
National Taiwan Ocean University
In Partial Fulfillment of the Requirements
for the Degree of
Master of Science
in
Harbor and River Engineering
June 2006
Keelung, Taiwan, Republic of China

中華民國 96 年 7 月

誌 謝

夕陽近，黑夜降臨時，鬼魅游移，恐懼在破曉的前一刻揮發；畢業在即，口試逼近，委員們狂風怒吼，猶如颱風橫掃整個會場，漫天的落葉，在委員們簽名的那一剎那，塵埃落定，只是沒想到，離校前的最終試驗竟是誌謝！想到結束，就想起一開始請求陳正宗教授收留我的那天，雖不是風雨交加，但也不算風和日麗，但總覺得老師周圍有股殺氣，阿~原來是老師剛結束 GROUP MEETING，本以為會被用脣槍舌劍狠狠的刮，沒想到老師居然拿出我的偏微分期中考卷說：「全班兩個及格，你就是其中一個。」心中正得意想著我有老本可以揮霍的時候，老師又接著說：「考試考的好，不一定研究就做的好，還是要認真啦！」正在失落之時，便已發現我已進入了光榮的力學聲響振動實驗室了。爾後，埋入於論文研究的工作中，本論文雖不是嘔心瀝血之作，但一定也不是囫圇吞棗所寫成的，當然，要感謝的人很多，族繁不及備載，但其中幾個須提出來，感謝陳正宗教授的兩年指導，在這兩年，我常犯一些「啞巴跟聾子說瞎子看到鬼」的錯誤，我的指導教授還是有辦法讓我兩年就畢業，實屬不易。雖說這兩年對我來說是種磨練，但對老師來講也是種磨練，所以也不能說我對研究室沒有貢獻；第二個要感謝的就是我的女友，能夠在這兩年沒有鬧過自殺跳海。讓我完成艱苦的碩士學業，真的是感謝萬分；第三個要感謝的是我的父親，在我挫折難過之際，能夠伸出援手，伴我走過難關，也相當的不簡單。接著感謝陳義麟 博士、李為民 博士、呂學育 博士、陳桂鴻 博士在論文口試時不吝嗇給予雕刻，能夠讓本論文有如鑽石一般更加光彩奪目。也要感謝國科會計畫 NSC 95-2221-E019-065 提供碩士研究獎學金。最後，在人生接下來的旅程，必將拿出研究所兩年所學然後盡力發揮，盼不負力學聲響振動實驗室對我的期待。

廖奐禎 07/07/16 酒後筆

Analytical solutions for the Green's functions of Laplace and biharmonic problems with circular boundaries

Contents

Table captions

Figure captions

Notations

$A(\cdot)$	base of the degenerate kernel
a_n , $\overline{a}_n$	Fourier coefficients
b_n , $\overline{b}_n$	Fourier coefficients
B	boundary
$B(\cdot)$	base of the degenerate kernel
c_n	Fourier coefficient
C.P.V.	Cauchy principal value
d_n	Fourier coefficient
D	flexural rigidity
E	Young's modulus
g_n	Fourier coefficient
H.P.V	Hadamard principal value
h	plate thickness
h_n	Fourier coefficient
$G(x,\zeta)$	Green's function
$K_{\theta,x}(\cdot)$, $K_{\theta,s}(\cdot)$	slope operator
$K_{m,x}(\cdot)$, $K_{m,s}(\cdot)$	moment operator
$K_{v,x}(\cdot)$, $K_{v,s}(\cdot)$	effective shear force operator
$K_{\theta,x}[G(x,\zeta)]$	displacement
$K_{m,x}[G(x,\zeta)]$	normal moment
$K_{v,x}[G(x,\zeta)]$	effective shear force

M	terms of Fourier series
$M(s,x)$	kernel function
$M_\theta(s,x)$	kernel function
$M_m(s,x)$	kernel function
$M_v(s,x)$	kernel function
N_h	number of circular holes
N	number of circular boundaries
p_n, $\overline{p}_n$	Fourier coefficients
q_n, $\overline{q}_n$	Fourier coefficients
(R,θ)	polar coordinates of the source point
(R_ζ,θ_ζ)	polar coordinates of the concentrated load point
R.P.V	Riemann principal value
r	distance between the source point and the field point
s	source point
$U(s,x)$	kernel function
$U_\theta(s,x)$	kernel function
$U_m(s,x)$	kernel function
$U_v(s,x)$	kernel function
$V(s,x)$	kernel function
$V_\theta(s,x)$	kernel function
$V_m(s,x)$	kernel function
$V_v(s,x)$	kernel function
x	field point

∇^2	Laplacian operator
∇^4	biharmonic operator
$\delta(s-x)$	Dirac-Delta function
ζ	Location of a concentrated load
ε	observed distance for boundary-layer effect
ν	Poisson ratio
Ω	domain
Ω^c	complementary domain
(ρ,ϕ)	polar coordinates of the field point
$\Theta(s,x)$	kernel function
$\Theta_\theta(s,x)$	kernel function
$\Theta_m(s,x)$	kernel function
$\Theta_v(s,x)$	kernel function
$\sigma_{z\theta}$	normal and tangential components of shear stresses
τ_∞	magnitude of applied shear stress at infinity
β	impedance coefficient

摘要

本文採用邊界積分方程法結合傅立葉級數與退化核來求解含圓形邊界拉普拉斯或雙諧和方程之格林函數。其中退化核即為分離核，係基本解中將場、源點分離所導得的級數形式，藉由退化核的內外域表示式可避免主值積分的計算。而未知的邊界密度函數則以傅立葉級數做展開。求得未知的傅立葉係數之後，將之代回邊界積分方程中可得場解。本方法在單圓與同心圓的領域下可屬於解析法，其主要誤差來源為所截取的傅立葉項數，經由項數的增加，可收斂到正解。本文所得之解析解將與有限元素法套裝軟體 (ABAQUS) 之執行結果與一些學者做一比較，以驗證本法的可行性。

關鍵字：拉普拉斯方程，雙諧和方程，退化核，零場積分方程，邊界積分方程，傅立葉級數

.

Abstract

In this thesis, the boundary integral equation methods (BIEMs) in conjunction with Fourier series and degenerate kernels are proposed to solve the Green's function of Laplace or biharmonic equations with circular boundaries. The degenerate kernels in the direct BIEM are expanded by separating the field point and source point in the fundamental solution. The singular boundary integrals are avoided since the appropriate interior and exterior expansion of degenerate kernels are used. All the unknown boundary densities are expressed in terms of Fourier series. After determining the unknown Fourier coefficients, the Green's function can be obtained by using the boundary integral equations. The present method can be regarded as an analytical approach in the circular and annular domain since error only occurs in truncating the Fourier terms. Finally, the analytical solutions are compared with the finite element method software (ABAQUS) data and Adewale's and Melnikov's results to demonstrate the validity of the present method.

Keyword: Laplace and biharmonic equation, degenerate kernel, null-field integral equation, boundary integral equation, Fourier series

Chapter 1 Introduction

1.1 Overview of BEM and motivation

The boundary element method (BEM) by discretizing the boundary integral equation (BIE) has been applied extensively for certain engineering problems [8, 11, 15, 46, 62] with general geometries as shown in Fig. 1-1, more than domain type methods, *e.g.* finite element method (FEM) or finite difference method (FDM). The finite element method had been, for many years, the most widely used numerical technique for the solution of general problems as shown in Table 1-1. However, a few problems are not so easy tasks for FEM that another numerical method, thus BEM is born. The boundary element method, sometimes referred to as the boundary integral equation method, is now establishing a position as a natural alternative to FEM in many fields of mechanics. BEM is suited for many engineering problems, in general, for all types of external fields and infinite or semi-infinite domains which FEM can not do it well. Domain type methods, FEM and FDM, have been deeply investigated in the engineering. Boundary type method, BEM, MFS, boundary collocation method and Trefftz method, have received attention in the recent decades. In analogy of clinical medicine, FEM behaves like operation. BEM is similar to Chinese medicine. Boundary collocation method resembles acupuncture and moxibustion. In other words, BEM and meshless methods can be seen as a supplement of FEM. BEM utilizes the discretization concept of FEM as well as the limitation. Whether the supplement is needed or not depends on its absolutely superior area than FEM. Two areas in crack and large scale problems can be well solved by BEM. For the crack problems, dual BEM with the hypersingularity is the key to solve. Degenerate kernel plays the role for modeling large scale problems using fast multipole method. Although BEM has been involved as an alternative numerical method for solving engineering problems, five critical issues are of concern:

(1) Treatment of singularity and hypersingularity. Most of the efforts have been focused on the singular boundary integral equation for problems with ordinary boundaries. In some situations, the singular boundary integral equation is not sufficient, *e.g.* degenerate boundary, fictitious frequency and spurious eigenvalue. Therefore, the hypersingular equation is required. The role of hypersingularity in computational mechanics has been examined in the review article of Chen and Hong [17]. In the past, several regularizations for hypersingularity were offered to

handle it in direct and indirect ways. Hong and Chen [62] have developed the theory of dual BIEM and dual BEM with hypersingular kernels. Recently, Chen and Chiu [19] had derived the separable expression of fundamental solution and can avoid calculating the improper integrals along the boundary. The singularity and hypersingularity disappear in boundary integral equation after describing the potential into two parts. Singularity can be transformed to summability of Fourier series.

(2) Boundary-layer effect. Boundary-layer effect in BEM has received attention in the recent years. In real applications, data near boundary can be smoothened since maximum principle always exists for potential problems. Nevertheless, it also deserves study to know how to manipulate the nearly singular integrals in applied mathematics. How to eliminate the boundary-layer effect in BEM is vital for researchers. In this thesis, boundary layer effect is eliminated by using the null-field equation. A demonstration is shown in Fig. 1-2 which was done by Wu [59].

(3) Convergence rate. BEM is very popular for boundary value problems with general geometries since it requires discretization on the boundary only. Regarding to constant, linear and quadratic elements, the discretization scheme does not take the special geometry into consideration. It leads to the slow convergence rate. Exponential convergence rate using null-field integral equation was achieved as demonstrated in Fig. 1-3 which was done by Hsiao [27]. Moreover, the present method can be directly applied to problems with general boundaries without any difficulty once the fundamental solution can be separated in the other coordinate, *e.g.* Cartesian coordinate or elliptic coordinate.

(4) Ill-posed model. To avoid directly calculating the singular and hypersingular integrals by using null-field approach or fictitious BEM yields an ill-conditioned system. The influence matrix is not diagonally dominated and needs preconditioning. We may wonder is it possible to push the null-field point on the real boundary but free of facing the singular or hypersingular integrals. The answer is yes and the key idea is to describe the jump behavior of potential distribution in the separate region by using degenerate (separate) kernels for fundamental solutions. The resulted algebraic system is well-posed.

(5) Mesh domain. Mesh is not required since we collocate on the boundary only, and introduce the generalized Fourier coefficients for circular boundary.

Based on the null-field integral equations, Shen, Chen and Hsiao in 2005 had successfully solved the Laplace, Helmholtz and biharmonic of boundary value problems with circular holes, respectively. Following the success of their experiences, Chen and Wu in 2006 have extended to inclusion problems. A dozen of papers were published as shown in Fig 1-4. The purpose of this thesis is to study the Green's function of Laplace and biharmonic equations with circular boundaries by using the null-field integral equation approach in conjunction with degenerate kernels and Fourier series. The displacement, slope, normal moment and effective shear force of the plate with circular boundaries can be obtained by using the boundary integral equations for the domain point.

1.2 Literature review

Boundary integral equations (BIEs) for the plate problems were acquired from the Rayleigh-Green identity [20] and the null-field integral equations were derived by moving the field points outside the domain. A null-field integral equation in conjunction with degenerate kernel is proposed to solve the biharmonic equations with circular boundaries. The circular boundary density is expressed in terms of Fourier series to fully capture geometric shape. It is well known that Fourier series is always incorporated to formulate the solution for problems with circular boundaries. For the regular straight boundary, the unknown boundary density in the BIEs can be expanded by Legendre polynomials. In the past, Shen [49] applied the null-field integral formulation, Fourier series and degenerate kernels to solve Laplace problems with circular boundaries. Based on this idea, the applications to the plate problems with multiple holes were proposed by Hsiao [27]. Here, we will extend to solve the Green's function of circular plates. In this thesis, the annular plate subject to a concentrated load is the main concern.

Annular plate problems occur in engineering applications, for example in the design of structures where a load is supported by a circular overhang. Some of the early

attempts to solve the annular plate problems included the work of Conway [23] who considered an annular plate with linearly varying thickness subject to a uniformly distributed load and a line load uniformly distributed along the edge of the hole. Bird and Steele [9, 10] presented a Fourier series procedure to solve circular plate problems containing multiple circular holes in a similar way of Trefftz method by adopting the interior and exterior T-complete sets. Recently, Sharafutdinov [48] had considered the problems of an annular plate subject to a concentrated load along its edges using the theory of functions of a complex variable. Lately, the problem of an isotropic annular plate clamped along one edge and free at the other and subject to a concentrated force was solved by Adewale [1]. The same case will be revisited by using the present method, and the details will be addressed in chapter 3.

Green's function is another concern in this thesis. Green's function was widely applicable to the qualitative analysis of initial and boundary value problems for equations of all the standard (elliptic, parabolic and hyperbolic) types in mathematical physics. Wang and Sudak [56] derived two-dimensional antiplane time-harmonic Green's functions for a circular inhomogeneity with an imperfect interface. Time-harmonic Green's functions can be applied to formulate the boundary element method for the time-harmonic problems, and can also be employed to investigate the dynamic Echelby problem and scattering problems in elastodynamics. A semi-analytical technique had earlier been developed and can successfully be utilized for computing Green's functions for a certain class of multiply connected regions. In Melnikov's paper [38], a semi-analytical approach is applied to the construction of Green's functions and matrices of Green's type for Laplace and Klein-Gordon equation in two dimensions. Mixed boundary value problems posed in multiply connected regions were also concerned by Melnikov [39]. Melnikov [41] also investigated the Green's function of the plate problems. The Green's function of a boundary value problem for a partial differential equation that models bending of a thin plate is usually referred to as its influence function. According to this, the work in [41] was devoted to the construction of representations of influence functions for a circular Poisson-Kirchhoff plate that are suitable for immediate computational applications.

The purpose of this thesis is to study the Green's function of the annular plate by using the null-field integral equation approach in conjunction with degenerate kernels and Fourier series. The unknown boundary densities of the displacement, slope, normal

moment and effective shear force are expressed in terms of Fourier series. It is noticed that all the improper integrals are avoided when the degenerate kernels are used. After determining the unknown Fourier coefficients, the displacement, slope, normal moment and effective shear force of the plate with circular boundaries can be obtained by using the boundary integral equations for the domain point. Finally, FEM program will play an important role in verifying the validity of the present method.

1.3 Organization of the thesis

The main concern in this thesis is that an analytical approach is proposed to solve the plate problems with circular boundaries under a concentrated load. In chapter 2, the derivation to the Green's function of Robin problem for Laplace equation with a circular domain is considered. Although the present formulation is suitable for the Laplacian, Helmholtz, biharmonic and biHelmholtz operators in one, two and three dimensional problems, only two-dimensional Laplace problems are adopted here. The Green's function of Robin Laplace equation is presented to demonstrate the validity of the present method and is compared with the Melnikov's solution [37]. The mathematical equivalence for the analytical solution of Melnikov's results and present method is proved.

In chapter 3, the analytical solution for the Green's function of biharmonic equations is derived using null-field integral equation in conjunction with Fourier expansion. The displacement, slope, normal moment and effective shear force of the plate with circular boundaries can be obtained by using the boundary integral equations for the domain point. A closed-form solution is obtained for the concentrated load on the center of the circular plate and is verified by the Szilard's solution [51]. For the eccentric loading, the analytical solution is derived and is compared with the Melnikov's solution [42]. Regarding the annular case, Adewale's results [1] are reexamined. FEM program, ABAQUS, and the present method are used to verify the validity of Adewale's results. Three annular examples solved by using the present method are compared with ABAQUS results. Finally, some conclusions are made and the further researches are indicated in chapter 4.

Table 1-1 Number of Papers of FEM, BEM and FDM

Numerical method	*Search phrase in topic field*	*No. of entries*	*Rank*	*Ratio*
FEM	“Finite element” or “finite elements”	66237	1	66.77%
FDM	“Finite difference” or “Finite differences”	19531	2	19.69%
BEM	“Boundary element” or “Boundary elements” or “boundary integral”	10126	3	10.21%
FVM	“Finite volume method” or “finite volume methods”	1695	4	1.71%
CM	“Collocation method” or “collocation methods”	1615	5	1.63%

Search data: May, 3, 2004

Data from: Prof. Cheng A. H. D.

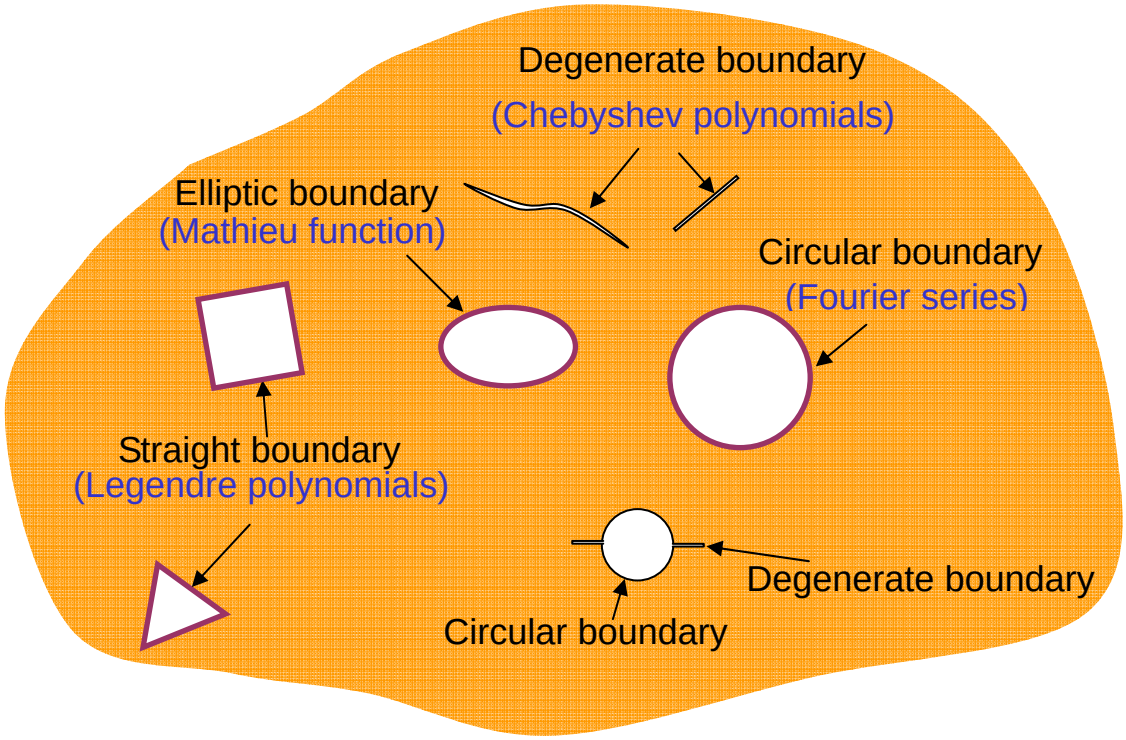

Fig. 1-1 The Laplace or biharmonic problems with arbitrary boundaries

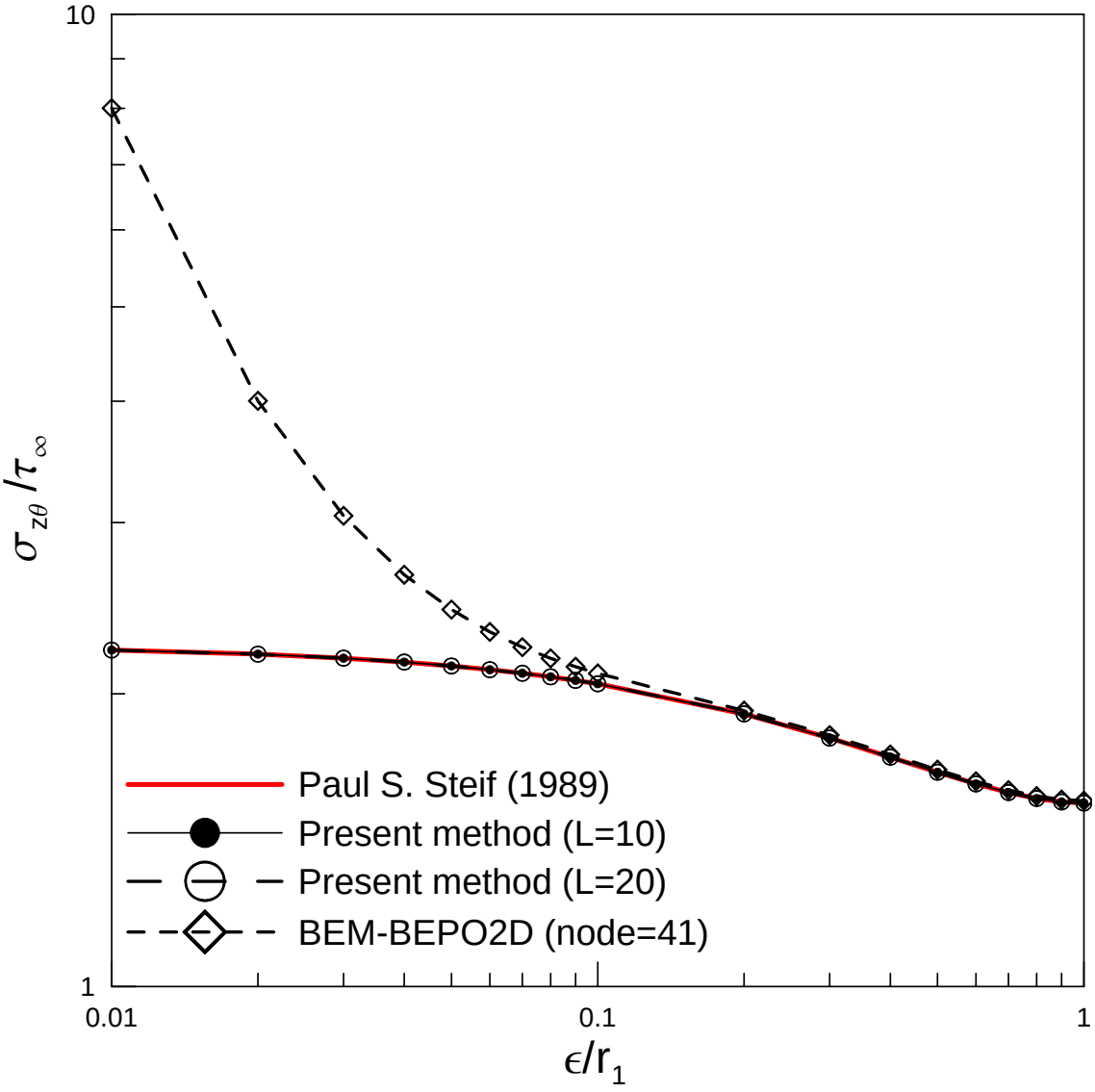

Fig. 1-2 Boundary-layer effect analysis [59]

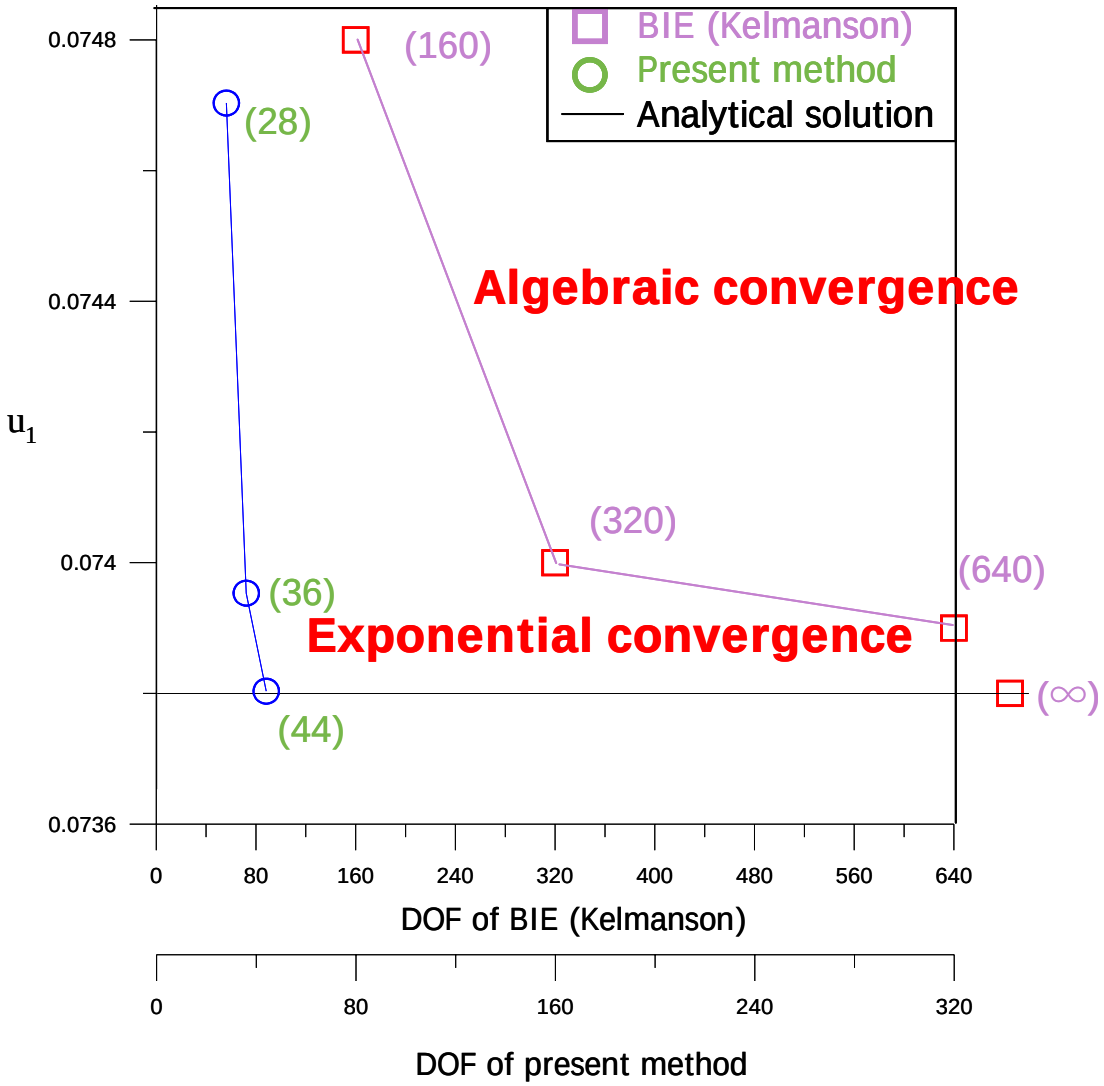

Fig. 1-3 Comparison for convergence rate [27]

Fig. 1-4 Flowchart research topics of NTOU / MSVLAB on null-field BIE (2003-2007)

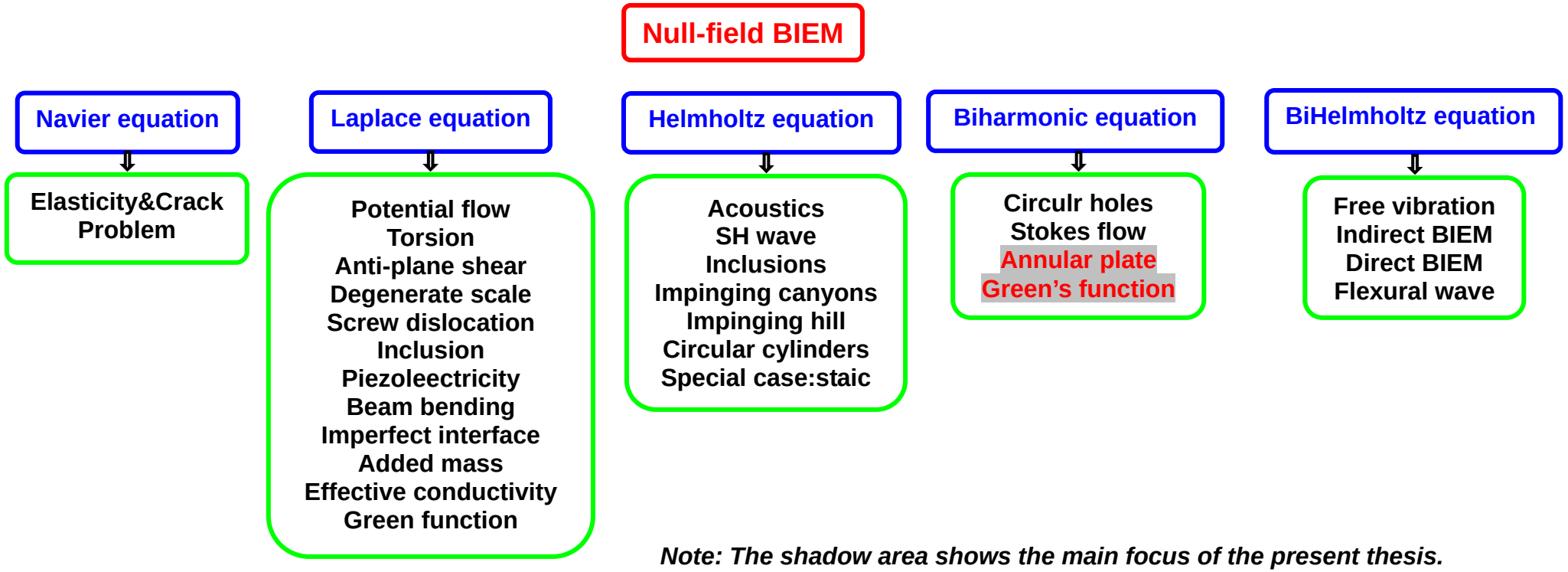

Note: The shadow area shows the main focus of the present thesis.

Chapter 2 Green's function for Laplace equation

Summary

In this chapter, an analytical approach for the Green's function of a circular domain is presented. Null-field integral equation is employed to solve the Robin problem while the kernel functions in the null-field integral equation are expanded to degenerate kernels which can separate the field and source points in the fundamental solution. The unknown boundary densities are expressed in terms of Fourier series. It is noticed that all the improper integrals are avoided when the degenerate kernels are used. By matching the boundary conditions at the collocation points, a linear algebraic system is obtained. After determining the unknown Fourier coefficients in the algebraic system, the potential can be obtained by using the boundary integral equations. The present method can be regarded as an analytical approach since error only occurs in truncating the Fourier terms. Finally, the Green's function for the Robin problem solved by Melnikov [37] is revisited to demonstrate the validity of the present method. Also, the mathematical equivalence between the Melnikov solution and ours is proved as shown in Appendix 1. The convergence rates of the Melnikov's result and the present solution are also our concern.

2.1 Dual boundary integral equations and dual null-field integral equations for constructing the Green's function

Supposing there are N randomly distributed circular holes bounded to the contours B_k ($k = 0, 1, 2, \cdots, N$) as shown in Fig. 2-1. We define

$$B = \bigcup_{k=0}^{N} B_k \ . \tag{2-1}$$

In mathematical physics, the Green's function satisfies the governing equation,

$$\Im G(\mathrm{x}, \zeta) = \delta(x - \zeta), \quad \mathrm{x} \in \Omega, \tag{2-2}$$

subject to boundary conditions, where $\Im$ may be the Laplacian, Helmholtz, biharmonic or biHelmholtz operators, $G(\mathrm{x}, \zeta)$ is the Green's function and can be seen as the potential function, $\delta(\mathrm{x} - \zeta)$ denotes the Dirac-delta function of source at ζ and Ω is the domain of interest. In order to employ the Green's third identity as follows

$$\iint_D [u(x)\nabla^2 v(x) - v(x)\nabla^2 u(x)] d\Omega(x) = \int_B [(u(x)\frac{\partial v(x)}{\partial n} - v(x)\frac{\partial u(x)}{\partial n}] dB(x) \tag{2-3}$$

We need two systems, $u(x)$ and $v(x)$. We choose $u(x)$ as $G(x,\zeta)$ and set $v(x)$ as the fundamental solution $U(x,s)$. For the two-dimensional second-order operators of Laplacian and Helmholtz, the boundary integral equation for the domain point can be derived from Eq. (2-3) as shown below

$$2\pi G(\mathrm{x},\zeta)=\int_B T(\mathrm{s},\mathrm{x})G(\mathrm{s},\zeta)dB(\mathrm{s})-\int_B U(\mathrm{s},\mathrm{x})\frac{\partial G(\mathrm{s},\zeta)}{\partial \mathrm{n}_\mathrm{s}}dB(\mathrm{s}) +U(\zeta,\mathrm{x}),\quad \mathrm{x}\in\Omega \tag{2-4}$$

$$2\pi\frac{\partial G(\mathrm{x},\zeta)}{\partial \mathrm{n}_\mathrm{x}}=\int_B M(\mathrm{s},\mathrm{x})G(\mathrm{s},\zeta)dB(\mathrm{s})-\int_B L(\mathrm{s},\mathrm{x})\frac{\partial G(\mathrm{s},\zeta)}{\partial \mathrm{n}_\mathrm{s}}dB(\mathrm{s}) +L(\zeta,\mathrm{x}),\quad \mathrm{x}\in\Omega \tag{2-5}$$

where s and x are the source and field points, respectively, B is the boundary, n_x denotes the outward normal vector at the field and point x, n_s is the outward normal vector at the source point s and the kernel function $U(\mathrm{s},\mathrm{x})$ is the fundamental solution which satisfies

$$\Im U(\mathrm{s},\mathrm{x})=2\pi\delta(\mathrm{x}-\mathrm{s}), \tag{2-6}$$

The other kernel functions, $T(\mathrm{s},\mathrm{x})$, $L(\mathrm{s},\mathrm{x})$ and $M(\mathrm{s},\mathrm{x})$, are defined by

$$T(\mathrm{s},\mathrm{x})\equiv\frac{\partial U(\mathrm{s},\mathrm{x})}{\partial \mathrm{n}_\mathrm{s}},\quad L(\mathrm{s},\mathrm{x})\equiv\frac{\partial U(\mathrm{s},\mathrm{x})}{\partial \mathrm{n}_\mathrm{x}},\quad M(\mathrm{s},\mathrm{x})\equiv\frac{\partial^2 U(\mathrm{s},\mathrm{x})}{\partial \mathrm{n}_\mathrm{s}\partial \mathrm{n}_\mathrm{x}}, \tag{2-7}$$

By moving the field point to the boundary, Eqs. (2-4) and (2-5) reduce to

$$\pi G(\mathrm{x},\zeta)=C.P.V.\int_B T(\mathrm{s},\mathrm{x})G(\mathrm{s},\zeta)dB(\mathrm{s})-R.P.V.\int_B U(\mathrm{s},\mathrm{x})\frac{\partial G(\mathrm{s},\zeta)}{\partial \mathrm{n}_\mathrm{s}}dB(\mathrm{s}) +U(\zeta,\mathrm{x}),\quad \mathrm{x}\in B \tag{2-8}$$

$$\pi\frac{\partial G(\mathrm{x},\zeta)}{\partial \mathrm{n}_\mathrm{x}}=H.P.V.\int_B M(\mathrm{s},\mathrm{x})G(\mathrm{s},\zeta)dB(\mathrm{s})-C.P.V.\int_B L(\mathrm{s},\mathrm{x})\frac{\partial G(\mathrm{s},\zeta)}{\partial \mathrm{n}_\mathrm{s}}dB(\mathrm{s}) +L(\zeta,\mathrm{x}),\quad \mathrm{x}\in B \tag{2-9}$$

where $C.P.V.$, $R.P.V.$ and $H.P.V.$ denote the Cauchy principal value, Riemann principal value and Hadamard principal value, respectively. Once the field point x locates outside the domain, the null-field integral equation of the direct method in Eqs. (2-4) and (2-5) yield

$$0=\int_B T(\mathrm{s},\mathrm{x})G(\mathrm{s},\zeta)dB(\mathrm{s})-\int_B U(\mathrm{s},\mathrm{x})\frac{\partial G(\mathrm{s},\zeta)}{\partial \mathrm{n}_\mathrm{s}}dB(\mathrm{s}) +U(\zeta,\mathrm{x}),\quad \mathrm{x}\in\Omega^c \tag{2-10}$$

$$0 = \int_B M(\mathrm{s},\mathrm{x}) G(\mathrm{s},\zeta) dB(\mathrm{s}) - \int_B L(\mathrm{s},\mathrm{x}) \frac{\partial G(\mathrm{s},\zeta)}{\partial \mathrm{n}_\mathrm{s}} dB(\mathrm{s}) + L(\zeta,\mathrm{x}), \quad \mathrm{x} \in \Omega^c \tag{2-11}$$

where Ω^c is the complementary domain. Note that the conventional null-field integral equations are not singular since s and x never coincide. If the kernel function in Eqs. (2-4), (2-5), (2-10) and (2-11) can be described as degenerate (separate) forms for the inside Ω or outside Ω^c domain, we have

$$2\pi G(\mathrm{x},\zeta) = \int_B T(\mathrm{s},\mathrm{x}) G(\mathrm{s},\zeta) dB(\mathrm{s}) - \int_B U(\mathrm{s},\mathrm{x}) \frac{\partial G(\mathrm{s},\zeta)}{\partial \mathrm{n}_\mathrm{s}} dB(\mathrm{s}) + U(\zeta,\mathrm{x}), \quad \mathrm{x} \in \Omega \cup B \tag{2-12}$$

$$2\pi \frac{\partial G(\mathrm{x},\zeta)}{\partial \mathrm{n}_\mathrm{x}} = \int_B M(\mathrm{s},\mathrm{x}) G(\mathrm{s},\zeta) dB(\mathrm{s}) - \int_B L(\mathrm{s},\mathrm{x}) \frac{\partial G(\mathrm{s},\zeta)}{\partial \mathrm{n}_\mathrm{s}} dB(\mathrm{s}) + L(\zeta,\mathrm{x}), \quad \mathrm{x} \in \Omega \cup B \tag{2-13}$$

$$0 = \int_B T(\mathrm{s},\mathrm{x}) G(\mathrm{s},\zeta) dB(\mathrm{s}) - \int_B U(\mathrm{s},\mathrm{x}) \frac{\partial G(\mathrm{s},\zeta)}{\partial \mathrm{n}_\mathrm{s}} dB(\mathrm{s}) + U(\zeta,\mathrm{x}), \quad \mathrm{x} \in \Omega^c \cup B \tag{2-14}$$

$$0 = \int_B M(\mathrm{s},\mathrm{x}) G(\mathrm{s},\zeta) dB(\mathrm{s}) - \int_B L(\mathrm{s},\mathrm{x}) \frac{\partial G(\mathrm{s},\zeta)}{\partial \mathrm{n}_\mathrm{s}} dB(\mathrm{s}) + L(\zeta,\mathrm{x}), \quad \mathrm{x} \in \Omega^c \cup B \tag{2-15}$$

For simplicity, Table 2-1 summarizes the main difference between the present formulation and conventional BEM. It is noted that the boundary integral equation for the domain point and the null-field integral equation for the null-field point can include the collocation point on the real boundary since the appropriate kernel can be used as elaborated on later in the following section.

2.2 Expansions of fundamental solution and boundary density

Now, we adopt the mathematical tools, degenerate kernels and Fourier series, for the purpose of analytical study. The combination of degenerate kernels and Fourier series plays the major role in handling problems with circular boundaries. Instead of directly calculating the *C.P.V.*, *R.P.V.* and *H.P.V.* in Eqs. (2-8) and (2-9), we obtain the linear algebraic system from the null-field integral equation of Eqs. (2-14) and (2-15) through the kernel expansion by “exactly” collocating the point on the real boundary.

Based on the separable property, the kernel function $U(\mathrm{s},\mathrm{x})$ can be expanded into the separable form by dividing the source and field points:

$$U(\mathrm{s},\mathrm{x})=\begin{cases} U^{i}(\mathrm{s},\mathrm{x})=\sum_{j} A_j(\mathrm{s})B_j(\mathrm{x}),\ |\mathrm{s}|\geq|\mathrm{x}| \\ U^{e}(\mathrm{s},\mathrm{x})=\sum_{j} A_j(\mathrm{x})B_j(\mathrm{s}),\ |\mathrm{x}|>|\mathrm{s}| \end{cases}, \tag{2-16}$$

where the bases of $A(\cdot)$ and $B(\cdot)$ can be found for the Laplacian, Helmholtz, biharmonic and biHelmholtz operators and the superscripts " i " and " e " denote the interior ($|\mathrm{s}|\geq|\mathrm{x}|$) and exterior ($|\mathrm{x}|>|\mathrm{s}|$) cases, respectively. To classify the interior (left, 1-D) and exterior (right, 1-D) regions, Fig. 2-2 shows for one, two and three dimensional cases. For the degenerate form of T, L and M kernels, they can be derived according to their definitions in Eq. (2-7). Regarding the multiply-connected domain problems, the interior "i" and exterior "e" expansions for the kernel should be taken with care. Although the mathematical tools of degenerate kernels, are suitable for the Laplacian, Helmholtz, biharmonic and biHelmholtz operators in one, two and three dimensional problems, we focus on the two-dimensional Laplace problems in this chapter as explained below.

Degenerate kernels for fundamental solutions

Based on the separable property, the kernel function $U(\mathrm{s},\mathrm{x})=\ln r$, ($r\equiv|\mathrm{x}-\mathrm{s}|$), is expanded into the degenerate form by separating the source point and field point in the polar coordinate [19]:

$$U(\mathrm{s},\mathrm{x})=\begin{cases} U^{i}(R,\theta;\rho,\phi)=\ln R-\sum_{m=1}^{\infty}\frac{1}{m}(\frac{\rho}{R})^{m}\cos m(\theta-\phi),\ R\geq\rho \\ U^{e}(R,\theta;\rho,\phi)=\ln \rho-\sum_{m=1}^{\infty}\frac{1}{m}(\frac{R}{\rho})^{m}\cos m(\theta-\phi),\ \rho>R \end{cases}, \tag{2-17}$$

where the superscripts "i" and "e" denote the interior ($R\geq\rho$) and exterior ($\rho>R$) cases, respectively. The origin of the observer system to describe x and s for the degenerate kernel is $(0,0)$. Figure 2-3 shows the graph of the separate expression of fundamental solutions where source point s located at $R=10.0$ and $\theta=\pi/3$. By setting the origin for the observer system, a circle with radius R from the origin to the

source point s is plotted. If the field point x is situated inside the circular region, the degenerate kernel belongs to the interior expression of U^i; otherwise, it is the exterior case. It is noted that the leading term and numerator term in Eq. (2-17) involve the larger argument to ensure the log singularity and series convergence, respectively. After taking the normal derivative $\partial / \partial R$ with respect to Eq. (2-17), the $T(\mathrm{s},\mathrm{x})$ kernel yields

$$T(\mathrm{s},\mathrm{x}) = \begin{cases} T^i(R,\theta;\rho,\phi) = \dfrac{1}{R} + \displaystyle\sum_{m=1}^{\infty} \left(\frac{\rho^m}{R^{m+1}}\right) \cos m(\theta-\phi), & R > \rho \\ T^e(R,\theta;\rho,\phi) = -\displaystyle\sum_{m=1}^{\infty} \left(\frac{R^{m-1}}{\rho^m}\right) \cos m(\theta-\phi), & \rho > R \end{cases}, \tag{2-18}$$

and the higher-order kernel functions, $L(\mathrm{s},\mathrm{x})$ and $M(\mathrm{s},\mathrm{x})$, are shown below

$$L(\mathrm{s},\mathrm{x}) = \begin{cases} L^i(R,\theta;\rho,\phi) = -\displaystyle\sum_{m=1}^{\infty} \left(\frac{\rho^{m-1}}{R^m}\right) \cos m(\theta-\phi), & R > \rho \\ L^e(R,\theta;\rho,\phi) = \dfrac{1}{\rho} + \displaystyle\sum_{m=1}^{\infty} \left(\frac{R^m}{\rho^{m+1}}\right) \cos m(\theta-\phi), & \rho > R \end{cases}, \tag{2-19}$$

$$M(\mathrm{s},\mathrm{x}) = \begin{cases} M^i(R,\theta;\rho,\phi) = \displaystyle\sum_{m=1}^{\infty} \left(\frac{m\rho^{m-1}}{R^{m+1}}\right) \cos m(\theta-\phi), & R \geq \rho \\ M^e(R,\theta;\rho,\phi) = \displaystyle\sum_{m=1}^{\infty} \left(\frac{mR^{m-1}}{\rho^{m+1}}\right) \cos m(\theta-\phi), & \rho > R \end{cases}. \tag{2-20}$$

Since the potentials resulted from $T(\mathrm{s},\mathrm{x})$ and $L(\mathrm{s},\mathrm{x})$ kernels are discontinuous across the boundary, the potentials of $T(\mathrm{s},\mathrm{x})$ and $L(\mathrm{s},\mathrm{x})$ for $R \to \rho^+$ and $R \to \rho^-$ are different as shown in [59]. This is the reason why $R = \rho$ is not included for degenerate kernels of $T(\mathrm{s},\mathrm{x})$ and $L(\mathrm{s},\mathrm{x})$ in Eqs. (2-18) and (2-19).

Fourier series expansions for unknown boundary densities

For problems with circular boundaries, we apply the Fourier series expansions to approximate the potential and its normal derivative on the boundary B_k as

$$G(\mathrm{s}_k,\zeta) = a_0^k + \sum_{n=1}^{M} (a_n^k \cos n\theta_k + b_n^k \sin n\theta_k), \quad \mathrm{s}_k \in B_k, \quad k = 0, 1, 2, \cdots, N, \tag{2-20}$$

$$\frac{\partial G(\mathrm{s}_k,\zeta)}{\partial \mathrm{n}_\mathrm{s}} = p_0^k + \sum_{n=1}^{M}(p_n^k \cos n\theta_k + q_n^k \sin n\theta_k),\ \ \mathrm{s}_k \in B_k,\ \ k = 0, 1, 2, \cdots, N, \qquad (2\text{-}21)$$

where a_n^k, b_n^k, p_n^k and q_n^k ($n = 0, 1, 2, \cdots, M$) are the Fourier coefficients and θ_k is the polar angle. In the real computation, only $2M+1$ finite terms are considered where M indicates the truncated terms of Fourier series.

2.3 Derivation of analytical solution for Green's function of Laplace problem with the impedance boundary condition

For the Robin problem subject to a concentrated load as shown in Fig. 2-4, the unknown Fourier series can be analytically derived. By collocating x on (a^+,ϕ), the null-field equations yields

$$\begin{aligned} 0 = &\int_B \left[-\sum_{m=1}^{\infty}\frac{1}{a}\cos m(\theta-\phi)\right]\left[p_0 + \sum_{n=1}^{\infty} p_n \cos n\theta + q_n \sin n\theta\right] a d\theta \\ &- \int_B \left[\ln a - \sum_{m=1}^{\infty}\frac{1}{m}\cos m(\theta-\phi)\right]\left[-\beta\left(p_0 + \sum_{n=1}^{\infty} p_n \cos n\theta + q_n \sin n\theta\right)\right] a d\theta \\ &+ \ln a - \sum_{m=1}^{\infty}\frac{1}{m}\left(\frac{R_\zeta}{a}\right)^m \cos m(\theta_\zeta - \phi), \quad x \to (a^+,\phi) \end{aligned} \qquad (2\text{-}22)$$

where a and β are the radius and impedance coefficient. For the Robin case, the explicit form for the unknown Fourier series can be obtained as

$$p_0 = -\frac{1}{2\pi a\beta},\ \ p_n = -\frac{\left(\frac{R_\zeta}{a}\right)^n}{\pi(n+a\beta)}\cos n\theta_\zeta,\ \ q_n = -\frac{\left(\frac{R_\zeta}{a}\right)^n}{\pi(n+a\beta)}\sin n\theta_\zeta \qquad (2\text{-}23)$$

where p_0, p_n and q_n are the Fourier coefficients and the boundary densities as shown below

$$G(s,\zeta) = \sum_{n=0}^{\infty} p_n \cos n\theta + q_n \sin n\theta, \quad s \in \text{boundary} \qquad (2\text{-}24)$$

$$\frac{\partial G(s,\zeta)}{\partial n_s} = -\beta\sum_{n=0}^{\infty} p_n \cos n\theta + q_n \sin n\theta, \quad s \in \text{boundary} \qquad (2\text{-}25)$$

By substituting all the boundary densities into the integral representation for the domain point, we have the series-form Green's function as shown below:

$$G(x,\zeta) = (1 + a\beta \ln a)\, p_0 + \sum_{n=1}^{\infty}\frac{\rho^n}{a^n}\frac{n-a\beta}{2n}(p_n \cos n\phi + q_n \sin n\phi) + \frac{\ln|x-\zeta|}{2\pi} \qquad (2\text{-}26)$$

Also, two limiting cases are our concern. One is the free boundary condition case of β to zero and the other is the fixed boundary condition case for β to infinity. Here, we

present a Green's function for the Robin problem with a circular boundary. This problem was also analytically solved by Melnikov, and the analysis of the convergence is compared between the present method and the Melnikov's result. The present method is shows consistency with the Melnikov's approach in the convergence rate as shown in Fig. 2-5. Another matter is, equivalence is also derived. It will be equivalence after rearranging between the present solution and the Melnikov's result as shown in Appendix 1. Finally, two potential contours are plotted by using the present solution and the Melnikov's result as shown in Figs 2-6 and 2-7. Good agreement is obtained.

2.4 Concluding remarks

For the Robin problem of Laplace equation, we have proposed an analytical approach to construct the Green's function by using degenerate kernels and Fourier series. Our result is also compared with the Melnikov's series form solution. The convergence rates of the present method and Melnokov's result is also addressed. The present solution and Melnikov's result will converge at the same value. It is found that our series solution converges shows consistency with that of Melnikov's. In addition. The mathematical equivalence for the two series solutions, ours and Melnikov's were also proved. Following the success of Laplace case, we will extend to biharmonic equation in the next chapter.

Table 2-1 Comparison of formulation between the present approach and conventional BEM

	Conventional BEM	***Present formulation***
Essential formulation	$2\pi G(\mathrm{x},\zeta)=U(\zeta,\mathrm{x})+\int_B T(\mathrm{s},\mathrm{x})G(\mathrm{s},\zeta)dB(\mathrm{s})-\int_B U(\mathrm{s},\mathrm{x})\frac{\partial G(\mathrm{s},\zeta)}{\partial \mathrm{n}_\mathrm{s}}dB(\mathrm{s}),\ \mathrm{x}\in\Omega$ $\pi G(\mathrm{x},\zeta)=U(\zeta,\mathrm{x})+C.P.V.\int_B T(\mathrm{s},\mathrm{x})G(\mathrm{s},\zeta)dB(\mathrm{s})-R.P.V.\int_B U(\mathrm{s},\mathrm{x})\frac{\partial G(\mathrm{s},\zeta)}{\partial \mathrm{n}_\mathrm{s}}dB(\mathrm{s}),\quad \mathrm{x}\in B$ $0=U(\zeta,\mathrm{x})+\int_B T^e(\mathrm{s},\mathrm{x})G(\mathrm{s},\zeta)dB(\mathrm{s})-\int_B U^e(\mathrm{s},\mathrm{x})\frac{\partial G(\mathrm{s},\zeta)}{\partial \mathrm{n}_\mathrm{s}}dB(\mathrm{s}),\ \mathrm{x}\in\Omega^c$	$2\pi G(\mathrm{x},\zeta)=U(\zeta,\mathrm{x})+\int_B T^i(\mathrm{s},\mathrm{x})G(\mathrm{s},\zeta)dB(\mathrm{s})-\int_B U^i(\mathrm{s},\mathrm{x})\frac{\partial G(\mathrm{s},\zeta)}{\partial \mathrm{n}_\mathrm{s}}dB(\mathrm{s}),\ \mathrm{x}\in\Omega\cup B$ $0=U(\zeta,\mathrm{x})+\int_B T^e(\mathrm{s},\mathrm{x})G(\mathrm{s},\zeta)dB(\mathrm{s})-\int_B U^e(\mathrm{s},\mathrm{x})\frac{\partial G(\mathrm{s},\zeta)}{\partial \mathrm{n}_\mathrm{s}}dB(\mathrm{s}),\ \mathrm{x}\in\Omega^c\cup B$
Natural formulation	$2\pi\frac{\partial G(\mathrm{x},\zeta)}{\partial \mathrm{n}_\mathrm{x}}=L(\zeta,\mathrm{x})+\int_B M(\mathrm{s},\mathrm{x})G(\mathrm{s},\zeta)dB(\mathrm{s})-\int_B L(\mathrm{s},\mathrm{x})\frac{\partial G(\mathrm{s},\zeta)}{\partial \mathrm{n}_\mathrm{s}}dB(\mathrm{s}),\quad \mathrm{x}\in\Omega$ $\pi\frac{\partial G(\mathrm{x},\zeta)}{\partial \mathrm{n}_\mathrm{x}}=L(\zeta,\mathrm{x})+H.P.V.\int_B M(\mathrm{s},\mathrm{x})G(\mathrm{s},\zeta)dB(\mathrm{s})-C.P.V.\int_B L(\mathrm{s},\mathrm{x})\frac{\partial G(\mathrm{s},\zeta)}{\partial \mathrm{n}_\mathrm{s}}dB(\mathrm{s}),\quad \mathrm{x}\in B$ $0=L(\zeta,\mathrm{x})+\int_B M^e(\mathrm{s},\mathrm{x})G(\mathrm{s},\zeta)dB(\mathrm{s})-\int_B L^e(\mathrm{s},\mathrm{x})\frac{\partial G(\mathrm{s},\zeta)}{\partial \mathrm{n}_\mathrm{s}}dB(\mathrm{s}),\ \mathrm{x}\in\Omega^c$	$2\pi\frac{\partial G(\mathrm{x},\zeta)}{\partial \mathrm{n}_\mathrm{x}}=L(\zeta,\mathrm{x})+\int_B M^i(\mathrm{s},\mathrm{x})G(\mathrm{s},\zeta)dB(\mathrm{s})-\int_B L^i(\mathrm{s},\mathrm{x})\frac{\partial G(\mathrm{s},\zeta)}{\partial \mathrm{n}_\mathrm{s}}dB(\mathrm{s}),\ \mathrm{x}\in\Omega\cup B$ $0=L(\zeta,\mathrm{x})+\int_B M^e(\mathrm{s},\mathrm{x})G(\mathrm{s},\zeta)dB(\mathrm{s})-\int_B L^e(\mathrm{s},\mathrm{x})\frac{\partial G(\mathrm{s},\zeta)}{\partial \mathrm{n}_\mathrm{s}}dB(\mathrm{s}),\ \mathrm{x}\in\Omega^c\cup B$

where CPV, RPV and HPV are the Cauchy principal value, Riemann principal value and Hadamard principal value, respectively. It is noted that the kernel in the present method should be properly expanded in terms of interior and exterior expressions of degenerate kernels. Mathematically speaking, our domain is a closed set ($\Omega\cup B$) instead of the open set (Ω only) of conventional method.

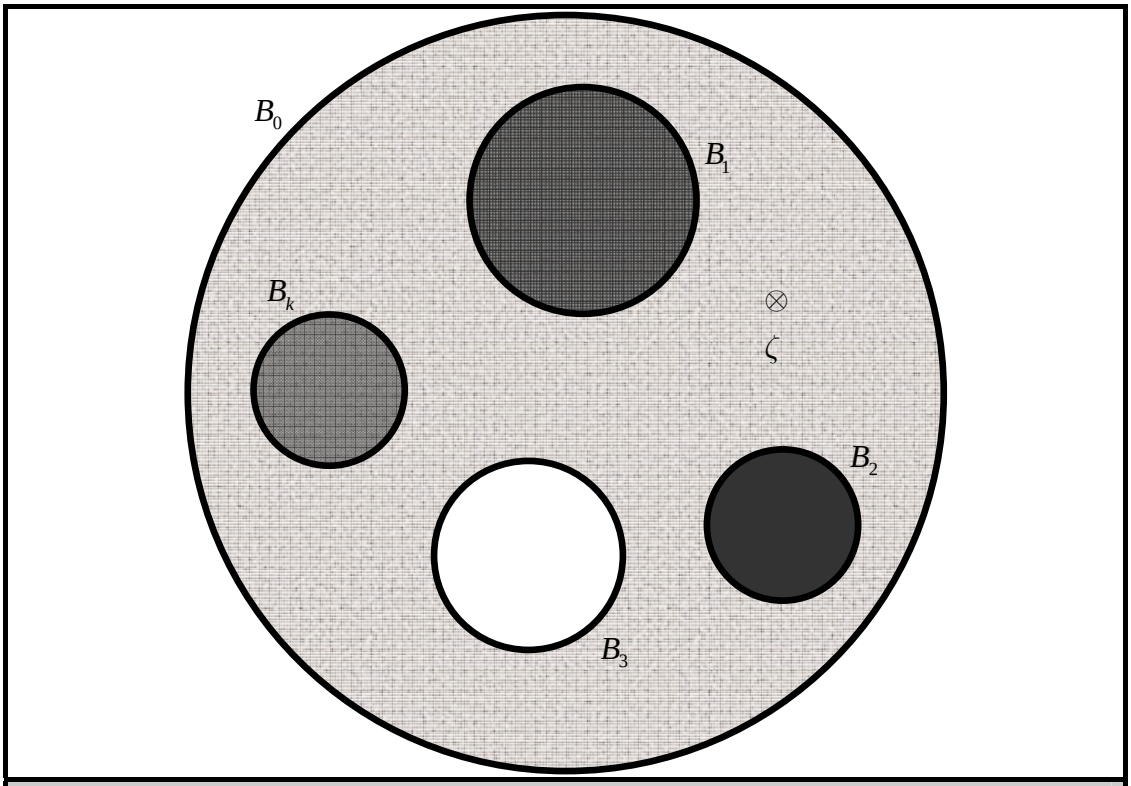

Fig. 2-1 Randomly distributed circular inclusions or holes bounded to the contour B_k

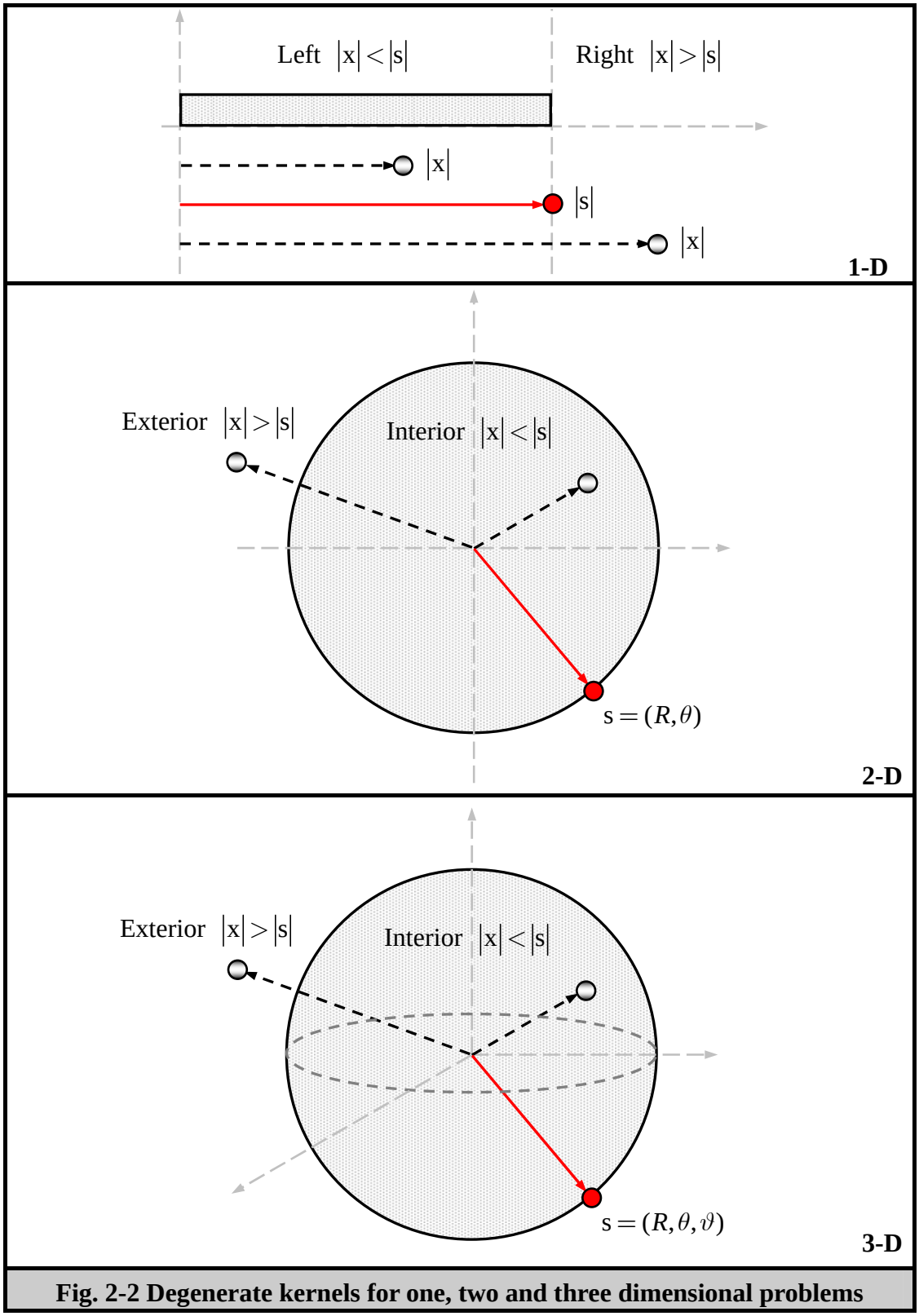

Fig. 2-2 Degenerate kernels for one, two and three dimensional problems

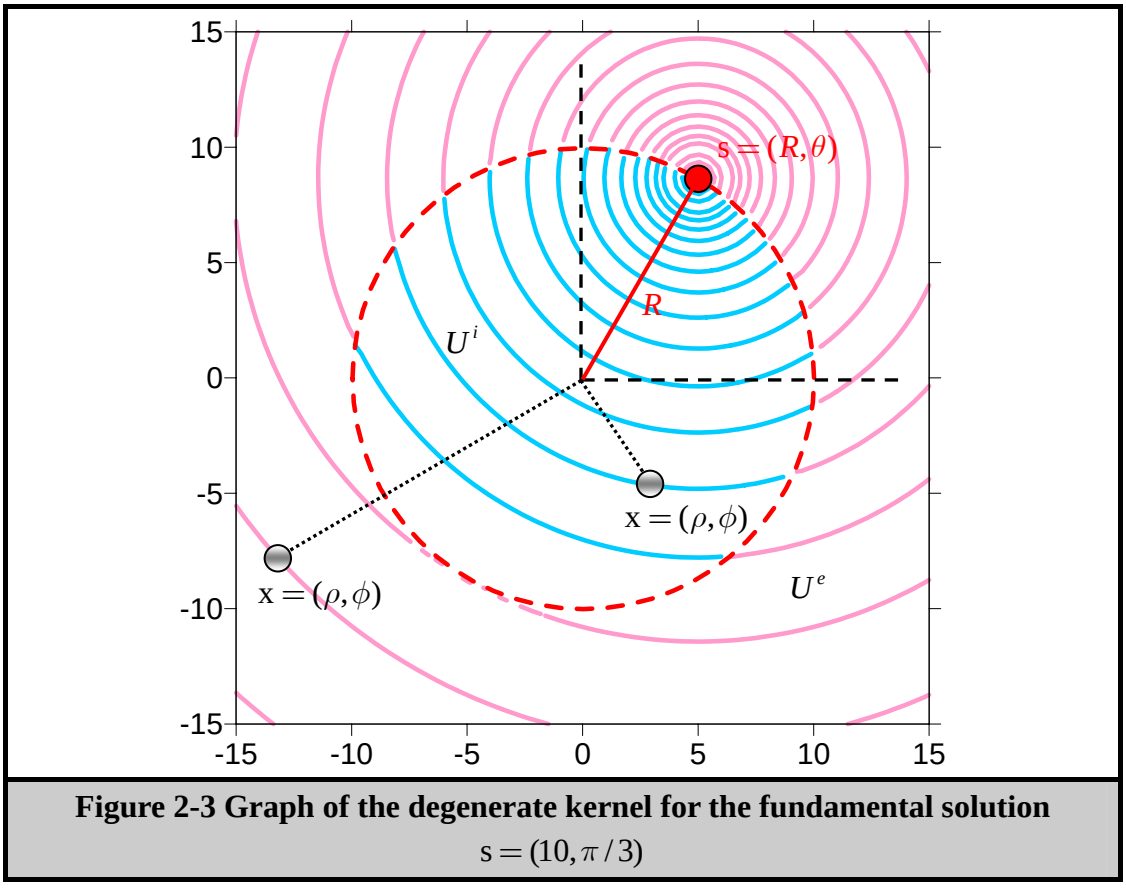

Figure 2-3 Graph of the degenerate kernel for the fundamental solution $s = (10, \pi / 3)$

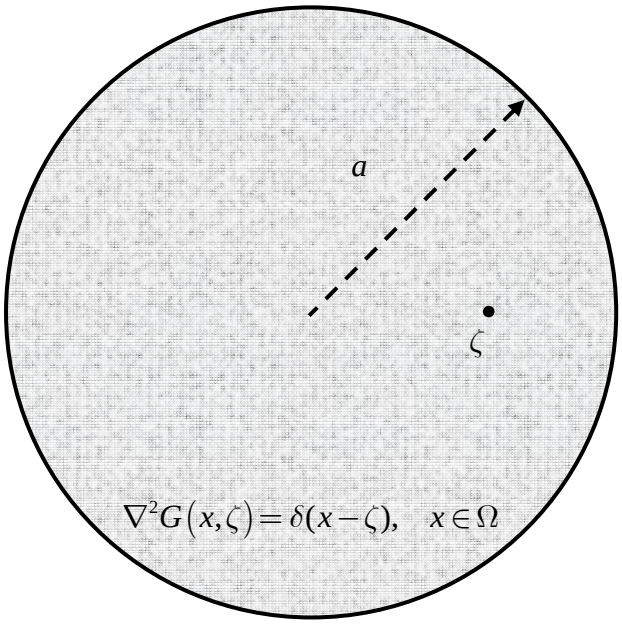

Fig. 2-4 Green's function for the Laplace problem subjected to the Robin boundary condition

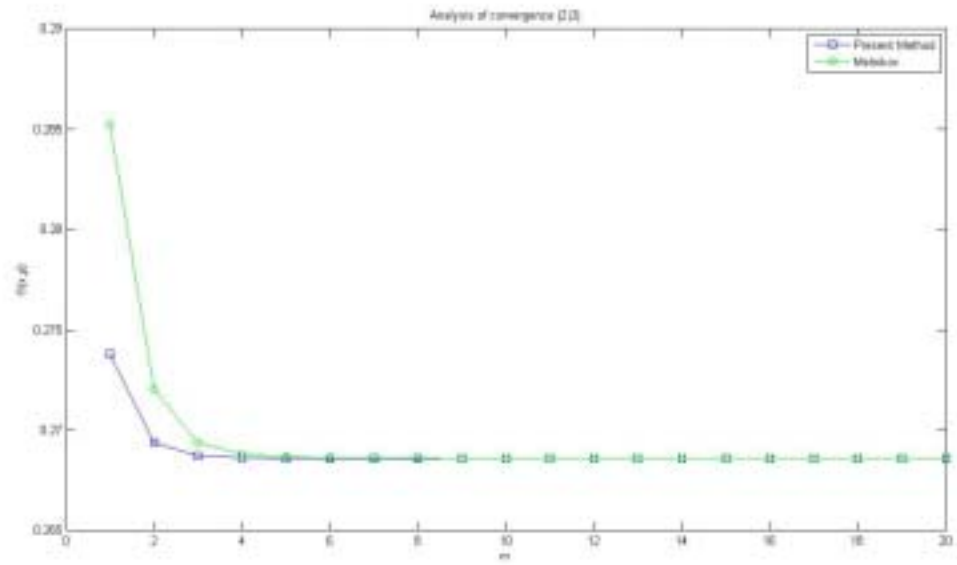

$(\rho,\phi)=(2,0)$

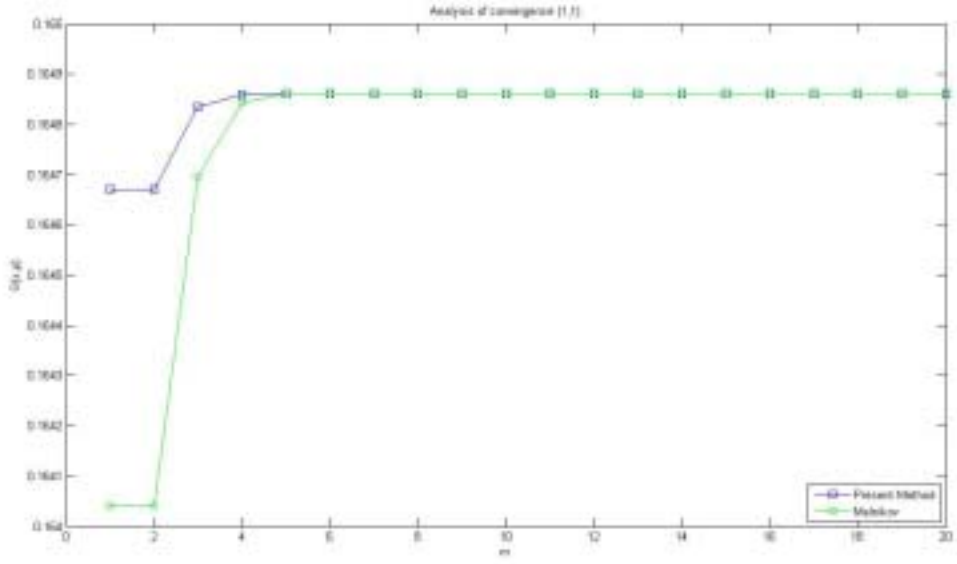

$(\rho,\phi)=\left(\sqrt{2},\frac{\pi}{4}\right)$

Fig. 2-5 Convergence study between the Melnikov's approach and the present method

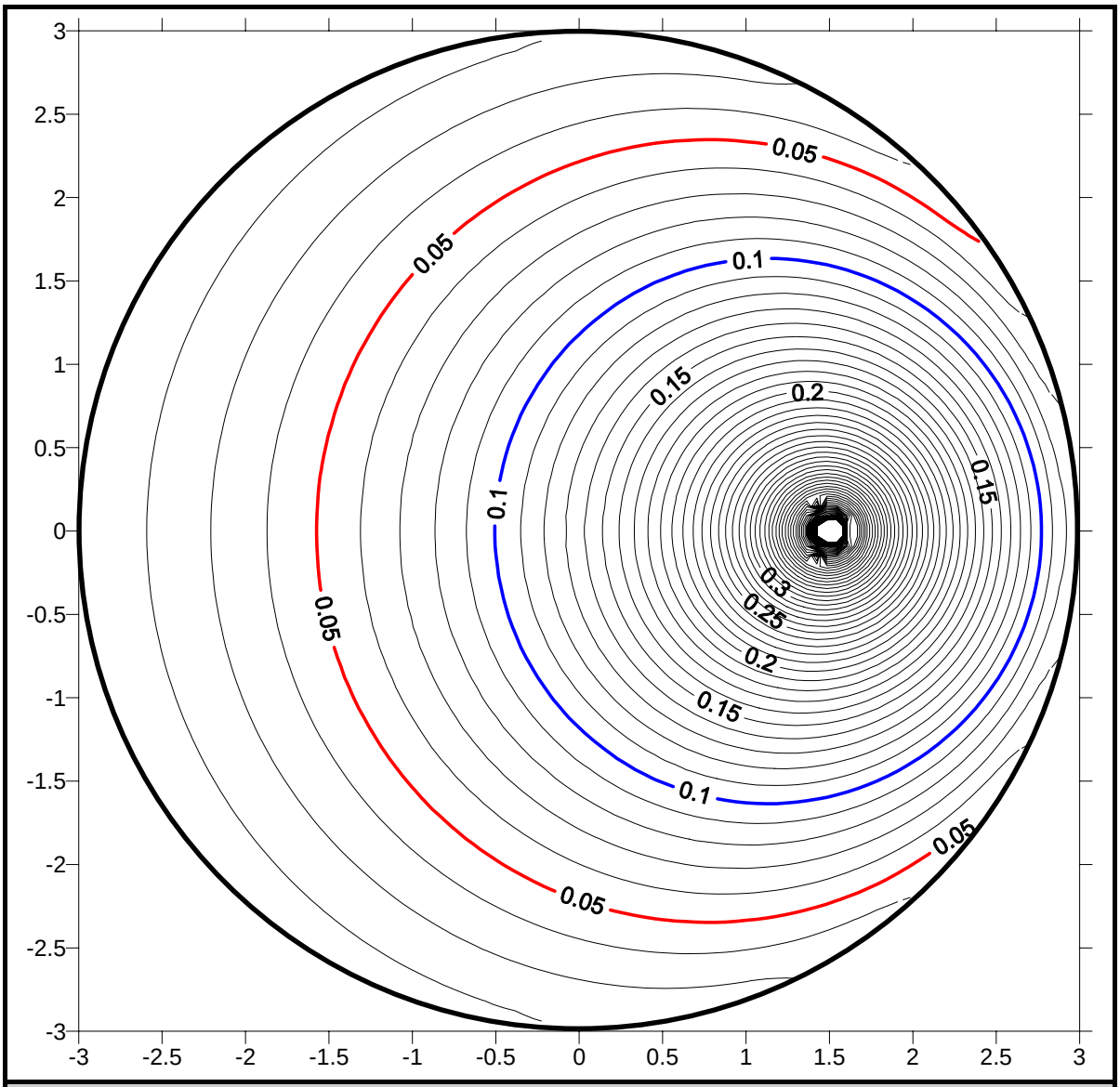

Fig. 2-6 Potential contour of the Green's function for the Laplace problem subjected to the Robin boundary condition using the Melnikov' approach

$R_\zeta = 1.5,\ \theta_\zeta = 0,\ \beta = 2,\ M = 20$

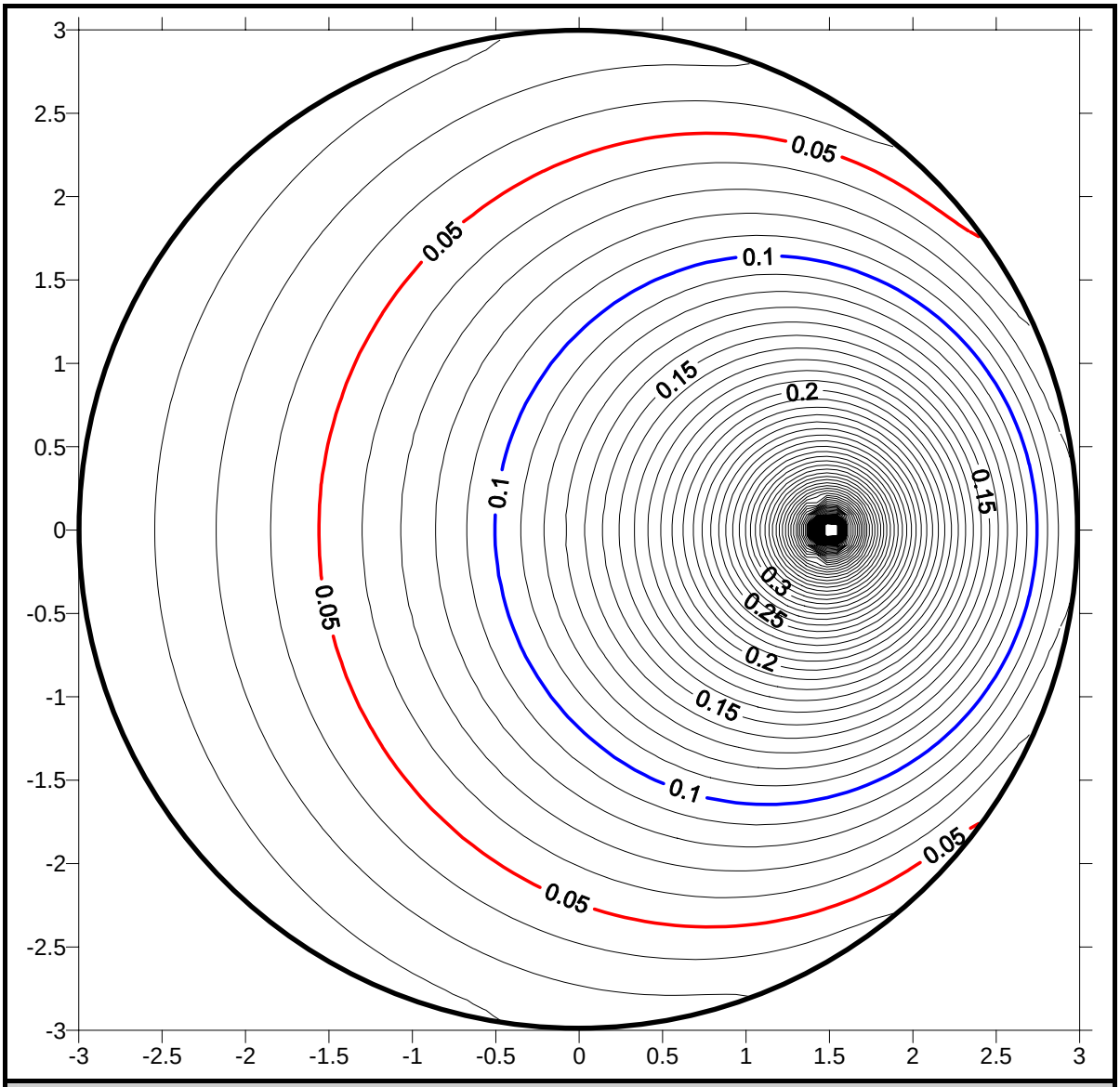

Fig. 2-7 Potential contour of the Green's function for the Laplace problem subjected to the Robin boundary condition using the present method

$R_\zeta = 1.5,\ \theta_\zeta = 0,\ \beta = 2,\ M = 20$

Chapter 3 Green's function for biharmonic equation

Summary

In this chapter, an analytical approach for deriving the Green's function of circular and annular plates is presented. Null-field integral equations are employed to solve the plate problems while kernel functions are expanded to degenerate kernels. The unknown boundary data of the displacement, slope, normal moment and effective shear force are expressed in terms of Fourier series. It is noticed that all the improper integrals are avoided when the degenerate kernels are used. By matching the boundary conditions, a linear algebraic system is obtained. After determining the unknown Fourier coefficients in the algebraic system, the displacement, slope, normal moment and effective shear force of the plate can be obtained by using the boundary integral equations. The present approach is seen as an "analytical" approach since error only ascribes to the truncated Fourier terms. Finally, several numerical examples are utilized to demonstrate the validity of the present method. We also examine the Adewale's results [1] by using our approach and FEM (ABAQUS). Other results are compared well between the present method and FEM using ABAQUS.

3.1 Problem statement for a plate

Considering a Kirchhoff plate for the two-dimensional domain under the concentrated load, the governing equation is written as follows:

$$\nabla^4 G(x,\zeta) = \frac{\delta(x-\zeta)}{D}, \quad x \in \Omega, \tag{3-1}$$

where $G(x,\zeta)$ is the Green's function and can be seen as the displacement, $\delta(x-\zeta)$ denotes the Dirac-delta function of source at ζ, Ω is the domain of the thin plate and D is the flexural rigidity of the plate which is expressed as

$$D = \frac{Eh^3}{12(1-\nu^2)}, \tag{3-2}$$

in which E is the Young's modulus, ν denotes the Poisson ratio, and h is the plate thickness. In order to employ the Rayleigh-Green identity [20], we need two systems, $u(x)$ and $v(x)$. We choose for $G(x,\zeta)$ as $u(x)$ and $U(s,x)$ as the fundamental solution $v(x)$. The fundamental solution satisfies

$$\nabla^4 U(s,x) = 8\pi\delta(s-x), \tag{3-3}$$

and we have

$$U(s,x)=r^2\ln r, \tag{3-4}$$

in which r is the distance between source point s and field point x $\left(r\equiv|x-s|\right)$. After exchanging with the variables x and s, we have four boundary integral equations as shown in the next section.

3.2 Boundary integral and null-field equations

The boundary integral equations for the domain point can be derived from the Rayleigh-Green identity [20] as shown below:

$$\begin{aligned}8\pi G(x,\zeta)=&-\int_B U(s,x)K_{v,s}[G(s,\zeta)]dB(s)+\int_B \Theta(s,x)K_{m,s}[G(s,\zeta)]dB(s)\\&-\int_B M(s,x)K_{\theta,s}[G(s,\zeta)]dB(s)+\int_B V(s,x)G(s,\zeta)dB(s)\\&+U(\zeta,x),\quad x\in\Omega\end{aligned} \tag{3-5}$$

$$\begin{aligned}8\pi K_{\theta,x}[G(x,\zeta)]=&-\int_B U_\theta(s,x)K_{v,s}[G(s,\zeta)]dB(s)+\int_B \Theta_\theta(s,x)K_{m,s}[G(s,\zeta)]dB(s)\\&-\int_B M_\theta(s,x)K_{\theta,s}[G(s,\zeta)]dB(s)+\int_B V_\theta(s,x)G(s,\zeta)dB(s)\\&+U_\theta(\zeta,x),\quad x\in\Omega\end{aligned} \tag{3-6}$$

$$\begin{aligned}8\pi K_{m,x}[G(x,\zeta)]=&-\int_B U_m(s,x)K_{v,s}[G(s,\zeta)]dB(s)+\int_B \Theta_m(s,x)K_{m,s}[G(s,\zeta)]dB(s)\\&-\int_B M_m(s,x)K_{\theta,s}[G(s,\zeta)]dB(s)+\int_B V_m(s,x)G(s,\zeta)dB(s)\\&+U_m(\zeta,x),\quad x\in\Omega\end{aligned} \tag{3-7}$$

$$\begin{aligned}8\pi K_{v,x}[G(x,\zeta)]=&-\int_B U_v(s,x)K_{v,s}[G(s,\zeta)]dB(s)+\int_B \Theta_v(s,x)K_{m,s}[G(s,\zeta)]dB(s)\\&-\int_B M_v(s,x)K_{\theta,s}[G(s,\zeta)]dB(s)+\int_B V_v(s,x)G(s,\zeta)dB(s)\\&+U_v(\zeta,x),\quad x\in\Omega\end{aligned} \tag{3-8}$$

where B is the boundary of the domain Ω, $G(x,\zeta)$, $K_{\theta,s}[G(x,\zeta)]$, $K_{m,s}[G(x,\zeta)]$ and $K_{v,s}[G(x,\zeta)]$ are the displacement, slope, normal moment and effective shear force, $K_{\theta,x}[\cdot]$, $K_{m,x}[\cdot]$ and $K_{v,x}[\cdot]$ are the slope, moment and shear force operators with respect to the point x, respectively. The kernel functions U, Θ, M, V, U_θ, Θ_θ, M_θ, V_θ, U_m, Θ_m, M_m, V_m, U_v, Θ_v, M_v and V_v in Eqs.(3-5)-(3-8) which are expanded to degenerate kernels by using the separation of source point and field point will be elaborated on later. The $K_{\theta,s}[\cdot]$, $K_{m,s}[\cdot]$ and $K_{v,s}[\cdot]$ are the slope, moment and shear force operators and defined as follows:

$$K_{\theta,x}[\cdot]=\frac{\partial}{\partial n_x}, \tag{3-9}$$

$$K_{m,x}[\cdot]=\nu\nabla_x^2+(1-\nu)\frac{\partial^2}{\partial^2 n_x}, \tag{3-10}$$

$$K_{v,x}[\cdot]=\frac{\partial\nabla_x^2}{\partial n_x}+(1-\nu)\frac{\partial}{\partial t_x}\left[\frac{\partial}{\partial n_x}\left(\frac{\partial}{\partial t_x}\right)\right], \tag{3-11}$$

where $\partial/\partial n_x$ is the normal derivative with respect to the field point x, $\partial/\partial t_x$ is the tangential derivative with respect to the field point x, ∇_x^2 means the Laplacian operator. By moving the field point to the boundary, Eqs. (3-5) ~ (3-8) reduce to

$$\begin{aligned}4\pi G(x,\zeta)=&-R.P.V.\int_B U(s,x)K_{v,s}[G(s,\zeta)]dB(s)+R.P.V.\int_B \Theta(s,x)K_{m,s}[G(s,\zeta)]dB(s)\\&-R.P.V.\int_B M(s,x)K_{\theta,s}[G(s,\zeta)]dB(s)+C.P.V\int_B V(s,x)G(s,\zeta)dB(s)\\&+U(\zeta,x),\quad x\in B\end{aligned} \tag{3-12}$$

$$\begin{aligned}4\pi K_{\theta,x}[G(x,\zeta)]=&-R.P.V.\int_B U_\theta(s,x)K_{v,s}[G(s,\zeta)]dB(s)+R.P.V.\int_B \Theta_\theta(s,x)K_{m,s}[G(s,\zeta)]dB(s)\\&-C.P.V.\int_B M_\theta(s,x)K_{\theta,s}[G(s,\zeta)]dB(s)+H.P.V.\int_B V_\theta(s,x)G(s,\zeta)dB(s)\\&+U_\theta(\zeta,x),\quad x\in B\end{aligned} \tag{3-13}$$

$$\begin{aligned}4\pi K_{m,x}[G(x,\zeta)]=&-R.P.V.\int_B U_m(s,x)K_{v,s}[G(s,\zeta)]dB(s)+C.P.V.\int_B \Theta_m(s,x)K_{m,s}[G(s,\zeta)]dB(s)\\&-H.P.V.\int_B M_m(s,x)K_{\theta,s}[G(s,\zeta)]dB(s)+F.P.\int_B V_m(s,x)G(s,\zeta)dB(s)\\&+U_m(\zeta,x),\quad x\in B\end{aligned} \tag{3-14}$$

$$\begin{aligned}4\pi K_{v,x}[G(x,\zeta)]=&-C.P.V.\int_B U_v(s,x)K_{v,s}[G(s,\zeta)]dB(s)+H.P.V.\int_B \Theta_v(s,x)K_{m,s}[G(s,\zeta)]dB(s)\\&-F.P.\int_B M_v(s,x)K_{\theta,s}[G(s,\zeta)]dB(s)+F.P.\int_B V_v(s,x)G(s,\zeta)dB(s)\\&+U_v(\zeta,x),\quad x\in B\end{aligned} \tag{3-15}$$

where C.P.V., R.P.V., H.P.V. and F.P. denote the Cauchy principal value, Riemann principal value, Hadamard principal value and finite part [60], respectively. The null-field integral equations by moving the field point x outside the domain are shown follows:

$$\begin{aligned}0=&-\int_B U(s,x)K_{v,s}[G(s,\zeta)]dB(s)+\int_B \Theta(s,x)K_{m,s}[G(s,\zeta)]dB(s)\\&-\int_B M(s,x)K_{\theta,s}[G(s,\zeta)]dB(s)+\int_B V(s,x)G(s,\zeta)dB(s)+U(\zeta,x),\quad x\in\Omega^c\end{aligned} \tag{3-16}$$

$$\begin{aligned}0=&-\int_B U_\theta(s,x)K_{v,s}[G(s,\zeta)]dB(s)+\int_B \Theta_\theta(s,x)K_{m,s}[G(s,\zeta)]dB(s)\\&-\int_B M_\theta(s,x)K_{\theta,s}[G(s,\zeta)]dB(s)+\int_B V_\theta(s,x)G(s,\zeta)dB(s)+U_\theta(\zeta,x),\quad x\in\Omega^c\end{aligned} \tag{3-17}$$

$$\begin{aligned}0=&-\int_B U_m(s,x)K_{v,s}[G(s,\zeta)]dB(s)+\int_B \Theta_m(s,x)K_{m,s}[G(s,\zeta)]dB(s)\\&-\int_B M_m(s,x)K_{\theta,s}[G(s,\zeta)]dB(s)+\int_B V_m(s,x)G(s,\zeta)dB(s)+U_m(\zeta,x),\quad x\in\Omega^c\end{aligned} \tag{3-18}$$

$$\begin{aligned}0=&-\int_B U_v(s,x)K_{v,s}[G(s,\zeta)]dB(s)+\int_B \Theta_v(s,x)K_{m,s}[G(s,\zeta)]dB(s)\\&-\int_B M_v(s,x)K_{\theta,s}[G(s,\zeta)]dB(s)+\int_B V_v(s,x)G(s,\zeta)dB(s)+U_v(\zeta,x),\quad x\in\Omega^c\end{aligned} \tag{3-19}$$

where Ω^C is the complementary domain of Ω. If the kernel functions in Eqs. (3-5) ~ (3-8)

and (3-16) ~ (3-19) can be expressed by degenerate (separate) forms for Ω or Ω^c domain, we have

$$\begin{aligned} 8\pi G(x,\zeta) = &-\int_B U(s,x)K_{v,s}[G(s,\zeta)]dB(s) + \int_B \Theta(s,x)K_{m,s}[G(s,\zeta)]dB(s) \\ &-\int_B M(s,x)K_{\theta,s}[G(s,\zeta)]dB(s) + \int_B V(s,x)G(s,\zeta)dB(s) \\ &+U(\zeta,x), \quad x\in\Omega\cup B \end{aligned} \tag{3-20}$$

$$\begin{aligned} 8\pi K_{\theta,x}[G(x,\zeta)] = &-\int_B U_\theta(s,x)K_{v,s}[G(s,\zeta)]dB(s) + \int_B \Theta_\theta(s,x)K_{m,s}[G(s,\zeta)]dB(s) \\ &-\int_B M_\theta(s,x)K_{\theta,s}[G(s,\zeta)]dB(s) + \int_B V_\theta(s,x)G(s,\zeta)dB(s) \\ &+U_\theta(\zeta,x), \quad x\in\Omega\cup B \end{aligned} \tag{3-21}$$

$$\begin{aligned} 8\pi K_{m,x}[G(x,\zeta)] = &-\int_B U_m(s,x)K_{v,s}[G(s,\zeta)]dB(s) + \int_B \Theta_m(s,x)K_{m,s}[G(s,\zeta)]dB(s) \\ &-\int_B M_m(s,x)K_{\theta,s}[G(s,\zeta)]dB(s) + \int_B V_m(s,x)G(s,\zeta)dB(s) \\ &+U_m(\zeta,x), \quad x\in\Omega\cup B \end{aligned} \tag{3-22}$$

$$\begin{aligned} 8\pi K_{v,x}[G(x,\zeta)] = &-\int_B U_v(s,x)K_{v,s}[G(s,\zeta)]dB(s) + \int_B \Theta_v(s,x)K_{m,s}[G(s,\zeta)]dB(s) \\ &-\int_B M_v(s,x)K_{\theta,s}[G(s,\zeta)]dB(s) + \int_B V_v(s,x)G(s,\zeta)dB(s) \\ &+U_v(\zeta,x), \quad x\in\Omega\cup B \end{aligned} \tag{3-23}$$

$$\begin{aligned} 0 = &-\int_B U(s,x)K_{v,s}[G(s,\zeta)]dB(s) + \int_B \Theta(s,x)K_{m,s}[G(s,\zeta)]dB(s) \\ &-\int_B M(s,x)K_{\theta,s}[G(s,\zeta)]dB(s) + \int_B V(s,x)G(s,\zeta)dB(s) \\ &+U(\zeta,x), \quad x\in\Omega^c\cup B \end{aligned} \tag{3-24}$$

$$\begin{aligned} 0 = &-\int_B U_\theta(s,x)K_{v,s}[G(s,\zeta)]dB(s) + \int_B \Theta_\theta(s,x)K_{m,s}[G(s,\zeta)]dB(s) \\ &-\int_B M_\theta(s,x)K_{\theta,s}[G(s,\zeta)]dB(s) + \int_B V_\theta(s,x)G(s,\zeta)dB(s) \\ &+U_\theta(\zeta,x), \quad x\in\Omega^c\cup B \end{aligned} \tag{3-25}$$

$$\begin{aligned} 0 = &-\int_B U_m(s,x)K_{v,s}[G(s,\zeta)]dB(s) + \int_B \Theta_m(s,x)K_{m,s}[G(s,\zeta)]dB(s) \\ &-\int_B M_m(s,x)K_{\theta,s}[G(s,\zeta)]dB(s) + \int_B V_m(s,x)G(s,\zeta)dB(s) \\ &+U_m(\zeta,x), \quad x\in\Omega^c\cup B \end{aligned} \tag{3-26}$$

$$\begin{aligned} 0 = &-\int_B U_v(s,x)K_{v,s}[G(s,\zeta)]dB(s) + \int_B \Theta_v(s,x)K_{m,s}[G(s,\zeta)]dB(s) \\ &-\int_B M_v(s,x)K_{\theta,s}[G(s,\zeta)]dB(s) + \int_B V_v(s,x)G(s,\zeta)dB(s) \\ &+U_v(\zeta,x), \quad x\in\Omega^c\cup B \end{aligned} \tag{3-27}$$

Although the four equations of Eqs. (3-24) ~ (3-27) in the plate formulation are provided, only the first two equations are employed to solve boundary unknowns for simplicity. In the real implementation, the collocation point in the null-field integral equation can be exactly located on the real boundary from Ω^C once the kernel functions is expressed in terms of

interior and exterior appropriate forms of degenerate kernels. In other words, Eqs. (3-24)-(3-27) can be implemented for $x \in \Omega^c \cup B$ if kernels of degenerate forms are used. Novelly, all the improper integrals disappear in the BIEs since the potential across the boundary can be determined in both sides by using degenerate kernels. For simplicity, Table 3-1 summarizes the main difference between the present method and conventional BEM.

3.3 Expansion of fundamental solution and boundary densities

The displacement $G(s,\zeta)$, slope $K_{\theta,s}[G(s,\zeta)]$, normal moment $K_{m,s}[G(s,\zeta)]$ and effective shear force $K_{v,s}[G(s,\zeta)]$ along the circular boundaries in the null-field integral equations are expanded in terms of Fourier series respectively, which are expressed as follows:

$$G(s,\zeta) = c_0 + \sum_{n=1}^{M}(c_n \cos n\theta + d_n \sin n\theta), \quad s \in B, \tag{3-28}$$

$$K_{\theta,s}[G(s,\zeta)] = g_0 + \sum_{n=1}^{M}(g_n \cos n\theta + h_n \sin n\theta), \quad s \in B, \tag{3-29}$$

$$K_{m,s}[G(s,\zeta)] = a_0 + \sum_{n=1}^{M}(a_n \cos n\theta + b_n \sin n\theta), \quad s \in B, \tag{3-30}$$

$$K_{v,s}[G(s,\zeta)] = p_0 + \sum_{n=1}^{M}(p_n \cos n\theta + q_n \sin n\theta), \quad s \in B, \tag{3-31}$$

where a_0, a_n, b_n, c_0, c_n, d_n, g_0, g_n, h_n, p_0, p_n and q_n are the Fourier coefficients and M is the number of Fourier series terms.

3.3.1 Expansion of kernels

For the kernel function $U(s,x)$, it can be expanded in terms of degenerate kernels in a series form as shown below:

$$U(s,x) = \begin{cases} U^I(s,x) = \rho^2(1+\ln R) + R^2 \ln R - [R\rho(1+2\ln R) + \frac{1}{2}\frac{\rho^3}{R}]\cos(\theta-\phi) \\ \qquad - \sum_{m=2}^{\infty}[\frac{1}{m(m+1)}\frac{\rho^{m+2}}{R^m} - \frac{1}{m(m-1)}\frac{\rho^m}{R^{m-2}}]\cos[m(\theta-\phi)], \quad R \geq \rho \end{cases} \tag{3-32,a}$$

$$\begin{cases} U^E(s,x) = R^2(1+\ln \rho) + \rho^2 \ln \rho - [\rho R(1+2\ln \rho) + \frac{1}{2}\frac{R^3}{\rho}]\cos(\theta-\phi) \\ \qquad - \sum_{m=2}^{\infty}[\frac{1}{m(m+1)}\frac{R^{m+2}}{\rho^m} - \frac{1}{m(m-1)}\frac{R^m}{\rho^{m-2}}]\cos[m(\theta-\phi)], \quad \rho > R \end{cases} \tag{3-32,b}$$

where the superscripts " I " and " E " denote the interior and exterior cases of $U(s,x)$ kernel depending on the geometry as shown in Fig. 3-1. The other kernels in the boundary integral equations can be obtained by utilizing the operators of Eqs.(3-9) ~ (3-11) with respect to the $U(s,x)$ kernel. The degenerate kernels U, Θ, M, V, U_θ, Θ_θ, M_θ, V_θ, U_m, Θ_m,

M_m, V_m, U_v, Θ_v, M_v and V_v in Eqs. (3-20) ~ (3-23) are listed in the Appendix 3. It is noted that the interior and exterior cases of U, Θ, M, U_θ, Θ_θ and U_m are the same when they both approach to the boundary ($\rho = R$), since the degenerate kernels are continuous functions across the boundary as shown in Table 3-2. Then, the kernel function with the superscript "I" is chosen while the field point is inside the circular region; otherwise, the kernels with the superscript "E" are chosen.

3.3.2 Series representation for the Green's function of the clamped-free annular plate

For the annular case as shown in Fig. 3-2 subject to the fixed-free boundary condition, the unknown Fourier series can be analytically derived. By collocating x on (b^+, ϕ) and (a^-, ϕ), the null-field equations yield

$$
\begin{aligned}
0 = &-\int_{B_1}\left[b^2(1+\ln b)+b^2\ln b-\left[b^2(1+2\ln b)+\frac{b^2}{2}\right]\cos(\theta-\phi)-\sum_{m=2}^{\infty}\left[\frac{b^2}{m(m+1)}-\frac{b^2}{m(m-1)}\right]\cos m(\theta-\phi)\right]\\
&\left[a_0+\sum_{n=1}^{\infty}a_n\cos n\theta+b_n\sin n\theta\right]bd\theta\\
&+\int_{B_1}\left[2b(1+\ln b)-\left[b(1+2\ln b)+\frac{3}{2}b\right]\cos(\theta-\phi)-\sum_{m=2}^{\infty}\left[\frac{m+2}{m(m+1)}b-\frac{1}{m-1}b\right]\cos m(\theta-\phi)\right]\\
&\left[\overline{a_0}+\sum_{n=1}^{\infty}\overline{a_n}\cos n\theta+\overline{b_n}\sin n\theta\right]bd\theta\\
&-\int_{B_2}\left[2(1+\nu)(1+\ln b)-(\nu+3)\frac{a}{b}\cos(\theta-\phi)+\sum_{m=2}^{\infty}\left[\frac{m(\nu-1)-2(\nu+1)}{m}\frac{a^m}{b^m}+(1-\nu)\frac{a^{m-2}}{b^{m-2}}\right]\cos m(\theta-\phi)\right]\\
&\left[p_0+\sum_{n=1}^{\infty}p_n\cos n\theta+q_n\sin n\theta\right]ad\theta\\
&+\int_{B_2}\left[(-3-\nu)\frac{1}{b}\cos(\theta-\phi)+\sum_{m=2}^{\infty}\left[(m(1-\nu)-4)\frac{a^{m-1}}{b^m}-m(1-\nu)\frac{a^{m-3}}{b^{m-2}}\right]\cos m(\theta-\phi)\right]\\
&\left[\overline{p_0}+\sum_{n=1}^{\infty}\overline{p_n}\cos n\theta+\overline{q_n}\sin n\theta\right]ad\theta\\
&+R_\zeta^{\,2}(1+\ln b)+b^2\ln b-\left[bR_\zeta(1+2\ln b)+\frac{1}{2}\frac{R_\zeta^{\,3}}{b}\right]\cos(\theta_\zeta-\phi)-\sum_{m=2}^{\infty}\left[\frac{1}{m(m+1)}\frac{R_\zeta^{\,m+2}}{b^m}-\frac{1}{m(m-1)}\frac{R_\zeta^{\,m}}{b^{m-2}}\right]\cos m(\theta_\zeta-\phi)
\end{aligned}
\qquad (3\text{-}33)
$$

, $x=(b^+,\phi)$,

$$
\begin{aligned}
0 = &-\int_{B_1}\left[b+b(1+2\ln b)-\left[b(3+2\ln b)-\frac{1}{2}b\right]\cos(\theta-\phi)+\sum_{m=2}^{\infty}\left[\frac{1}{m+1}b-\frac{m-2}{m(m-1)}b\right]\cos m(\theta-\phi)\right]\\
&\left[a_0+\sum_{n=1}^{\infty}a_n\cos n\theta+b_n\sin n\theta\right]bd\theta\\
&+\int_{B_1}\left[2-\left[(3+2\ln b)-\frac{3}{2}\right]\cos(\theta-\phi)+\sum_{m=2}^{\infty}\left[\frac{m+2}{m+1}-\frac{m-2}{m-1}\right]\cos m(\theta-\phi)\right]\\
&\left[\overline{a_0}+\sum_{n=1}^{\infty}\overline{a_n}\cos n\theta+\overline{b_n}\sin n\theta\right]bd\theta\\
&-\int_{B_2}\left[\frac{2(1+\nu)}{b}+(\nu+3)\frac{a}{b^2}\cos(\theta-\phi)-\sum_{m=2}^{\infty}\left[\left(m(\nu-1)-2(\nu+1)\right)\frac{a^m}{b^{m+1}}+(m-2)(1-\nu)\frac{a^{m-2}}{b^{m-1}}\right]\cos m(\theta-\phi)\right]\\
&\left[p_0+\sum_{n=1}^{\infty}p_n\cos n\theta+q_n\sin n\theta\right]ad\theta\\
&+\int_{B_2}\left[(3+\nu)\frac{1}{b^2}\cos(\theta-\phi)-\sum_{m=2}^{\infty}\left[m\left(m(1-\nu)-4\right)\frac{a^{m-1}}{b^{m+1}}-m(m-2)(1-\nu)\frac{a^{m-3}}{b^{m-1}}\right]\cos m(\theta-\phi)\right]\\
&\left[\overline{p_0}+\sum_{n=1}^{\infty}\overline{p_n}\cos n\theta+\overline{q_n}\sin n\theta\right]ad\theta\\
&+\frac{R_\zeta^{\,2}}{b}+b(1+2\ln b)-\left[R_\zeta(3+2\ln b)-\frac{1}{2}\frac{R_\zeta^{\,3}}{b^2}\right]\cos(\theta_\zeta-\phi)+\sum_{m=2}^{\infty}\left[\frac{1}{m+1}\frac{R_\zeta^{\,m+2}}{b^{m+1}}-\frac{m-2}{m(m-1)}\frac{R_\zeta^{\,m}}{b^{m-1}}\right]\cos m(\theta_\zeta-\phi)
\end{aligned}
\tag{3-34}
$$

, $x=(b^+,\phi)$,

$$
\begin{aligned}
0 = &-\int_{B_1}\left[a^2(1+\ln b)+b^2\ln b-\left[ba(1+2\ln b)+\frac{1}{2}\frac{a^3}{b}\right]\cos(\theta-\phi)-\sum_{m=2}^{\infty}\left[\frac{1}{m(m+1)}\frac{a^{m+2}}{b^m}-\frac{1}{m(m-1)}\frac{a^m}{b^{m-2}}\right]\cos m(\theta-\phi)\right]\\
&\left[a_0+\sum_{n=1}^{\infty}a_n\cos n\theta+b_n\sin n\theta\right]bd\theta\\
&+\int_{B_1}\left[\frac{a^2}{b}+b(1+2\ln b)-\left[a(3+2\ln b)-\frac{1}{2}\frac{a^3}{b^2}\right]\cos(\theta-\phi)+\sum_{m=2}^{\infty}\left[\frac{1}{m+1}\frac{a^{m+2}}{b^{m+1}}-\frac{m-2}{m(m-1)}\frac{a^m}{b^{m-1}}\right]\cos m(\theta-\phi)\right]\\
&\left[\overline{a_0}+\sum_{n=1}^{\infty}\overline{a_n}\cos n\theta+\overline{b_n}\sin n\theta\right]bd\theta\\
&-\int_{B_2}\left[(\nu-1)+(\nu+3)+2(\nu+1)\ln a-\left[2(\nu+1)-(\nu-1)\right]\cos(\theta-\phi)+\sum_{m=2}^{\infty}\left[(\nu-1)+\frac{m(1-\nu)-2(1+\nu)}{m}\right]\cos m(\theta-\phi)\right]\\
&\left[p_0+\sum_{n=1}^{\infty}p_n\cos n\theta+q_n\sin n\theta\right]ad\theta\\
&+\int_{B_2}\left[\frac{4}{a}+\left[\frac{2}{a}(3-\nu)-\frac{1}{a}(1-\nu)\right]\cos(\theta-\phi)-\sum_{m=2}^{\infty}\left[m(1-\nu)\frac{1}{a}-\left(4+m(1-\nu)\right)\frac{1}{a}\right]\cos m(\theta-\phi)\right]\\
&\left[\overline{p_0}+\sum_{n=1}^{\infty}\overline{p_n}\cos n\theta+\overline{q_n}\sin n\theta\right]ad\theta\\
&+a^2(1+\ln R_\zeta)+R_\zeta^{\,2}\ln R_\zeta-\left[R_\zeta a(1+2\ln R_\zeta)+\frac{1}{2}\frac{a^3}{R_\zeta}\right]\cos(\theta_\zeta-\phi)-\sum_{m=2}^{\infty}\left[\frac{1}{m(m+1)}\frac{a^{m+2}}{R_\zeta^{\,m}}-\frac{1}{m(m-1)}\frac{a^m}{R_\zeta^{\,m-2}}\right]\cos m(\theta_\zeta-\phi)
\end{aligned}
\tag{3-35}
$$

, $x=(a^-,\phi)$,

$$
\begin{aligned}
0 = &-\int_{B_1}\left[2a(1+\ln b)-\left[b(1+2\ln b)+\frac{3}{2}\frac{a^2}{b}\right]\cos(\theta-\phi)-\sum_{m=2}^{\infty}\left[\frac{m+2}{m(m+1)}\frac{a^{m+1}}{b^m}-\frac{1}{m-1}\frac{a^{m-1}}{b^{m-2}}\right]\cos m(\theta-\phi)\right]\\
&\left[a_0+\sum_{n=1}^{\infty}a_n\cos n\theta+b_n\sin n\theta\right]bd\theta\\
&+\int_{B_1}\left[\frac{2a}{b}-\left[(3+2\ln b)-\frac{3}{2}\frac{a^2}{b^2}\right]\cos(\theta-\phi)+\sum_{m=2}^{\infty}\left[\frac{m+2}{m+1}\frac{a^{m+1}}{b^{m+1}}-\frac{m-2}{m-1}\frac{a^{m-1}}{b^{m-1}}\right]\cos m(\theta-\phi)\right]\\
&\left[\overline{a_0}+\sum_{n=1}^{\infty}\overline{a_n}\cos n\theta+\overline{b_n}\sin n\theta\right]bd\theta\\
&-\int_{B_2}\left[\frac{2}{a}(\nu-1)-\left[\frac{2}{a}(\nu+1)-3(\nu-1)\frac{1}{a}\right]\cos(\theta-\phi)+\sum_{m=2}^{\infty}\left[(m+2)(\nu-1)\frac{1}{a}+\left(m(1-\nu)-2(1+\nu)\right)\frac{1}{a}\right]\cos m(\theta-\phi)\right]\\
&\left[p_0+\sum_{n=1}^{\infty}p_n\cos n\theta+q_n\sin n\theta\right]ad\theta\\
&+\int_{B_2}\left[\left[\frac{2}{a^2}(3-\nu)-3(1-\nu)\frac{1}{a^2}\right]\cos(\theta-\phi)-\sum_{m=2}^{\infty}\left[m(m+2)(1-\nu)\frac{1}{a^2}-m\left(4+m(1-\nu)\right)\frac{1}{a^2}\right]\cos m(\theta-\phi)\right]\\
&\left[\overline{p_0}+\sum_{n=1}^{\infty}\overline{p_n}\cos n\theta+\overline{q_n}\sin n\theta\right]ad\theta\\
&+2a(1+\ln R_\zeta)-\left[R_\zeta(1+2\ln R_\zeta)+\frac{3}{2}\frac{a^2}{R_\zeta}\right]\cos(\theta_\zeta-\phi)-\sum_{m=2}^{\infty}\left[\frac{m+2}{m(m+1)}\frac{a^{m+1}}{{R_\zeta}^m}-\frac{1}{m-1}\frac{a^{m-1}}{{R_\zeta}^{m-2}}\right]\cos m(\theta_\zeta-\phi)
\end{aligned}
\tag{3-36}
$$

, $x=(a^-,\phi)$,

where a and b are the inner and outer radii, respectively. For the fixed-free case, the explicit form for the unknown Fourier series can be obtained. The Fourier expansions of the boundary densities for the radial slope, normal moment and shear force are shown below:

$$K_{v,s}[G(s,\zeta)]=a_0+a_1\cos\theta+b_1\sin\theta+\sum_{n=2}^{M}(a_n\cos n\theta+b_n\sin n\theta),\quad s\in B_1 \tag{3-37}$$

$$K_{m,s}[G(s,\zeta)]=\overline{a}_0+\overline{a}_1\cos\theta+\overline{b}_1\sin\theta+\sum_{n=2}^{M}(\overline{a}_n\cos n\theta+\overline{b}_n\sin n\theta),\quad s\in B_1 \tag{3-38}$$

$$K_{\theta,s}[G(s,\zeta)]=p_0+p_1\cos\theta+q_1\sin\theta+\sum_{n=2}^{M}(p_n\cos n\theta+q_n\sin n\theta),\quad s\in B_2 \tag{3-39}$$

$$G(s,\zeta)=\overline{p}_0+\overline{p}_1\cos\theta+\overline{q}_1\sin\theta+\sum_{n=2}^{M}(\overline{p}_n\cos n\theta+\overline{q}_n\sin n\theta),\quad s\in B_2 \tag{3-40}$$

where the unknown coefficients can be obtained according to Eqs. (3-37) ~ (3-40) and are shown below:

$$a_0=\frac{1}{2b\pi} \tag{3-41}$$

$$\begin{aligned}\overline{a}_0=&-(b^2(\nu-1)+2a^2(\nu+1)(\ln b+\ln R_\zeta)\\&-(\nu-1)R_\zeta^2)/(4\pi(-b^2(\nu-1)+a^2(\nu+1)))\end{aligned} \tag{3-42}$$

$$\begin{aligned}p_0=&(a(b^2(-1+2\ln b-2\ln R_\zeta)+R_\zeta^2))\\&/(4\pi(-b^2(-1+\nu)+a^2(1+\nu)))\end{aligned} \tag{3-43}$$

$$\bar{p}_0 = (\frac{2a^2(1+\nu)((a^2-b^2)+2b^2(\ln b-\ln a))(1+\ln R_\zeta)}{-b^2(-1+\nu)+a^2(1+\nu)} + \frac{((b^2-a^2)(-1+\nu)+2a^2(1+\nu)(\ln a-\ln b))(b^2(1+2\ln b)+R_\zeta^2)}{-b^2(-1+\nu)+a^2(1+\nu)} + 2(b^2\ln b+(1+\ln b)R_\zeta^2)-2a^2(1+\ln R_\zeta)+R_\zeta^2\ln R_\zeta)/16\pi \tag{3-44}$$

$$a_1 = -((a^4b^2(3+\nu)+(-3b^4(-1+\nu)+a^4(3+\nu))R_\zeta^2+b^2(-1+\nu)R_\zeta^4))\cos\theta_\zeta /(2b^2\pi(b^4(-1+\nu)-a^4(3+\nu))R_\zeta) \tag{3-45}$$

$$\bar{a}_1 = ((b^2-R_\zeta^2)(-a^4(3+\nu)+b^2(-1+\nu)R_\zeta^2))\cos\theta_\zeta /(2b\pi(b^4(-1+\nu)-a^4(3+\nu))R_\zeta) \tag{3-46}$$

$$p_1 = -((-a^2b^2(-b^2(-3+\nu)+a^2(3+\nu))+(-2a^2b^2(-3+\nu) + b^4(-1+\nu)+a^4(3+\nu)+2(-b^4(-1+\nu)+a^4(3+\nu))(\ln b-\ln R_\zeta))R_\zeta^2 + (a^2(-3+\nu)-b^2(-1+\nu))R_\zeta^4))\cos\theta_\zeta /(8\pi(-b^4(-1+\nu)+a^4(3+\nu))R_\zeta) \tag{3-47}$$

$$\bar{p}_1 = (a(a^2b^2(-b^2(1+\nu)+a^2(3+\nu))+(-(a-b)(a+b)(-b^2(-1+\nu) + a^2(3+\nu))+2(-b^4(-1+\nu)+a^4(3+\nu))(-\ln b+\ln R_\zeta))R_\zeta^2 - (-b^2(-1+\nu)+a^2(1+\nu))R_\zeta^4))\cos\theta_\zeta /(8\pi(-b^4(-1+\nu)+a^4(3+\nu))R_\zeta) \tag{3-48}$$

$$b_1 = -((a^4b^2(3+\nu)+(-3b^4(-1+\nu)+a^4(3+\nu))R_\zeta^2+b^2(-1+\nu)R_\zeta^4))\sin\theta_\zeta /(2b^2\pi(b^4(-1+\nu)-a^4(3+\nu))R_\zeta) \tag{3-49}$$

$$\bar{b}_1 = ((b^2-R_\zeta^2)(-a^4(3+\nu)+b^2(-1+\nu)R_\zeta^2))\sin\theta_\zeta /(2b\pi(b^4(-1+\nu)-a^4(3+\nu))R_\zeta) \tag{3-50}$$

$$q_1 = -((-a^2b^2(-b^2(-3+\nu)+a^2(3+\nu))+(-2a^2b^2(-3+\nu)+b^4(-1+\nu) + a^4(3+\nu)+2(-b^4(-1+\nu)+a^4(3+\nu))(\ln b-\ln R_\zeta))R_\zeta^2+(a^2(-3+\nu) - b^2(-1+\nu))R_\zeta^4))\sin\theta_\zeta /(8\pi(-b^4(-1+\nu)+a^4(3+\nu))R_\zeta) \tag{3-51}$$

$$\bar{q}_1 = (a(a^2b^2(-b^2(1+\nu)+a^2(3+\nu))+(-(a-b)(a+b)(-b^2(-1+\nu) + a^2(3+\nu))+2(-b^4(-1+\nu)+a^4(3+\nu))(-\ln b+\ln R_\zeta))R_\zeta^2 - (-b^2(-1+\nu)+a^2(1+\nu))R_\zeta^4))\sin\theta_\zeta /(8\pi(-b^4(-1+\nu)+a^4(3+\nu))R_\zeta) \tag{3-52}$$

$$
\begin{aligned}
a_n = {} & (b^{-1+n} R_\zeta^{-n} (a^{2(1+n)} (a^{2n} b^2 (-2+n)(-1+\nu)(3+\nu) + b^{2n} (-b^2 (-2+n+n^2)(-1 \\
& +\nu)^2 + a^2 (n^2 (-1+\nu)^2 + 8(1+\nu)))) + a^{2n} n(-1+\nu)(b^{2n} (-a^2 (1+n) + b^2 (2 \\
& +n))(-1+\nu) - a^{2(1+n)} (3+\nu)) R_\zeta^2 + R_\zeta^{2n} (-a^2 b^{2n} (-1+\nu)(3+\nu)(b^2 (2 \\
& +n) - n R_\zeta^2) + a^{2n} (a^2 (-b^2 (-2+n)(1+n)(-1+\nu)^2 + a^2 (n^2 (-1+\nu)^2 \\
& +8(1+\nu))) - (-b^2 (-2+n) + a^2 (-1+n)) n (-1+\nu)^2 R_\zeta^2)))) \cos n\theta_\zeta \\
& /(2\pi(-a^{2+4n} b^2 (-1+\nu)(3+\nu) - a^2 b^{2+4n} (-1+\nu)(3+\nu) + a^{2n} b^{2n} (b^4 n^2 (-1 \\
& +\nu)^2 - 2a^2 b^2 (-1+n^2)(-1+\nu)^2 + a^4 (n^2 (-1+\nu)^2 + 8(1+\nu)))))
\end{aligned}
\tag{3-53}
$$

$$
\begin{aligned}
\bar{a}_n = {} & -(b^n R_\zeta^{-n} (a^{2(1+n)} (a^{2n} b^2 n(-1+\nu)(3+\nu) + b^{2n} (b^2 (-1+n) n (-1+\nu)^2 \\
& -a^2 (n^2 (-1+\nu)^2 + 8(1+\nu)))) + a^{2n} n(-1+\nu)(b^{2n} (-b^2 n + a^2 (1+n)) \\
& (-1+\nu) - a^{2(1+n)} (3+\nu)) R_\zeta^2 + R_\zeta^{2n} (a^2 b^{2n} n(-1+\nu)(3+\nu)(b^2 - R_\zeta^2) + a^{2n} (a^2 \\
& (-b^2 n(1+n)(-1+\nu)^2 + a^2 (n^2 (-1+\nu)^2 + 8(1+\nu))) - n(a^2 (-1+n) \\
& -b^2 n)(-1+\nu)^2 R_\zeta^2)))) \cos n\theta_\zeta / (2n\pi(-a^{2+4n} b^2 (-1+\nu)(3+\nu) \\
& -a^2 b^{2+4n} (-1+\nu)(3+\nu) + a^{2n} b^{2n} (b^4 n^2 (-1+\nu)^2 - 2a^2 b^2 (-1+n^2) \\
& (-1+\nu)^2 + a^4 (n^2 (-1+\nu)^2 + 8(1+\nu)))))
\end{aligned}
\tag{3-54}
$$

$$
\begin{aligned}
p_n = {} & (a^{1+n} R_\zeta^{-n} (b^{2(1+n)} (-1+n)(-a^2 b^{2n} (-4+n(-1+\nu)) \\
& + a^{2n} (a^2 (1+n)(4+n(-1+\nu)) - b^2 n^2 (-1+\nu))) + b^{2n} n(1+n)(b^{2(1+n)} \\
& (-1+\nu) + a^{2n} (b^2 (-1+n)(-1+\nu) + a^2 (-4+n-n\nu))) R_\zeta^2 \\
& + R_\zeta^{2n} (b^2 (1+n)(a^{2(1+n)} (4+n(-1+\nu)) + b^{2n} (a^2 (-1+n)(-4+n(-1+\nu)) \\
& -b^2 n^2 (-1+\nu))) + (-1+n) n (-a^{2n} b^2 (-1+\nu) + b^{2n} (b^2 (1+n)(-1+\nu) \\
& + a^2 (4+n-n\nu))) R_\zeta^2))) \cos n\theta_\zeta / (2(-1+n) n(1+n)\pi(-a^{2+4n} b^2 (-1+\nu) \\
& (3+\nu) - a^2 b^{2+4n} (-1+\nu)(3+\nu) + a^{2n} b^{2n} (b^4 n^2 (-1+\nu)^2 - 2a^2 b^2 (-1+n^2) \\
& (-1+\nu)^2 + a^4 (n^2 (-1+\nu)^2 + 8(1+\nu)))))
\end{aligned}
\tag{3-55}
$$

$$
\begin{aligned}
\bar{p}_n = {} & (a^{2+n} R_\zeta^{-n} (b^{2(1+n)} (-1+n)(a^2 b^{2n} (2-n+(2+n)\nu) \\
& + a^{2n} (-b^2 n^2 (-1+\nu) + a^2 (1+n)(n(-1+\nu) - 2(1+\nu)))) \\
& + b^{2n} n(1+n)(-b^{2(1+n)} (-1+\nu) + a^{2n} (b^2 (-1+n)(-1+\nu) \\
& + a^2 (2+n+2\nu-n\nu))) R_\zeta^2 + R_\zeta^{2n} (b^2 (1+n)(a^{2(1+n)} (n(-1+\nu) \\
& -2(1+\nu)) + b^{2n} (b^2 n^2 (-1+\nu) - a^2 (-1+n)(2-n+(2+n)\nu))) \\
& + (-1+n) n (-a^{2n} b^2 (-1+\nu) + b^{2n} (-b^2 (1+n)(-1+\nu) + a^2 (2-n \\
& + (2+n)\nu))) R_\zeta^2))) \cos n\theta_\zeta / (2(1-n) n^2 (1+n)\pi(-a^{2+4n} b^2 (-1+\nu)(3+\nu) \\
& -a^2 b^{2+4n} (-1+\nu)(3+\nu) + a^{2n} b^{2n} (b^4 n^2 (-1+\nu)^2 - 2a^2 b^2 (-1+n^2) \\
& (-1+\nu)^2 + a^4 (n^2 (-1+\nu)^2 + 8(1+\nu)))))
\end{aligned}
\tag{3-56}
$$

$$
\begin{aligned}
b_n = {} & (b^{-1+n}R_\zeta^{-n}(a^{2(1+n)}(a^{2n}b^2(-2+n)(-1+\nu)(3+\nu)+b^{2n}(-b^2(-2+n+n^2)(-1\\
& +\nu)^2+a^2(n^2(-1+\nu)^2+8(1+\nu))))+a^{2n}n(-1+\nu)(b^{2n}(-a^2(1+n)+b^2(2\\
& +n))(-1+\nu)-a^{2(1+n)}(3+\nu))R_\zeta^2+R_\zeta^{2n}(-a^2b^{2n}(-1+\nu)(3+\nu)(b^2(2\\
& +n)-nR_\zeta^2)+a^{2n}(a^2(-b^2(-2+n)(1+n)(-1+\nu)^2+a^2(n^2(-1+\nu)^2\\
& +8(1+\nu)))-(-b^2(-2+n)+a^2(-1+n))n(-1+\nu)^2R_\zeta^2))))\sin n\theta_\zeta\\
& /(2\pi(-a^{2+4n}b^2(-1+\nu)(3+\nu)-a^2b^{2+4n}(-1+\nu)(3+\nu)+a^{2n}b^{2n}(b^4n^2(-1\\
& +\nu)^2-2a^2b^2(-1+n^2)(-1+\nu)^2+a^4(n^2(-1+\nu)^2+8(1+\nu)))))
\end{aligned}
\tag{3-57}
$$

$$
\begin{aligned}
\overline{b}_n = {} & -(b^nR_\zeta^{-n}(a^{2(1+n)}(a^{2n}b^2n(-1+\nu)(3+\nu)+b^{2n}(b^2(-1+n)n(-1+\nu)^2\\
& -a^2(n^2(-1+\nu)^2+8(1+\nu))))+a^{2n}n(-1+\nu)(b^{2n}(-b^2n+a^2(1+n))\\
& (-1+\nu)-a^{2(1+n)}(3+\nu))R_\zeta^2+R_\zeta^{2n}(a^2b^{2n}n(-1+\nu)(3+\nu)(b^2-R_\zeta^2)+a^{2n}(a^2\\
& (-b^2n(1+n)(-1+\nu)^2+a^2(n^2(-1+\nu)^2+8(1+\nu)))-n(a^2(-1+n)\\
& -b^2n)(-1+\nu)^2R_\zeta^2))))\sin n\theta_\zeta/(2n\pi(-a^{2+4n}b^2(-1+\nu)(3+\nu)\\
& -a^2b^{2+4n}(-1+\nu)(3+\nu)+a^{2n}b^{2n}(b^4n^2(-1+\nu)^2-2a^2b^2(-1+n^2)\\
& (-1+\nu)^2+a^4(n^2(-1+\nu)^2+8(1+\nu)))))
\end{aligned}
\tag{3-58}
$$

$$
\begin{aligned}
q_n = {} & (a^{1+n}R_\zeta^{-n}(b^{2(1+n)}(-1+n)(-a^2b^{2n}(-4+n(-1+\nu))\\
& +a^{2n}(a^2(1+n)(4+n(-1+\nu))-b^2n^2(-1+\nu)))+b^{2n}n(1+n)(b^{2(1+n)}\\
& (-1+\nu)+a^{2n}(b^2(-1+n)(-1+\nu)+a^2(-4+n-n\nu)))R_\zeta^2\\
& +R_\zeta^{2n}(b^2(1+n)(a^{2(1+n)}(4+n(-1+\nu))+b^{2n}(a^2(-1+n)(-4+n(-1+\nu))\\
& -b^2n^2(-1+\nu)))+(-1+n)n(-a^{2n}b^2(-1+\nu)+b^{2n}(b^2(1+n)(-1+\nu)\\
& +a^2(4+n-n\nu)))R_\zeta^2)))\sin n\theta_\zeta/(2(-1+n)n(1+n)\pi(-a^{2+4n}b^2(-1+\nu)\\
& (3+\nu)-a^2b^{2+4n}(-1+\nu)(3+\nu)+a^{2n}b^{2n}(b^4n^2(-1+\nu)^2-2a^2b^2(-1+n^2)\\
& (-1+\nu)^2+a^4(n^2(-1+\nu)^2+8(1+\nu)))))
\end{aligned}
\tag{3-59}
$$

$$
\begin{aligned}
\overline{q}_n = {} & (a^{2+n}R_\zeta^{-n}(b^{2(1+n)}(-1+n)(a^2b^{2n}(2-n+(2+n)\nu)\\
& +a^{2n}(-b^2n^2(-1+\nu)+a^2(1+n)(n(-1+\nu)-2(1+\nu))))\\
& +b^{2n}n(1+n)(-b^{2(1+n)}(-1+\nu)+a^{2n}(b^2(-1+n)(-1+\nu)\\
& +a^2(2+n+2\nu-n\nu)))R_\zeta^2+R_\zeta^{2n}(b^2\left(1+n\right)(a^{2(1+n)}(n(-1+\nu)\\
& -2(1+\nu))+b^{2n}(b^2n^2(-1+\nu)-a^2(-1+n)(2-n+(2+n)\nu)))\\
& +(-1+n)n(-a^{2n}b^2(-1+\nu)+b^{2n}(-b^2(1+n)(-1+\nu)+a^2(2-n\\
& +(2+n)\nu)))R_\zeta^2)))\sin n\theta_\zeta/(2(1-n)n^2(1+n)\pi(-a^{2+4n}b^2(-1+\nu)(3+\nu)\\
& -a^2b^{2+4n}(-1+\nu)(3+\nu)+a^{2n}b^{2n}(b^4n^2(-1+\nu)^2-2a^2b^2(-1+n^2)\\
& (-1+\nu)^2+a^4(n^2(-1+\nu)^2+8(1+\nu)))))
\end{aligned}
\tag{3-60}
$$

where $n=2,3,4\cdots$. By substituting all the boundary densities into the integral representation for the domain point, we have the series-form Green's function as shown below:

$$
\begin{aligned}
8\pi G(x,\zeta) &= -2\pi b\left[\rho^2\left(1+\ln b\right)+b^2\ln b\right]a_0+2\pi b\left[\frac{\rho^2}{b}+b\left(1+2\ln b\right)\right]\overline{a_0}-2\pi a\left[2\left(1+\nu\right)\left(1+\ln\rho\right)\right]p_0\\
&+\left[b\rho\left(1+2\ln b\right)+\frac{1}{2}\frac{\rho^3}{b}\right]\pi b\left(a_1\cos\phi+b_1\sin\phi\right)-\left[\rho\left(3+2\ln b\right)-\frac{1}{2}\frac{\rho^3}{b^2}\right]\pi b\left(\overline{a_1}\cos\phi+\overline{b_1}\sin\phi\right)\\
&+\left[\left(\nu+3\right)\frac{a}{\rho}\right]\pi a\left(p_1\cos\phi+q_1\sin\phi\right)+\left(-3-\nu\right)\frac{1}{\rho}\pi a\left(\overline{p_1}\cos\phi+\overline{q_1}\sin\phi\right)\\
&+\sum_{m=2}^{\infty}\left[\frac{1}{m\left(m+1\right)}\frac{\rho^{m+2}}{b^m}-\frac{1}{m\left(m-1\right)}\frac{\rho^m}{b^{m-2}}\right]\pi b\left(a_m\cos m\phi+b_m\sin m\phi\right)\\
&+\sum_{m=2}^{\infty}\left[\frac{1}{m+1}\frac{\rho^{m+2}}{b^{m+1}}-\frac{m-2}{m\left(m-1\right)}\frac{\rho^m}{b^{m-1}}\right]\pi b\left(\overline{a_m}\cos m\phi+\overline{b_m}\sin m\phi\right)\\
&-\sum_{m=2}^{\infty}\left[\frac{m\left(\nu-1\right)-2\left(\nu+1\right)}{m}\frac{a^m}{\rho^m}+\left(1-\nu\right)\frac{a^{m-2}}{\rho^{m-2}}\right]\pi a\left(p_m\cos m\phi+q_m\sin m\phi\right)\\
&+\sum_{m=2}^{\infty}\left[\left(m\left(1-\nu\right)-4\right)\frac{a^{m-1}}{\rho^m}-m\left(1-\nu\right)\frac{a^{m-3}}{\rho^{m-2}}\right]\pi a\left(\overline{p_m}\cos m\phi+\overline{q_m}\sin m\phi\right)\\
&+U(\zeta,x)\quad ,a\le\rho\le b,
\end{aligned}
\tag{3-61}
$$

If we expand the $U(\zeta,x)$ function, we have

$$
\begin{aligned}
8\pi G(x,\zeta) &= -2\pi b\left[\rho^2\left(1+\ln b\right)+b^2\ln b\right]a_0+2\pi b\left[\frac{\rho^2}{b}+b\left(1+2\ln b\right)\right]\overline{a_0}-2\pi a\left[2\left(1+\nu\right)\left(1+\ln\rho\right)\right]p_0\\
&+R_\zeta{}^2\left(1+\ln\rho\right)+\rho^2\ln\rho\\
&+\left[b\rho\left(1+2\ln b\right)+\frac{1}{2}\frac{\rho^3}{b}\right]\pi b\left(a_1\cos\phi+b_1\sin\phi\right)-\left[\rho\left(3+2\ln b\right)-\frac{1}{2}\frac{\rho^3}{b^2}\right]\pi b\left(\overline{a_1}\cos\phi+\overline{b_1}\sin\phi\right)\\
&+\left[\left(\nu+3\right)\frac{a}{\rho}\right]\pi a\left(p_1\cos\phi+q_1\sin\phi\right)+\left(-3-\nu\right)\frac{1}{\rho}\pi a\left(\overline{p_1}\cos\phi+\overline{q_1}\sin\phi\right)\\
&-\left[\rho R_\zeta\left(1+2\ln\rho\right)+\frac{1}{2}\frac{R_\zeta{}^3}{\rho}\right]\cos\left(\theta_s-\phi\right)\\
&+\sum_{m=2}^{\infty}\left[\frac{1}{m\left(m+1\right)}\frac{\rho^{m+2}}{b^m}-\frac{1}{m\left(m-1\right)}\frac{\rho^m}{b^{m-2}}\right]\pi b\left(a_m\cos m\phi+b_m\sin m\phi\right)\\
&+\sum_{m=2}^{\infty}\left[\frac{1}{m+1}\frac{\rho^{m+2}}{b^{m+1}}-\frac{m-2}{m\left(m-1\right)}\frac{\rho^m}{b^{m-1}}\right]\pi b\left(\overline{a_m}\cos m\phi+\overline{b_m}\sin m\phi\right)\\
&-\sum_{m=2}^{\infty}\left[\frac{m\left(\nu-1\right)-2\left(\nu+1\right)}{m}\frac{a^m}{\rho^m}+\left(1-\nu\right)\frac{a^{m-2}}{\rho^{m-2}}\right]\pi a\left(p_m\cos m\phi+q_m\sin m\phi\right)\\
&+\sum_{m=2}^{\infty}\left[\left(m\left(1-\nu\right)-4\right)\frac{a^{m-1}}{\rho^m}-m\left(1-\nu\right)\frac{a^{m-3}}{\rho^{m-2}}\right]\pi a\left(\overline{p_m}\cos m\phi+\overline{q_m}\sin m\phi\right)\\
&-\sum_{m=2}^{\infty}\left[\frac{1}{m\left(m+1\right)}\frac{R_\zeta{}^{m+2}}{\rho^m}-\frac{1}{m\left(m-1\right)}\frac{R_\zeta{}^m}{\rho^{m-2}}\right]\cos m\left(\theta_s-\phi\right)\quad ,R_\zeta\le\rho\le b,
\end{aligned}
\tag{3-62}
$$

$$
\begin{aligned}
8\pi G(x,\zeta) = & -2\pi b\left[\rho^2\left(1+\ln b\right)+b^2\ln b\right]a_0+2\pi b\left[\frac{\rho^2}{b}+b\left(1+2\ln b\right)\right]\overline{a_0}-2\pi a\left[2\left(1+\nu\right)\left(1+\ln\rho\right)\right]p_0 \\
& +\rho^2\left(1+\ln R_\zeta\right)+{R_\zeta}^2\ln R_\zeta \\
& +\left[b\rho\left(1+2\ln b\right)+\frac{1}{2}\frac{\rho^3}{b}\right]\pi b\left(a_1\cos\phi+b_1\sin\phi\right)-\left[\rho\left(3+2\ln b\right)-\frac{1}{2}\frac{\rho^3}{b^2}\right]\pi b\left(\overline{a_1}\cos\phi+\overline{b_1}\sin\phi\right) \\
& +\left[\left(\nu+3\right)\frac{a}{\rho}\right]\pi a\left(p_1\cos\phi+q_1\sin\phi\right)+\left(-3-\nu\right)\frac{1}{\rho}\pi a\left(\overline{p_1}\cos\phi+\overline{q_1}\sin\phi\right) \\
& -\left[R_\zeta\rho\left(1+2\ln R_\zeta\right)+\frac{1}{2}\frac{\rho^3}{R_\zeta}\right]\cos\left(\theta_\zeta-\phi\right) \\
& +\sum_{m=2}^{\infty}\left[\frac{1}{m\left(m+1\right)}\frac{\rho^{m+2}}{b^m}-\frac{1}{m\left(m-1\right)}\frac{\rho^m}{b^{m-2}}\right]\pi b\left(a_m\cos m\phi+b_m\sin m\phi\right) \\
& +\sum_{m=2}^{\infty}\left[\frac{1}{m+1}\frac{\rho^{m+2}}{b^{m+1}}-\frac{m-2}{m\left(m-1\right)}\frac{\rho^m}{b^{m-1}}\right]\pi b\left(\overline{a_m}\cos m\phi+\overline{b_m}\sin m\phi\right) \\
& -\sum_{m=2}^{\infty}\left[\frac{m\left(\nu-1\right)-2\left(\nu+1\right)}{m}\frac{a^m}{\rho^m}+\left(1-\nu\right)\frac{a^{m-2}}{\rho^{m-2}}\right]\pi a\left(p_m\cos m\phi+q_m\sin m\phi\right) \\
& +\sum_{m=2}^{\infty}\left[\left(m\left(1-\nu\right)-4\right)\frac{a^{m-1}}{\rho^m}-m\left(1-\nu\right)\frac{a^{m-3}}{\rho^{m-2}}\right]\pi a\left(\overline{p_m}\cos m\phi+\overline{q_m}\sin m\phi\right) \\
& -\sum_{m=2}^{\infty}\left[\frac{1}{m\left(m+1\right)}\frac{\rho^{m+2}}{{R_\zeta}^m}-\frac{1}{m\left(m-1\right)}\frac{\rho^m}{{R_\zeta}^{m-2}}\right]\cos m\left(\theta_\zeta-\phi\right)\quad,a\le\rho\le R_\zeta,
\end{aligned}
\tag{3-63}
$$

where a_n, b_n, $\overline{a}_n$, $\overline{b}_n$, p_n, q_n, $\overline{p}_n$ and $\overline{q}_n$ ($n=0,1,2\cdots$) are shown in Eqs. (3-41)~(3-60).

3.4 Discussions on Adewale's results

In the Adewale's paper [1], the Green's function of clamped-free annular plate was also solved. The problem domain was divided into two parts by the cylindrical section where a concentrated load was applied [1]. The author used the Trefftz method to construct the homogeneous solution

$$
u=\sum_{m=0}^{\infty}R_m\left(r\right)\cos m\theta\,, \tag{3-64}
$$

in each part. By substituting Eq. (3-64) into the governing equation, the author could determine $R_m(r)$. Mathematically speaking, the series in Eq. (3-64) can be seen as the summation of Trefftz bases. Chen et al. have found that the base of the Trefftz method is imbedded in the degenerate kernel [22]. To simulate the concentrated force, a ring-distributed force using the Fourier series was used. Then, the author utilized two B.C.s in each part, two continuity and two equilibrium conditions on the interface to determine the eight unknown coefficients. Variation of deflection coefficients, radial moment coefficients and shear coefficients along radial positions and angles were presented. However, some results are misleading. To investigate these inconsistencies, both null-field integral formulation and FEM using the ABAQUS are adopted to revisit this problem. In addition, two unclear issues in [1] are discussed. One is the simulation of concentrated load and the other is the operator of shear

force.

3.4.1 Concentrated Load

In Adewale's paper [1], the author expanded the concentrated load to the Fourier series,

$$P \approx P\left[\frac{1}{2}+\sum_{k=1}^{\infty}\frac{2\sin\frac{(2k-1)\pi}{2}}{(2k-1)\pi}\cos(2k-1)\theta\right], 0\le\theta\le\frac{\pi}{2} \tag{3-65}$$

By summing the series of Eq. (3-65), the result converges to one as shown in Fig. 3-3, which does not show the behavior of the Dirac-Delta function. The author seems to improperly transform the concentrated load to a ring-distributed one. Is it reasonable ? If this load is distributed along angle from 0 to $\pi/2$, the results of deflection coefficient in Fig. 5 of [1] would be untrue. In addition, the Dirac-Delta function $\delta(x)$ should satisfy the identity as follows

$$\int_{-\infty}^{\infty}\delta(x)dx=1 \tag{3-66}$$

Equation (3-65) can not satisfy the Eq. (3-66) such that the strength of the concentrated loading is one.

3.4.2 Definition of shear force

For the clamped-free annular plate problem as shown in Fig. 3-2, the moment and the shear force on the inner circle are zero for the free boundary on the inner circle. Therefore the author obtained the moment and shear force

$$\left(\frac{\partial^2}{\partial r^2}+\nu\left(\frac{1}{r}\frac{\partial}{\partial r}-\frac{m^2}{r^2}\frac{\partial}{\partial r}\right)\right)R_m(r)\Big|_{r=a}=0, \text{ moment free,} \tag{3-67}$$

$$\left(\frac{\partial^3}{\partial r^3}-\frac{1}{r^2}\frac{\partial}{\partial r}+\frac{1}{r}\frac{\partial^2}{\partial r^2}-\frac{m^2}{r^2}\frac{\partial}{\partial r}\right)R_m(r)\Big|_{r=a}=0, \text{ shear force free,} \tag{3-68}$$

respectively, where ν is the Poisson ratio. Equation (3-68) is unreasonable since it dose not involve the Poisson ratio. According to the displacement of Eq. (3-64) and the definition of moment and shear force in the Szilard's book [51], the moment and shear can be derived as

$$\frac{\partial^2 R_m(r)}{\partial r^2}+\nu\left(\frac{1}{r}\frac{\partial R_m(r)}{\partial r}-\frac{m^2}{r^2}R_m(r)\right) \text{ for moment} \tag{3-69}$$

$$\frac{\partial^3 R_m(r)}{\partial r^3}-\frac{1}{r^2}\frac{\partial R_m(r)}{\partial r}+\frac{1}{r}\frac{\partial^2 R_{m(r)}}{\partial r^2}+\frac{2m^2}{r^3}R_m(r)$$
$$-\frac{m^2}{r^2}\frac{\partial R_m(r)}{\partial r}+(1-\nu)\left[\frac{m^2}{r^3}R_m(r)-\frac{m^2}{r^2}\frac{\partial R_m(r)}{\partial r}\right] \quad \text{for shear force} \tag{3-70}$$

In the literature, many articles had reported the definitions of the moment and shear force, *e.g.* Szilard [51], Leissa [31], Adewale [1] and Chen et al. [21]. We summarize the moment and shear force in Table 3-3. After careful comparisons, Adewale's shear force of Eq. (3-68) differs from the others and consequently this difference may cause inconsistent results. All the definitions are found to be the same except the shear force in [1].

3.4.3 Results and discussions

In order to verify the accuracy of the Adewale's results, two alternatives, null-field approach and FEM using ABAQUS, are employed to revisit the annular problem. For the clamped-free boundary condition, Figs. 3-4 and 3-5 show the potential contours of Green's function by using FEM (ABAQUS) and the present method, respectively. Good agreement is obtained between our analytical solution and FEM result although Adewale [1] did not provide the displacement contour of his analytical solution. To compare with the available results of [1], Figs. 3-6~3-8 show the variation of deflection coefficients, moment coefficients and shear force coefficients along radial positions for different values of inner radius. It is also found that FEM results match well with our solutions but deviates from the analytical solution of [1]. The larger the inner radius is, the less the deflection coefficient of free edge is as shown in Fig. 3-6. Figure 3-8(a) shows the smooth discontinuity of shear force coefficients due to the Dirac-Delta function. The jump of shear force in Fig. 3-8(a) is not obvious, while Figs. 3-8(b) and (c) have a discontinuity at the position of the concentrated loading. According to the equilibrium of force, the shear force can be considered as the reaction force on the outer edge which direction should be inverse of the applied load. But in [1], the direction of shear force on the outer edge is the same as the applied concentrated load as shown in Fig. 3-8(a), which is unreasonable. Furthermore, the shear force in [1] is always positive, which implies that the moment will always increase according to the relation of shear force and moment. But the tendency of moment in [1] is not the case, which may be wrong. The above misleading phenomena do not happen in our results and FEM data. Variation of deflection coefficients versus the radial angle for different values of inner radius is shown in Fig. 3-9. Also, FEM data agree well with our analytical formula but deviates from the Adewale's solution. To verify the accuracy of the Adewale's results and examine the response of the clamped-free annular plate subjected to a concentrated load, the null-field integral formulation was

employed to solve this problem. The transverse displacement, moment and shear force along the radial positions and angles for different inner radii were determined by using the present method in comparison with the FEM results using the ABAQUS. Good agreements between our analytical results and those of ABAQUS are made but deviating the Adewale's data. The outcome of the Adewale's results remains uncertain.

3.5 Illustrative examples

Case 1: Green's function of the biharmonic equation for the circular plate problem

A circular plate subjected to a concentrated load as shown in Fig. 3-10 has been solved by Szilard [51] and Melnikov [42]. The load is at the center of the plate in the Szilard's solution. Here, we resolve the same problem to obtain an analytical solution, and then verify the validity of our approach after comparing with Szilard and Melnikov solutions. Appendix 2 shows the equivalence among the Szilard, Melnikov and present solutions. The displacement contours of a circular plate subjected to a concentrated load which is located on the center of the plate are plotted in Fig. 3-11. Good agreement is obtained. Also, two displacement contours with the source at different directions and radial positions are plotted by using the Melnikov's solution and the present analytical solution as shown in Figs 3-12~3-15. Good agreement is made.

Case 2: Green's function of the biharmonic equation for the clamped-free annular plate problem

The radial slope, normal moment and shear force contours as shown in Figs 3-16~3-18. For the clamped-free annular plate problem, the moment and the shear force on the inner circle are zero for the free boundary, and the displacement and the slope on the outer circle are zero for the clamped boundary. Good results are obtained. But we do not show the validity with any figures and just offer an indication. Next, we present different cases.

Case 3: Green's function of the biharmonic equation for the clamped-clamped annular plate problem

For the clamped-clamped annular plate problem, the displacement and the slope on the outer and inner circles are both zero for the clamped boundary. Figures 3-19 and 3-20 are the displacement contours by using the present method and the ABAQUS program. Good agreement is obtained.

Case 4: Green's function of the biharmonic equation for the free-simply supported annular plate problem with circular

For the free-simply supported annular plate problem, the moment and the shear force on the inner circle are zero for the free boundary and the displacement and the moment on the outer circle are zero for the simply supported boundary. Figures 3-21 and 3-22 are the displacement contours using the present method and the ABAQUS program. Good agreement is obtained.

3.6 Concluding remarks

For plate problems with circular boundaries, an analytical approach by using degenerate kernels, null-field integral equation and Fourier series was obtained. The main advantage of the present method over BEM is that all the improper integrals are avoided when degenerate kernels are used. The potential on the boundary can be determined from both sides (interior and exterior). Also, discretzation of boundaries are not required. Once the Fourier coefficients of the unknown boundary densities were determined, the displacement, slope, normal moment and effective shear force of the circular plate can be easily determined by substituting the boundary densities into the boundary integral equations for the domain point. Not only the circular plate but also the annular problems have been solved easily and effectively by using the present method in comparison with available exact solution and FEM results. The present method can be applied to plate containing any number of circular holes.

Table 3-1 Comparisons of the conventional BIEM and the present method

Conventional BIEM

Domain point

$$8\pi G(x,\zeta) = -\int_B U(s,x)K_{v,s}[G(s,\zeta)]dB(s) + \int_B \Theta(s,x)K_{m,s}[G(s,\zeta)]dB(s)$$
$$-\int_B M(s,x)K_{\theta,s}[G(s,\zeta)]dB(s) + \int_B V(s,x)G(s,\zeta)dB(s) + U(\zeta,x), \quad x \in \Omega$$
$$8\pi K_{\theta,x}[G(x,\zeta)] = -\int_B U_\theta(s,x)K_{v,s}[G(s,\zeta)]dB(s) + \int_B \Theta_\theta(s,x)K_{m,s}[G(s,\zeta)]dB(s)$$
$$-\int_B M_\theta(s,x)K_{\theta,s}[G(s,\zeta)]dB(s) + \int_B V_\theta(s,x)G(s,\zeta)dB(s) + U_\theta(\zeta,x), \quad x \in \Omega$$
$$8\pi K_{m,x}[G(x,\zeta)] = -\int_B U_m(s,x)K_{v,s}[G(s,\zeta)]dB(s) + \int_B \Theta_m(s,x)K_{m,s}[G(s,\zeta)]dB(s)$$
$$-\int_B M_m(s,x)K_{\theta,s}[G(s,\zeta)]dB(s) + \int_B V_m(s,x)G(s,\zeta)dB(s) + U_m(\zeta,x), \quad x \in \Omega$$
$$8\pi K_{v,x}[G(x,\zeta)] = -\int_B U_v(s,x)K_{v,s}[G(s,\zeta)]dB(s) + \int_B \Theta_v(s,x)K_{m,s}[G(s,\zeta)]dB(s)$$
$$-\int_B M_v(s,x)K_{\theta,s}[G(s,\zeta)]dB(s) + \int_B V_v(s,x)G(s,\zeta)dB(s) + U_m(\zeta,x), \quad x \in \Omega$$

Boundary point

$$4\pi G(x,\zeta) = -R.P.V.\int_B U(s,x)K_{v,s}[G(s,\zeta)]dB(s) + R.P.V.\int_B \Theta(s,x)K_{m,s}[G(s,\zeta)]dB(s)$$
$$-R.P.V.\int_B M(s,x)K_{\theta,s}[G(s,\zeta)]dB(s) + C.P.V\int_B V(s,x)G(s,\zeta)dB(s) + U(\zeta,x), \quad x \in B$$
$$4\pi K_{\theta,x}[G(x,\zeta)] = -R.P.V.\int_B U_\theta(s,x)K_{v,s}[G(s,\zeta)]dB(s) + R.P.V.\int_B \Theta_\theta(s,x)K_{m,s}[G(s,\zeta)]dB(s)$$
$$-C.P.V.\int_B M_\theta(s,x)K_{\theta,s}[G(s,\zeta)]dB(s) + H.P.V.\int_B V_\theta(s,x)G(s,\zeta)dB(s) + U_\theta(\zeta,x), \quad x \in B$$
$$4\pi K_{m,x}[G(x,\zeta)] = -R.P.V.\int_B U_m(s,x)K_{v,s}[G(s,\zeta)]dB(s) + C.P.V.\int_B \Theta_m(s,x)K_{m,s}[G(s,\zeta)]dB(s)$$
$$-H.P.V.\int_B M_m(s,x)K_{\theta,s}[G(s,\zeta)]dB(s) + F.P.\int_B V_m(s,x)G(s,\zeta)dB(s) + U_m(\zeta,x), \quad x \in B$$
$$4\pi K_{v,x}[G(x,\zeta)] = -C.P.V.\int_B U_v(s,x)K_{v,s}[G(s,\zeta)]dB(s) + H.P.V.\int_B \Theta_v(s,x)K_{m,s}[G(s,\zeta)]dB(s)$$
$$-F.P.\int_B M_v(s,x)K_{\theta,s}[G(s,\zeta)]dB(s) + F.P.\int_B V_v(s,x)G(s,\zeta)dB(s) + U_m(\zeta,x), \quad x \in B$$

Null-field point

$$0 = -\int_B U(s,x)K_{v,s}[G(s,\zeta)]dB(s) + \int_B \Theta(s,x)K_{m,s}[G(s,\zeta)]dB(s)$$
$$-\int_B M(s,x)K_{\theta,s}[G(s,\zeta)]dB(s) + \int_B V(s,x)G(s,\zeta)dB(s) + U(\zeta,x), \quad x \in \Omega^c$$
$$0 = -\int_B U_\theta(s,x)K_{v,s}[G(s,\zeta)]dB(s) + \int_B \Theta_\theta(s,x)K_{m,s}[G(s,\zeta)]dB(s)$$
$$-\int_B M_\theta(s,x)K_{\theta,s}[G(s,\zeta)]dB(s) + \int_B V_\theta(s,x)G(s,\zeta)dB(s) + U_\theta(\zeta,x), \quad x \in \Omega^c$$
$$0 = -\int_B U_m(s,x)K_{v,s}[G(s,\zeta)]dB(s) + \int_B \Theta_m(s,x)K_{m,s}[G(s,\zeta)]dB(s)$$
$$-\int_B M_m(s,x)K_{\theta,s}[G(s,\zeta)]dB(s) + \int_B V_m(s,x)G(s,\zeta)dB(s) + U_m(\zeta,x), \quad x \in \Omega^c$$
$$0 = -\int_B U_v(s,x)K_{v,s}[G(s,\zeta)]dB(s) + \int_B \Theta_v(s,x)K_{m,s}[G(s,\zeta)]dB(s)$$
$$-\int_B M_v(s,x)K_{\theta,s}[G(s,\zeta)]dB(s) + \int_B V_v(s,x)G(s,\zeta)dB(s) + U_m(\zeta,x), \quad x \in \Omega^c$$

Continue

Present method	
Domain point including boundary	$8\pi G(x,\zeta) = -\int_B U(s,x)K_{v,s}[G(s,\zeta)]dB(s) + \int_B \Theta(s,x)K_{m,s}[G(s,\zeta)]dB(s)$ $-\int_B M(s,x)K_{\theta,s}[G(s,\zeta)]dB(s) + \int_B V(s,x)G(s,\zeta)dB(s) + U(\zeta,x), \quad x \in \Omega \cup B$
	$8\pi K_{\theta,x}[G(x,\zeta)] = -\int_B U_\theta(s,x)K_{v,s}[G(s,\zeta)]dB(s) + \int_B \Theta_\theta(s,x)K_{m,s}[G(s,\zeta)]dB(s)$ $-\int_B M_\theta(s,x)K_{\theta,s}[G(s,\zeta)]dB(s) + \int_B V_\theta(s,x)G(s,\zeta)dB(s) + U_\theta(\zeta,x), \quad x \in \Omega \cup B$
	$8\pi K_{m,x}[G(x,\zeta)] = -\int_B U_m(s,x)K_{v,s}[G(s,\zeta)]dB(s) + \int_B \Theta_m(s,x)K_{m,s}[G(s,\zeta)]dB(s)$ $-\int_B M_m(s,x)K_{\theta,s}[G(s,\zeta)]dB(s) + \int_B V_m(s,x)G(s,\zeta)dB(s) + U_m(\zeta,x), \quad x \in \Omega \cup B$
	$8\pi K_{v,x}[G(x,\zeta)] = -\int_B U_v(s,x)K_{v,s}[G(s,\zeta)]dB(s) + \int_B \Theta_v(s,x)K_{m,s}[G(s,\zeta)]dB(s)$ $-\int_B M_v(s,x)K_{\theta,s}[G(s,\zeta)]dB(s) + \int_B V_v(s,x)G(s,\zeta)dB(s) + U_m(\zeta,x), \quad x \in \Omega \cup B$
Null-field point including boundary	$0 = -\int_B U(s,x)K_{v,s}[G(s,\zeta)]dB(s) + \int_B \Theta(s,x)K_{m,s}[G(s,\zeta)]dB(s)$ $-\int_B M(s,x)K_{\theta,s}[G(s,\zeta)]dB(s) + \int_B V(s,x)G(s,\zeta)dB(s) + U(\zeta,x), \quad x \in \Omega^c \cup B$
	$0 = -\int_B U_\theta(s,x)K_{v,s}[G(s,\zeta)]dB(s) + \int_B \Theta_\theta(s,x)K_{m,s}[G(s,\zeta)]dB(s)$ $-\int_B M_\theta(s,x)K_{\theta,s}[G(s,\zeta)]dB(s) + \int_B V_\theta(s,x)G(s,\zeta)dB(s) + U_\theta(\zeta,x), \quad x \in \Omega^c \cup B$
	$0 = -\int_B U_m(s,x)K_{v,s}[G(s,\zeta)]dB(s) + \int_B \Theta_m(s,x)K_{m,s}[G(s,\zeta)]dB(s)$ $-\int_B M_m(s,x)K_{\theta,s}[G(s,\zeta)]dB(s) + \int_B V_m(s,x)G(s,\zeta)dB(s) + U_m(\zeta,x), \quad x \in \Omega^c \cup B$
	$0 = -\int_B U_v(s,x)K_{v,s}[G(s,\zeta)]dB(s) + \int_B \Theta_v(s,x)K_{m,s}[G(s,\zeta)]dB(s)$ $-\int_B M_v(s,x)K_{\theta,s}[G(s,\zeta)]dB(s) + \int_B V_v(s,x)G(s,\zeta)dB(s) + U_m(\zeta,x), \quad x \in \Omega^c \cup B$

where CPV, RPV, HPV, FP, $K_{\theta,s}[\cdot]$, $K_{m,s}[\cdot]$ and $K_{v,s}[\cdot]$ are the Cauchy principal value, Riemann principal value, Hadamard principal value, finite part, slope operator, normal moment operator and effective shear operator, respectively. It is noted that the kernels in the present method should be properly expanded in terms of interior and exterior expressions of degenerate kernels. Mathematically speaking, our domain is a closed set ($D \cup B$) instead of the open set (D only) of conventional method.

Table 3-2 Influence coefficients for the singularity distribution on the circular boundary

		Interior	Exterior
$U(s,x)$	Degenerate kernel	$U^i(R,\theta;\rho,\phi)=\rho^2(1+\ln R)+R^2\ln R$ $-\left[R\rho(1+2\ln R)+\frac{1}{2}\frac{\rho^3}{R}\right]\cos(\theta-\phi)$ $-\sum_{m=2}^{\infty}\left[\frac{1}{m(m+1)}\frac{\rho^{m+2}}{R^m}-\frac{1}{m(m-1)}\frac{\rho^m}{R^{m-2}}\right]\cos m(\theta-\phi),\ R>\rho$	$U^e(R,\theta;\rho,\phi)=R^2(1+\ln\rho)+\rho^2\ln\rho$ $-\left[\rho R(1+2\ln\rho)+\frac{1}{2}\frac{R^3}{\rho}\right]\cos(\theta-\phi)$ $-\sum_{m=2}^{\infty}\left[\frac{1}{m(m+1)}\frac{R^{m+2}}{\rho^m}-\frac{1}{m(m-1)}\frac{R^m}{\rho^{m-2}}\right]\cos m(\theta-\phi),\ \rho>R$
	Orthogonal process	$\int_0^{2\pi}[U^i][1]Rd\theta=2\pi R(\rho^2(1+\ln R)+R^2\ln R),\ R>\rho$ $\int_0^{2\pi}[U^i][\cos\theta]Rd\theta=-\pi R(R\rho(1+2\ln R)+\frac{1}{2}\frac{\rho^3}{R})\cos\phi,\ R>\rho$ $\int_0^{2\pi}[U^i][\sin\theta]Rd\theta=-\pi R(R\rho(1+2\ln R)+\frac{1}{2}\frac{\rho^3}{R})\sin\phi,\ R>\rho$ $\int_0^{2\pi}[U^i][\cos n\theta]Rd\theta=-\pi R(\frac{1}{n(n+1)}\frac{\rho^{n+2}}{R^n}-\frac{1}{n(n-1)}\frac{\rho^n}{R^{n-2}})\cos n\phi,\ R>\rho$ $\int_0^{2\pi}[U^i][\sin n\theta]Rd\theta=-\pi R(\frac{1}{n(n+1)}\frac{\rho^{n+2}}{R^n}-\frac{1}{n(n-1)}\frac{\rho^n}{R^{n-2}})\sin n\phi,\ R>\rho$	$\int_0^{2\pi}[U^e][1]Rd\theta=2\pi R(R^2(1+\ln\rho)+\rho^2\ln\rho),\ \rho>R$ $\int_0^{2\pi}[U^e][\cos\theta]Rd\theta=-\pi R(\rho R(1+2\ln\rho)+\frac{1}{2}\frac{R^3}{\rho})\cos\phi,\ \rho>R$ $\int_0^{2\pi}[U^e][\sin\theta]Rd\theta=-\pi R(\rho R(1+2\ln\rho)+\frac{1}{2}\frac{R^3}{\rho})\sin\phi,\ \rho>R$ $\int_0^{2\pi}[U^e][\cos n\theta]Rd\theta=-\pi R(\frac{1}{n(n+1)}\frac{R^{n+2}}{\rho^n}-\frac{1}{n(n-1)}\frac{R^n}{\rho^{n-2}})\cos n\phi,\ \rho>R$ $\int_0^{2\pi}[U^e][\sin n\theta]Rd\theta=-\pi R(\frac{1}{n(n+1)}\frac{R^{n+2}}{\rho^n}-\frac{1}{n(n-1)}\frac{R^n}{\rho^{n-2}})\sin n\phi,\ \rho>R$
	Limiting behavior across the boundary	$\lim_{\rho\to R}2\pi R(\rho^2(1+\ln R)+R^2\ln R)=2\pi R^3(1+2\ln R)$ $-\lim_{\rho\to R}\pi R(R\rho(1+2\ln R)+\frac{1}{2}\frac{\rho^3}{R})\cos\phi=-\pi R^3(\frac{3}{2}+2\ln R)\cos\phi$ $-\lim_{\rho\to R}\pi R(R\rho(1+2\ln R)+\frac{1}{2}\frac{\rho^3}{R})\sin\phi=-\pi R^3(\frac{3}{2}+2\ln R)\sin\phi$ $-\lim_{\rho\to R}\pi R(\frac{1}{n(n+1)}\frac{\rho^{n+2}}{R^n}-\frac{1}{n(n-1)}\frac{\rho^n}{R^{n-2}})\cos n\phi=\pi R^3\frac{2}{n(n^2-1)}\cos n\phi$ $-\lim_{\rho\to R}\pi R(\frac{1}{n(n+1)}\frac{\rho^{n+2}}{R^n}-\frac{1}{n(n-1)}\frac{\rho^n}{R^{n-2}})\sin n\phi=\pi R^3\frac{2}{n(n^2-1)}R\sin n\phi$	Continuous $(\rho^-\to R\leftarrow\rho^+)$	$\lim_{\rho\to R}2\pi R(R^2(1+\ln\rho)+\rho^2\ln\rho)=2\pi R^3(1+2\ln R)$ $-\lim_{\rho\to R}\pi R(\rho R(1+2\ln\rho)+\frac{1}{2}\frac{R^3}{\rho})\cos\phi=-\pi R^3(\frac{3}{2}+2\ln R)\cos\phi$ $-\lim_{\rho\to R}\pi R(\rho R(1+2\ln\rho)+\frac{1}{2}\frac{R^3}{\rho})\sin\phi=-\pi R^3(\frac{3}{2}+2\ln R)\sin\phi$ $-\lim_{\rho\to R}\pi R(\frac{1}{n(n+1)}\frac{R^{n+2}}{\rho^n}-\frac{1}{n(n-1)}\frac{R^n}{\rho^{n-2}})\cos n\phi=\pi R^3\frac{2}{n(n^2-1)}\cos n\phi$ $-\lim_{\rho\to R}\pi R(\frac{1}{n(n+1)}\frac{R^{n+2}}{\rho^n}-\frac{1}{n(n-1)}\frac{R^n}{\rho^{n-2}})\sin n\phi=\pi R^3\frac{2}{n(n^2-1)}R\sin n\phi$

Continue

$\Theta(s,x)$		Interior		Exterior
	Degenerate kernel	$\Theta^i(R,\theta;\rho,\phi)=\frac{\rho^2}{R}+R(1+2\ln R)$ $-\left[\rho(3+2\ln R)-\frac{1}{2}\frac{\rho^3}{R^2}\right]\cos(\theta-\phi)$ $+\sum_{m=2}^{\infty}\left[\frac{1}{m+1}\frac{\rho^{m+2}}{R^{m+1}}-\frac{m-2}{m(m-1)}\frac{\rho^m}{R^{m-1}}\right]\cos m(\theta-\phi),\ R>\rho$		$\Theta^e(R,\theta;\rho,\phi)=2R(1+\ln\rho)$ $-\left[\rho(1+2\ln\rho)+\frac{3}{2}\frac{R^2}{\rho}\right]\cos(\theta-\phi)$ $-\sum_{m=2}^{\infty}\left[\frac{m+2}{m(m+1)}\frac{R^{m+1}}{\rho^m}-\frac{1}{m-1}\frac{R^{m-1}}{\rho^{m-2}}\right]\cos m(\theta-\phi),\ \rho>R$
	Orthogonal process	$\int_0^{2\pi}[\Theta^i][1]Rd\theta=2\pi R(\frac{\rho^2}{R}+R(1+2\ln R)),\ R>\rho$ $\int_0^{2\pi}[\Theta^i][\cos\theta]Rd\theta=-\pi R(\rho(3+2\ln R)-\frac{1}{2}\frac{\rho^3}{R^2})\cos\phi,\ R>\rho$ $\int_0^{2\pi}[\Theta^i][\sin\theta]Rd\theta=-\pi R(\rho(3+2\ln R)-\frac{1}{2}\frac{\rho^3}{R^2})\sin\phi,\ R>\rho$ $\int_0^{2\pi}[\Theta^i][\cos n\theta]Rd\theta=\pi R(\frac{1}{n+1}\frac{\rho^{n+2}}{R^{n+1}}-\frac{n-2}{n(n-1)}\frac{\rho^n}{R^{n-1}})\cos n\phi,\ R>\rho$ $\int_0^{2\pi}[\Theta^i][\sin n\theta]Rd\theta=\pi R(\frac{1}{n+1}\frac{\rho^{n+2}}{R^{n+1}}-\frac{n-2}{n(n-1)}\frac{\rho^n}{R^{n-1}})\sin n\phi,\ R>\rho$		$\int_0^{2\pi}[\Theta^e][1]Rd\theta=2\pi R(2R(1+\ln\rho)),\ \rho>R$ $\int_0^{2\pi}[\Theta^e][\cos\theta]Rd\theta=-\pi R(\rho(1+2\ln\rho)+\frac{3}{2}\frac{R^2}{\rho})\cos\phi,\ \rho>R$ $\int_0^{2\pi}[\Theta^e][\sin\theta]Rd\theta=-\pi R(\rho(1+2\ln\rho)+\frac{3}{2}\frac{R^2}{\rho})\sin\phi,\ \rho>R$ $\int_0^{2\pi}[\Theta^e][\cos n\theta]Rd\theta=-\pi R(\frac{n+2}{n(n+1)}\frac{R^{n+1}}{\rho^n}-\frac{1}{n-1}\frac{R^{n-1}}{\rho^{n-2}})\cos n\phi,\ \rho>R$ $\int_0^{2\pi}[\Theta^e][\sin n\theta]Rd\theta=-\pi R(\frac{n+2}{n(n+1)}\frac{R^{n+1}}{\rho^n}-\frac{1}{n-1}\frac{R^{n-1}}{\rho^{n-2}})\sin n\phi,\ \rho>R$
	Limiting behavior across the boundary	$\lim_{\rho\to R}2\pi R(\frac{\rho^2}{R}+R(1+2\ln R))=4\pi R^2(1+\ln R)$ $-\lim_{\rho\to R}\pi R(\rho(3+2\ln R)-\frac{1}{2}\frac{\rho^3}{R^2})\cos\phi=-\pi R^2(\frac{5}{2}+2\ln R)\cos\phi$ $-\lim_{\rho\to R}\pi R(\rho(3+2\ln R)-\frac{1}{2}\frac{\rho^3}{R^2})\sin\phi=-\pi R^2(\frac{5}{2}+2\ln R)\sin\phi$ $\lim_{\rho\to R}\pi R(\frac{1}{n+1}\frac{\rho^{n+2}}{R^{n+1}}-\frac{n-2}{n(n-1)}\frac{\rho^n}{R^{n-1}})\cos n\phi=\pi R^2\frac{2}{n(n^2-1)}\cos n\phi$ $\lim_{\rho\to R}\pi R(\frac{1}{n+1}\frac{\rho^{n+2}}{R^{n+1}}-\frac{n-2}{n(n-1)}\frac{\rho^n}{R^{n-1}})\sin n\phi=\pi R^2\frac{2}{n(n^2-1)}\sin n\phi$	Continuous $(\rho^-\to R\leftarrow\rho^+)$	$\lim_{\rho\to R}2\pi R(2R(1+\ln\rho))=4\pi R^2(1+\ln R)$ $-\lim_{\rho\to R}\pi R(\rho(1+2\ln\rho)+\frac{3}{2}\frac{R^2}{\rho})\cos\phi=-\pi R^2(\frac{5}{2}+2\ln R)\cos\phi$ $-\lim_{\rho\to R}\pi R(\rho(1+2\ln\rho)+\frac{3}{2}\frac{R^2}{\rho})\sin\phi=-\pi R^2(\frac{5}{2}+2\ln R)\sin\phi$ $-\lim_{\rho\to R}\pi R(\frac{n+2}{n(n+1)}\frac{R^{n+1}}{\rho^n}-\frac{1}{n-1}\frac{R^{n-1}}{\rho^{n-2}})\cos n\phi=\pi R^2\frac{2}{n(n^2-1)}\cos n\phi$ $-\lim_{\rho\to R}\pi R(\frac{n+2}{n(n+1)}\frac{R^{n+1}}{\rho^n}-\frac{1}{n-1}\frac{R^{n-1}}{\rho^{n-2}})\sin n\phi=\pi R^2\frac{2}{n(n^2-1)}\sin n\phi$

Continue

		Interior		Exterior
$M(s,x)$	Degenerate kernel	$M^i(R,\theta;\rho,\phi)=(\nu-1)\frac{\rho^2}{R^2}+(\nu+3)+2(\nu+1)\ln R$ $-\left[(\nu+1)\frac{2\rho}{R}-(\nu-1)\frac{\rho^3}{R^3}\right]\cos(\theta-\phi)$ $-\sum_{m=2}^{\infty}\left[(\nu-1)\frac{\rho^{m+2}}{R^{m+2}}+\frac{m(1-\nu)-2(1+\nu)}{m}\frac{\rho^m}{R^m}\right]\cos m(\theta-\phi),\ R>\rho$		$M^e(R,\theta;\rho,\phi)=2(1+\nu)(1+\ln\rho)$ $-(\nu+3)\frac{R}{\rho}\cos(\theta-\phi)$ $+\sum_{m=2}^{\infty}\left[\frac{m(\nu-1)-2(\nu+1)}{m}\frac{R^m}{\rho^m}+(1-\nu)\frac{R^{m-2}}{\rho^{m-2}}\right]\cos m(\theta-\phi),\ \rho>R$
	Orthogonal process	$\int_0^{2\pi}[M^i][1]Rd\theta=2\pi R((\nu-1)\frac{\rho^2}{R^2}+(\nu+3)+2(\nu+1)\ln R),\ R>\rho$ $\int_0^{2\pi}[M^i][\cos\theta]Rd\theta=-\pi R((\nu+1)\frac{2\rho}{R}-(\nu-1)\frac{\rho^3}{R^3})\cos\phi,\ R>\rho$ $\int_0^{2\pi}[M^i][\sin\theta]Rd\theta=-\pi R((\nu+1)\frac{2\rho}{R}-(\nu-1)\frac{\rho^3}{R^3})\sin\phi,\ R>\rho$ $\int_0^{2\pi}[M^i][\cos n\theta]Rd\theta=-\pi R((\nu-1)\frac{\rho^{n+2}}{R^{n+2}}+\frac{n(1-\nu)-2(1+\nu)}{n}\frac{\rho^n}{R^n})\cos n\phi,\ R>\rho$ $\int_0^{2\pi}[M^i][\sin n\theta]Rd\theta=-\pi R((\nu-1)\frac{\rho^{n+2}}{R^{n+2}}+\frac{n(1-\nu)-2(1+\nu)}{n}\frac{\rho^n}{R^n})\sin n\phi,\ R>\rho$		$\int_0^{2\pi}[M^e][1]Rd\theta=2\pi R(2(1+\nu)(1+\ln\rho)),\ \rho>R$ $\int_0^{2\pi}[M^e][\cos\theta]Rd\theta=-\pi R((\nu+3)\frac{R}{\rho})\cos\phi,\ \rho>R$ $\int_0^{2\pi}[M^e][\sin\theta]Rd\theta=-\pi R((\nu+3)\frac{R}{\rho})\sin\phi,\ \rho>R$ $\int_0^{2\pi}[M^e][\cos n\theta]Rd\theta=\pi R(\frac{n(\nu-1)-2(\nu+1)}{n}\frac{R^n}{\rho^n}+(1-\nu)\frac{R^{n-2}}{\rho^{n-2}})\cos n\phi,\ \rho>R$ $\int_0^{2\pi}[M^e][\sin n\theta]Rd\theta=\pi R(\frac{n(\nu-1)-2(\nu+1)}{n}\frac{R^n}{\rho^n}+(1-\nu)\frac{R^{n-2}}{\rho^{n-2}})\sin n\phi,\ \rho>R$
	Limiting behavior across the boundary	$\lim_{\rho\to R}2\pi R((\nu-1)\frac{\rho^2}{R^2}+(\nu+3)+2(\nu+1)\ln R)=4\pi R(1+\nu)(1+\ln R)$ $-\lim_{\rho\to R}\pi R((\nu+1)\frac{2\rho}{R}-(\nu-1)\frac{\rho^3}{R^3})\cos\phi=-\pi R(\nu+3)\cos\phi$ $-\lim_{\rho\to R}\pi R((\nu+1)\frac{2\rho}{R}-(\nu-1)\frac{\rho^3}{R^3})\sin\phi=-\pi R(\nu+3)\sin\phi$ $-\lim_{\rho\to R}\pi R((\nu-1)\frac{\rho^{n+2}}{R^{n+2}}+\frac{n(1-\nu)-2(1+\nu)}{n}\frac{\rho^n}{R^n})\cos n\phi=\pi R\frac{2(1+\nu)}{n}\cos n\phi$ $-\lim_{\rho\to R}\pi R((\nu-1)\frac{\rho^{n+2}}{R^{n+2}}+\frac{n(1-\nu)-2(1+\nu)}{n}\frac{\rho^n}{R^n})\sin n\phi=\pi R\frac{2(1+\nu)}{n}\sin n\phi$	Continuous $(\rho^-\to R\leftarrow\rho^+)$	$\lim_{\rho\to R}2\pi R(2(1+\nu)(1+\ln\rho))=4\pi R(1+\nu)(1+\ln R)$ $-\lim_{\rho\to R}\pi R((\nu+3)\frac{R}{\rho})\cos\phi=-\pi R(\nu+3)\cos\phi$ $-\lim_{\rho\to R}\pi R((\nu+3)\frac{R}{\rho})\sin\phi=-\pi R(\nu+3)\sin\phi$ $-\lim_{\rho\to R}\pi R(\frac{n(\nu-1)-2(\nu+1)}{n}\frac{R^n}{\rho^n}+(1-\nu)\frac{R^{n-2}}{\rho^{n-2}})\cos n\phi=\pi R\frac{2(\nu+1)}{n}\cos n\phi$ $-\lim_{\rho\to R}\pi R(\frac{n(\nu-1)-2(\nu+1)}{n}\frac{R^n}{\rho^n}+(1-\nu)\frac{R^{n-2}}{\rho^{n-2}})\sin n\phi=\pi R\frac{2(\nu+1)}{n}\sin n\phi$

Continue

		Interior		Exterior
$V(s,x)$	Degenerate kernel	$V^i(R,\theta;\rho,\phi)=\frac{4}{R}$ $+\left[\frac{2\rho}{R^2}(3-\nu)-\frac{\rho^3}{R^4}(1-\nu)\right]\cos(\theta-\phi)$ $-\sum_{m=2}^{\infty}\left[m(1-\nu)\frac{\rho^{m+2}}{R^{m+3}}-(4+m(1-\nu))\frac{\rho^m}{R^{m+1}}\right]\cos m(\theta-\phi),\ R>\rho$		$V^e(R,\theta;\rho,\phi)=$ $(-3-\nu)\frac{1}{\rho}\cos(\theta-\phi)$ $+\sum_{m=2}^{\infty}\left[(m(1-\nu)-4)\frac{R^{m-1}}{\rho^m}-m(1-\nu)\frac{R^{m-3}}{\rho^{m-2}}\right]\cos m(\theta-\phi),\ \rho>R$
	Orthogonal process	$\int_0^{2\pi}[V^i][1]Rd\theta=2\pi R(\frac{4}{R}),\ R>\rho$ $\int_0^{2\pi}[V^i][\cos\theta]Rd\theta=\pi R(\frac{2\rho}{R^2}(3-\nu)-\frac{\rho^3}{R^4}(1-\nu))\cos\phi,\ R>\rho$ $\int_0^{2\pi}[v^i][\sin\theta]Rd\theta=\pi R(\frac{2\rho}{R^2}(3-\nu)-\frac{\rho^3}{R^4}(1-\nu))\sin\phi,\ R>\rho$ $\int_0^{2\pi}[V^i][\cos n\theta]Rd\theta=-\pi R(n(1-\nu)\frac{\rho^{n+2}}{R^{n+3}}-(4+n(1-\nu))\frac{\rho^n}{R^{n+1}})\cos n\phi,\ R>\rho$ $\int_0^{2\pi}[V^i][\sin n\theta]Rd\theta=-\pi R(n(1-\nu)\frac{\rho^{n+2}}{R^{n+3}}-(4+n(1-\nu))\frac{\rho^n}{R^{n+1}})\sin n\phi,\ R>\rho$		$\int_0^{2\pi}[V^e][1]Rd\theta=0,\ \rho>R$ $\int_0^{2\pi}[V^e][\cos\theta]Rd\theta=\pi R((-3-\nu)\frac{1}{\rho})\cos\phi,\ \rho>R$ $\int_0^{2\pi}[V^e][\sin\theta]Rd\theta=\pi R((-3-\nu)\frac{1}{\rho})\sin\phi,\ \rho>R$ $\int_0^{2\pi}[V^e][\cos n\theta]Rd\theta=\pi R((n(1-\nu)-4)\frac{R^{n-1}}{\rho^n}-n(1-\nu)\frac{R^{n-3}}{\rho^{n-2}})\cos n\phi,\ \rho>R$ $\int_0^{2\pi}[V^e][\sin n\theta]Rd\theta=\pi R((n(1-\nu)-4)\frac{R^{n-1}}{\rho^n}-n(1-\nu)\frac{R^{n-3}}{\rho^{n-2}})\sin n\phi,\ \rho>R$
	Limiting behavior across the boundary	$\lim_{\rho\to R}2\pi R(\frac{4}{R})=8\pi$ $\lim_{\rho\to R}\pi R(\frac{2\rho}{R^2}(3-\nu)-\frac{\rho^3}{R^4}(1-\nu))\cos\phi=\pi(5-\nu)\cos\phi$ $\lim_{\rho\to R}\pi R((\nu+1)\frac{2\rho}{R}-(\nu-1)\frac{\rho^3}{R^3})\sin\phi=\pi(5-\nu)\sin\phi$ $-\lim_{\rho\to R}\pi R(n(1-\nu)\frac{\rho^{n+2}}{R^{n+3}}-(4+n(1-\nu))\frac{\rho^n}{R^{n+1}})\cos n\phi=4\pi\cos n\phi$ $-\lim_{\rho\to R}\pi R(n(1-\nu)\frac{\rho^{n+2}}{R^{n+3}}-(4+n(1-\nu))\frac{\rho^n}{R^{n+1}})\sin n\phi=4\pi\sin n\phi$	Discontinuous $(\rho^-\to R\leftarrow\rho^+)$	$\lim_{\rho\to R}0=0$ $\lim_{\rho\to R}\pi R((-3-\nu)\frac{1}{\rho})\cos\phi=-\pi(\nu+3)\cos\phi$ $\lim_{\rho\to R}\pi R((-3-\nu)\frac{1}{\rho})\sin\phi=-\pi(\nu+3)\sin\phi$ $\lim_{\rho\to R}\pi R((n(1-\nu)-4)\frac{R^{n-1}}{\rho^n}-n(1-\nu)\frac{R^{n-3}}{\rho^{n-2}})\cos n\phi=-4\pi\cos n\phi$ $\lim_{\rho\to R}\pi R((n(1-\nu)-4)\frac{R^{n-1}}{\rho^n}-n(1-\nu)\frac{R^{n-3}}{\rho^{n-2}})\sin n\phi=-4\pi\sin n\phi$

Continue

		Interior	Exterior
$U_\theta(s,x)$	Degenerate kernel	$U_\theta^{\,i}(R,\theta;\rho,\phi)=2\rho(1+\ln R)$ $-\left[R(1+2\ln R)+\frac{3}{2}\frac{\rho^2}{R}\right]\cos(\theta-\phi)$ $-\sum_{m=2}^{\infty}\left[\frac{m+2}{m(m+1)}\frac{\rho^{m+1}}{R^m}-\frac{1}{m-1}\frac{\rho^{m-1}}{R^{m-2}}\right]\cos m(\theta-\phi),\ R>\rho$	$U_\theta^{\,e}(R,\theta;\rho,\phi)=\frac{R^2}{\rho}+\rho(1+2\ln\rho)$ $-\left[R(3+2\ln\rho)-\frac{1}{2}\frac{R^3}{\rho^2}\right]\cos(\theta-\phi)$ $+\sum_{m=2}^{\infty}\left[\frac{1}{m+1}\frac{R^{m+2}}{\rho^{m+1}}-\frac{m-2}{m(m-1)}\frac{R^m}{\rho^{m-1}}\right]\cos m(\theta-\phi),\ \rho>R$
	Orthogonal process	$\int_0^{2\pi}[U_\theta^{\,i}][1]Rd\theta=2\pi R(2\rho(1+\ln R)),\ R>\rho$ $\int_0^{2\pi}[U_\theta^{\,i}][\cos\theta]Rd\theta=-\pi R(R(1+2\ln R)+\frac{3}{2}\frac{\rho^2}{R})\cos\phi,\ R>\rho$ $\int_0^{2\pi}[U_\theta^{\,i}][\sin\theta]Rd\theta=-\pi R(R(1+2\ln R)+\frac{3}{2}\frac{\rho^2}{R})\sin\phi,\ R>\rho$ $\int_0^{2\pi}[U_\theta^{\,i}][\cos n\theta]Rd\theta=-\pi R(\frac{n+2}{n(n+1)}\frac{\rho^{n+1}}{R^n}-\frac{1}{n-1}\frac{\rho^{n-1}}{R^{n-2}})\cos n\phi,\ R>\rho$ $\int_0^{2\pi}[U_\theta^{\,i}][\sin n\theta]Rd\theta=-\pi R(\frac{n+2}{n(n+1)}\frac{\rho^{n+1}}{R^n}-\frac{1}{n-1}\frac{\rho^{n-1}}{R^{n-2}})\sin n\phi,\ R>\rho$	$\int_0^{2\pi}[U_\theta^{\,e}][1]Rd\theta=2\pi R(\frac{R^2}{\rho}+\rho(1+2\ln\rho)),\ \rho>R$ $\int_0^{2\pi}[U_\theta^{\,e}][\cos\theta]Rd\theta=-\pi R(R(3+2\ln\rho)-\frac{1}{2}\frac{R^3}{\rho^2})\cos\phi,\ \rho>R$ $\int_0^{2\pi}[U_\theta^{\,e}][\sin\theta]Rd\theta=-\pi R(R(3+2\ln\rho)-\frac{1}{2}\frac{R^3}{\rho^2})\sin\phi,\ \rho>R$ $\int_0^{2\pi}[U_\theta^{\,e}][\cos n\theta]Rd\theta=\pi R(\frac{1}{n+1}\frac{R^{n+2}}{\rho^{n+1}}-\frac{n-2}{n(n-1)}\frac{R^n}{\rho^{n-1}})\cos n\phi,\ \rho>R$ $\int_0^{2\pi}[U_\theta^{\,e}][\sin n\theta]Rd\theta=\pi R(\frac{1}{n+1}\frac{R^{n+2}}{\rho^{n+1}}-\frac{n-2}{n(n-1)}\frac{R^n}{\rho^{n-1}})\sin n\phi,\ \rho>R$
	Limiting behavior across the boundary	$\lim_{\rho\to R}2\pi R(2\rho(1+\ln R))=4\pi R^2(1+\ln R)$ $-\lim_{\rho\to R}\pi R(R(1+2\ln R)+\frac{3}{2}\frac{\rho^2}{R})\cos\phi=-\pi R^2(\frac{5}{2}+2\ln R)\cos\phi$ $-\lim_{\rho\to R}\pi R(R(1+2\ln R)+\frac{3}{2}\frac{\rho^2}{R})\sin\phi=-\pi R^2(\frac{5}{2}+2\ln R)\sin\phi$ $-\lim_{\rho\to R}\pi R(\frac{n+2}{n(n+1)}\frac{\rho^{n+1}}{R^n}-\frac{1}{n-1}\frac{\rho^{n-1}}{R^{n-2}})\cos n\phi=\pi R^2\frac{2}{n(n^2-1)}\cos n\phi$ $-\lim_{\rho\to R}\pi R(\frac{n+2}{n(n+1)}\frac{\rho^{n+1}}{R^n}-\frac{1}{n-1}\frac{\rho^{n-1}}{R^{n-2}})\sin n\phi=\pi R^2\frac{2}{n(n^2-1)}\sin n\phi$	Continuous $(\rho^-\to R\leftarrow\rho^+)$	$\lim_{\rho\to R}2\pi R(\frac{R^2}{\rho}+\rho(1+2\ln\rho))=4\pi R^2(1+\ln R)$ $-\lim_{\rho\to R}\pi R(R(3+2\ln\rho)-\frac{1}{2}\frac{R^3}{\rho^2})\cos\phi=-\pi R^2(\frac{5}{2}+2\ln R)\cos\phi$ $-\lim_{\rho\to R}\pi R(R(3+2\ln\rho)-\frac{1}{2}\frac{R^3}{\rho^2})\sin\phi=-\pi R^2(\frac{5}{2}+2\ln R)\sin\phi$ $\lim_{\rho\to R}\pi R(\frac{1}{n+1}\frac{R^{n+2}}{\rho^{n+1}}-\frac{n-2}{n(n-1)}\frac{R^n}{\rho^{n-1}})\cos n\phi=\pi R^2\frac{2}{n(n^2-1)}\cos n\phi$ $\lim_{\rho\to R}\pi R(\frac{1}{n+1}\frac{R^{n+2}}{\rho^{n+1}}-\frac{n-2}{n(n-1)}\frac{R^n}{\rho^{n-1}})\sin n\phi=\pi R^2\frac{2}{n(n^2-1)}\sin n\phi$

Continue

$\Theta_\theta(s,x)$		***Interior***		***Exterior***
	Degenerate kernel	$\Theta_\theta{}^i(R,\theta;\rho,\phi)=\frac{2\rho}{R}$ $-\left[\left(3+2\ln R\right)-\frac{3}{2}\frac{\rho^2}{R^2}\right]\cos\left(\theta-\phi\right)$ $+\sum_{m=2}^{\infty}\left[\frac{m+2}{m+1}\frac{\rho^{m+1}}{R^{m+1}}-\frac{m-2}{m-1}\frac{\rho^{m-1}}{R^{m-1}}\right]\cos m\left(\theta-\phi\right),\ R>\rho$		$\Theta_\theta{}^e(R,\theta;\rho,\phi)=\frac{2R}{\rho}$ $-\left[\left(3+2\ln\rho\right)-\frac{3}{2}\frac{R^2}{\rho^2}\right]\cos\left(\theta-\phi\right)$ $+\sum_{m=2}^{\infty}\left[\frac{m+2}{m+1}\frac{R^{m+1}}{\rho^{m+1}}-\frac{m-2}{m-1}\frac{R^{m-1}}{\rho^{m-1}}\right]\cos m\left(\theta-\phi\right),\ \rho>R$
	Orthogonal process	$\int_0^{2\pi}[\Theta_\theta{}^i][1]Rd\theta=2\pi R(\frac{2\rho}{R}),\ R>\rho$ $\int_0^{2\pi}[\Theta_\theta{}^i][\cos\theta]Rd\theta=-\pi R(\left(3+2\ln R\right)-\frac{3}{2}\frac{\rho^2}{R^2})\cos\phi,\ R>\rho$ $\int_0^{2\pi}[\Theta_\theta{}^i][\sin\theta]Rd\theta=-\pi R(\left(3+2\ln R\right)-\frac{3}{2}\frac{\rho^2}{R^2})\sin\phi,\ R>\rho$ $\int_0^{2\pi}[\Theta_\theta{}^i][\cos n\theta]Rd\theta=\pi R(\frac{n+2}{n+1}\frac{\rho^{n+1}}{R^{n+1}}-\frac{n-2}{n-1}\frac{\rho^{n-1}}{R^{n-1}})\cos n\phi,\ R>\rho$ $\int_0^{2\pi}[\Theta_\theta{}^i][\sin n\theta]Rd\theta=\pi R(\frac{n+2}{n+1}\frac{\rho^{n+1}}{R^{n+1}}-\frac{n-2}{n-1}\frac{\rho^{n-1}}{R^{n-1}})\sin n\phi,\ R>\rho$		$\int_0^{2\pi}[\Theta_\theta{}^e][1]Rd\theta=2\pi R(\frac{2R}{\rho}),\ \rho>R$ $\int_0^{2\pi}[\Theta_\theta{}^e][\cos\theta]Rd\theta=-\pi R(\left(3+2\ln\rho\right)-\frac{3}{2}\frac{R^2}{\rho^2})\cos\phi,\ \rho>R$ $\int_0^{2\pi}[\Theta_\theta{}^e][\sin\theta]Rd\theta=-\pi R(\left(3+2\ln\rho\right)-\frac{3}{2}\frac{R^2}{\rho^2})\sin\phi,\ \rho>R$ $\int_0^{2\pi}[\Theta_\theta{}^e][\cos n\theta]Rd\theta=\pi R(\frac{n+2}{n+1}\frac{R^{n+1}}{\rho^{n+1}}-\frac{n-2}{n-1}\frac{R^{n-1}}{\rho^{n-1}})\cos n\phi,\ \rho>R$ $\int_0^{2\pi}[\Theta_\theta{}^e][\sin n\theta]Rd\theta=\pi R(\frac{n+2}{n+1}\frac{R^{n+1}}{\rho^{n+1}}-\frac{n-2}{n-1}\frac{R^{n-1}}{\rho^{n-1}})\sin n\phi,\ \rho>R$
	Limiting behavior across the boundary	$\lim_{\rho\to R}2\pi R(\frac{2\rho}{R})=4\pi R$ $-\lim_{\rho\to R}\pi R(\left(3+2\ln R\right)-\frac{3}{2}\frac{\rho^2}{R^2})\cos\phi=-\pi R(\frac{3}{2}+2\ln R)\cos\phi$ $-\lim_{\rho\to R}\pi R(\left(3+2\ln R\right)-\frac{3}{2}\frac{\rho^2}{R^2})\sin\phi=-\pi R(\frac{3}{2}+2\ln R)\sin\phi$ $\lim_{\rho\to R}\pi R(\frac{n+2}{n+1}\frac{\rho^{n+1}}{R^{n+1}}-\frac{n-2}{n-1}\frac{\rho^{n-1}}{R^{n-1}})\cos n\phi=\pi R\frac{2n}{n^2-1}\cos n\phi$ $\lim_{\rho\to R}\pi R(\frac{n+2}{n+1}\frac{\rho^{n+1}}{R^{n+1}}-\frac{n-2}{n-1}\frac{\rho^{n-1}}{R^{n-1}})\sin n\phi=\pi R\frac{2n}{n^2-1}\sin n\phi$	Continuous $(\rho^-\to R\leftarrow\rho^+)$	$\lim_{\rho\to R}2\pi R(\frac{2R}{\rho})=4\pi R$ $-\lim_{\rho\to R}\pi R(\left(3+2\ln\rho\right)-\frac{3}{2}\frac{R^2}{\rho^2})\cos\phi=-\pi R(\frac{3}{2}+2\ln R)\cos\phi$ $-\lim_{\rho\to R}\pi R(\left(3+2\ln\rho\right)-\frac{3}{2}\frac{R^2}{\rho^2})\sin\phi=-\pi R(\frac{3}{2}+2\ln R)\sin\phi$ $\lim_{\rho\to R}\pi R(\frac{n+2}{n+1}\frac{R^{n+1}}{\rho^{n+1}}-\frac{n-2}{n-1}\frac{R^{n-1}}{\rho^{n-1}})\cos n\phi=\pi R\frac{2n}{n^2-1}\cos n\phi$ $\lim_{\rho\to R}\pi R(\frac{n+2}{n+1}\frac{R^{n+1}}{\rho^{n+1}}-\frac{n-2}{n-1}\frac{R^{n-1}}{\rho^{n-1}})\sin n\phi=\pi R\frac{2n}{n^2-1}\sin n\phi$

Continue

$M_\theta(s,x)$		Interior		Exterior
	Degenerate kernel	$M_\theta^{\,i}(R,\theta;\rho,\phi)=\frac{2\rho}{R^2}(\nu-1)$ $-\left[\frac{2}{R}(\nu+1)-3(\nu-1)\frac{\rho^2}{R^3}\right]\cos(\theta-\phi)$ $+\sum_{m=2}^{\infty}\left[(m+2)(\nu-1)\frac{\rho^{m+1}}{R^{m+2}}+\left(m(1-\nu)-2(1+\nu)\right)\frac{\rho^{m-1}}{R^m}\right]\cos m(\theta-\phi),\ R>\rho$		$M_\theta^{\,e}(R,\theta;\rho,\phi)=\frac{2(1+\nu)}{\rho}$ $+(\nu+3)\frac{R}{\rho^2}\cos(\theta-\phi)$ $-\sum_{m=2}^{\infty}\left[\left(m(\nu-1)-2(\nu+1)\right)\frac{R^m}{\rho^{m+1}}+(m-2)(1-\nu)\frac{R^{m-2}}{\rho^{m-1}}\right]\cos m(\theta-\phi),\ \rho>R$
	Orthogonal process	$\int_0^{2\pi}[M_\theta^{\,i}][1]Rd\theta=2\pi R(\frac{2\rho}{R^2}(\nu-1)),\ R>\rho$ $\int_0^{2\pi}[M_\theta^{\,i}][\cos\theta]Rd\theta=-\pi R(\frac{2}{R}(\nu+1)-3(\nu-1)\frac{\rho^2}{R^3})\cos\phi,\ R>\rho$ $\int_0^{2\pi}[M_\theta^{\,i}][\sin\theta]Rd\theta=-\pi R(\frac{2}{R}(\nu+1)-3(\nu-1)\frac{\rho^2}{R^3})\sin\phi,\ R>\rho$ $\int_0^{2\pi}[M_\theta^{\,i}][\cos n\theta]Rd\theta=\pi R((m+2)(\nu-1)\frac{\rho^{m+1}}{R^{m+2}}+\left(m(1-\nu)-2(1+\nu)\right)\frac{\rho^{m-1}}{R^m})\cos n\phi,\ R>\rho$ $\int_0^{2\pi}[M_\theta^{\,i}][\sin n\theta]Rd\theta=\pi R((m+2)(\nu-1)\frac{\rho^{m+1}}{R^{m+2}}+\left(m(1-\nu)-2(1+\nu)\right)\frac{\rho^{m-1}}{R^m})\sin n\phi,\ R>\rho$		$\int_0^{2\pi}[M_\theta^{\,e}][1]Rd\theta=2\pi R(\frac{2(1+\nu)}{\rho}),\ \rho>R$ $\int_0^{2\pi}[M_\theta^{\,e}][\cos\theta]Rd\theta=\pi R((\nu+3)\frac{R}{\rho^2})\cos\phi,\ \rho>R$ $\int_0^{2\pi}[M_\theta^{\,e}][\sin\theta]Rd\theta=\pi R((\nu+3)\frac{R}{\rho^2})\sin\phi,\ \rho>R$ $\int_0^{2\pi}[M_\theta^{\,e}][\cos n\theta]Rd\theta=-\pi R(\left(m(\nu-1)-2(\nu+1)\right)\frac{R^m}{\rho^{m+1}}+(m-2)(1-\nu)\frac{R^{m-2}}{\rho^{m-1}})\cos n\phi,\ \rho>R$ $\int_0^{2\pi}[M_\theta^{\,e}][\sin n\theta]Rd\theta=-\pi R(\left(m(\nu-1)-2(\nu+1)\right)\frac{R^m}{\rho^{m+1}}+(m-2)(1-\nu)\frac{R^{m-2}}{\rho^{m-1}})\sin n\phi,\ \rho>R$
	Limiting behavior across the boundary	$\lim_{\rho\to R}2\pi R(\frac{2\rho}{R^2}(\nu-1))=4\pi(\nu-1)$ $-\lim_{\rho\to R}\pi R(\frac{2}{R}(\nu+1)-3(\nu-1)\frac{\rho^2}{R^3})\cos\phi=-\pi(5-\nu)\cos\phi$ $-\lim_{\rho\to R}\pi R(\frac{2}{R}(\nu+1)-3(\nu-1)\frac{\rho^2}{R^3})\sin\phi=-\pi(5-\nu)\sin\phi$ $\lim_{\rho\to R}\pi R((n+2)(\nu-1)\frac{\rho^{n+1}}{R^{n+2}}+\left(n(1-\nu)-2(1+\nu)\right)\frac{\rho^{n-1}}{R^n})\cos n\phi$ $=-4\pi\cos n\phi$ $\lim_{\rho\to R}\pi R((n+2)(\nu-1)\frac{\rho^{m+1}}{R^{m+2}}+\left(n(1-\nu)-2(1+\nu)\right)\frac{\rho^{n-1}}{R^n})\sin n\phi$ $=-4\pi\sin n\phi$	Discontinuous $(\rho^-\to R\leftarrow\rho^+)$	$\lim_{\rho\to R}2\pi R(\frac{2(1+\nu)}{\rho})=4\pi(1+\nu)$ $\lim_{\rho\to R}\pi R((\nu+3)\frac{R}{\rho^2})\cos\phi=\pi(\nu+3)\cos\phi$ $\lim_{\rho\to R}\pi R((\nu+3)\frac{R}{\rho^2})\sin\phi=\pi(\nu+3)\sin\phi$ $-\lim_{\rho\to R}\pi R(\left(n(\nu-1)-2(\nu+1)\right)\frac{R^m}{\rho^{m+1}}+(n-2)(1-\nu)\frac{R^{n-2}}{\rho^{n-1}})\cos n\phi$ $=4\pi\cos n\phi$ $-\lim_{\rho\to R}\pi R(\left(n(\nu-1)-2(\nu+1)\right)\frac{R^m}{\rho^{m+1}}+(n-2)(1-\nu)\frac{R^{n-2}}{\rho^{n-1}})\sin n\phi$ $=4\pi\sin n\phi$

Continue

$V_\theta(s,x)$		Interior		Exterior
	Degenerate kernel	$V_\theta^{\,i}(R,\theta;\rho,\phi)=$ $\left[\frac{2}{R^2}(3-\nu)-3(1-\nu)\frac{\rho^2}{R^4}\right]\cos(\theta-\phi)$ $-\sum_{m=2}^{\infty}\left[m(m+2)(1-\nu)\frac{\rho^{m+1}}{R^{m+3}}-m\left(4+m(1-\nu)\right)\frac{\rho^{m-1}}{R^{m+1}}\right]\cos m(\theta-\phi),\ R>\rho$		$V_\theta^{\,e}(R,\theta;\rho,\phi)=$ $(3+\nu)\frac{1}{\rho^2}\cos(\theta-\phi)$ $-\sum_{m=2}^{\infty}\left[m\left(m(1-\nu)-4\right)\frac{R^{m-1}}{\rho^{m+1}}-m(m-2)(1-\nu)\frac{R^{m-3}}{\rho^{m-1}}\right]\cos m(\theta-\phi),\ \rho>R$
	Orthogonal process	$\int_0^{2\pi}[V_\theta^{\,i}][1]Rd\theta=0,\ R>\rho$ $\int_0^{2\pi}[V_\theta^{\,i}][\cos\theta]Rd\theta=\pi R(\frac{2}{R^2}(3-\nu)-3(1-\nu)\frac{\rho^2}{R^4})\cos\phi,\ R>\rho$ $\int_0^{2\pi}[V_\theta^{\,i}][\sin\theta]Rd\theta=\pi R(\frac{2}{R^2}(3-\nu)-3(1-\nu)\frac{\rho^2}{R^4})\sin\phi,\ R>\rho$ $\int_0^{2\pi}[V_\theta^{\,i}][\cos n\theta]Rd\theta=-\pi R(n(n+2)(1-\nu)\frac{\rho^{n+1}}{R^{n+3}}$ $-n\left(4+n(1-\nu)\right)\frac{\rho^{n-1}}{R^{n+1}})\cos n\phi,\ R>\rho$ $\int_0^{2\pi}[V_\theta^{\,i}][\sin n\theta]Rd\theta=-\pi R(n(n+2)(1-\nu)\frac{\rho^{n+1}}{R^{n+3}}$ $-n\left(4+n(1-\nu)\right)\frac{\rho^{n-1}}{R^{n+1}})\sin n\phi,\ R>\rho$		$\int_0^{2\pi}[V_\theta^{\,e}][1]Rd\theta=0,\ \rho>R$ $\int_0^{2\pi}[V_\theta^{\,e}][\cos\theta]Rd\theta=\pi R((3+\nu)\frac{1}{\rho^2})\cos\phi,\ \rho>R$ $\int_0^{2\pi}[V_\theta^{\,e}][\sin\theta]Rd\theta=\pi R((3+\nu)\frac{1}{\rho^2})\sin\phi,\ \rho>R$ $\int_0^{2\pi}[V_\theta^{\,e}][\cos n\theta]Rd\theta=-\pi R(n\left(n(1-\nu)-4\right)\frac{R^{n-1}}{\rho^{n+1}}$ $-n(n-2)(1-\nu)\frac{R^{n-3}}{\rho^{n-1}})\cos n\phi,\ \rho>R$ $\int_0^{2\pi}[V_\theta^{\,e}][\sin n\theta]Rd\theta=-\pi R(n\left(n(1-\nu)-4\right)\frac{R^{n-1}}{\rho^{n+1}}$ $-n(n-2)(1-\nu)\frac{R^{n-3}}{\rho^{n-1}})\sin n\phi,\ \rho>R$
	Limiting behavior across the boundary	$\lim_{\rho\to R}0=0$ $\lim_{\rho\to R}\pi R(\frac{2}{R^2}(3-\nu)-3(1-\nu)\frac{\rho^2}{R^4})\cos\phi=\pi\frac{(3+\nu)}{R}\cos\phi$ $\lim_{\rho\to R}\pi R(\frac{2}{R^2}(3-\nu)-3(1-\nu)\frac{\rho^2}{R^4})\sin\phi=\pi\frac{(3+\nu)}{R}\sin\phi$ $-\lim_{\rho\to R}\pi R(n(n+2)(1-\nu)\frac{\rho^{n+1}}{R^{n+3}}-n\left(4+n(1-\nu)\right)\frac{\rho^{n-1}}{R^{n+1}})\cos n\phi$ $=\frac{2n\pi(\nu+1)}{R}\cos n\phi$ $-\lim_{\rho\to R}\pi R(n(n+2)(1-\nu)\frac{\rho^{n+1}}{R^{n+3}}-n\left(4+n(1-\nu)\right)\frac{\rho^{n-1}}{R^{n+1}})\sin n\phi$ $=\frac{2n\pi(\nu+1)}{R}\sin n\phi$	Pseudo-continuous $(\rho^-\to R\leftarrow\rho^+)$	$\lim_{\rho\to R}0=0$ $\lim_{\rho\to R}\pi R((3+\nu)\frac{1}{\rho^2})\cos\phi=\pi\frac{(\nu+3)}{R}\cos\phi$ $\lim_{\rho\to R}\pi R((3+\nu)\frac{1}{\rho^2})\sin\phi=\pi\frac{(\nu+3)}{R}\sin\phi$ $-\lim_{\rho\to R}\pi R(n\left(n(1-\nu)-4\right)\frac{R^{n-1}}{\rho^{n+1}}-n(n-2)(1-\nu)\frac{R^{n-3}}{\rho^{n-1}})\cos n\phi$ $=\frac{2n\pi(1+\nu)}{R}\cos n\phi$ $-\lim_{\rho\to R}\pi R(n\left(n(1-\nu)-4\right)\frac{R^{n-1}}{\rho^{n+1}}-n(n-2)(1-\nu)\frac{R^{n-3}}{\rho^{n-1}})\sin n\phi$ $=\frac{2n\pi(1+\nu)}{R}\sin n\phi$

Continue

$U_m(s,x)$		***Interior***		***Exterior***
	Degenerate kernel	$U_m^{\,i}(R,\theta;\rho,\phi)=2(1+\nu)(1+\ln R)$ $-(\nu+3)\frac{\rho}{R}\cos(\theta-\phi)$ $+\sum_{m=2}^{\infty}\left[\frac{m(\nu-1)-2(\nu+1)}{m}\frac{\rho^m}{R^m}+(1-\nu)\frac{\rho^{m-2}}{R^{m-2}}\right]\cos m(\theta-\phi),\ R>\rho$		$U_m^{\,e}(R,\theta;\rho,\phi)=(3+\nu)+(\nu-1)\frac{R^2}{\rho^2}+2\ln\rho(\nu+1)$ $+\left[(\nu-1)\frac{R^3}{\rho^3}-2(\nu+1)\frac{R}{\rho}\right]\cos(\theta-\phi)$ $+\sum_{m=2}^{\infty}\left[\frac{m(1-\nu)-2(\nu+1)}{m}\frac{R^m}{\rho^m}-m(1-\nu)\frac{R^{m+2}}{\rho^{m+2}}\right]\cos m(\theta-\phi),\ \rho>R$
	Orthogonal process	$\int_0^{2\pi}[U_m^{\,i}][1]Rd\theta=2\pi R(2(1+\nu)(1+\ln R)),\ R>\rho$ $\int_0^{2\pi}[U_m^{\,i}][\cos\theta]Rd\theta=-\pi R((\nu+3)\frac{\rho}{R})\cos\phi,\ R>\rho$ $\int_0^{2\pi}[U_m^{\,i}][\sin\theta]Rd\theta=-\pi R((\nu+3)\frac{\rho}{R})\sin\phi,\ R>\rho$ $\int_0^{2\pi}[U_m^{\,i}][\cos n\theta]Rd\theta=\pi R(\frac{n(\nu-1)-2(\nu+1)}{n}\frac{\rho^n}{R^n}+(1-\nu)\frac{\rho^{n-2}}{R^{n-2}})\cos n\phi,\ R>\rho$ $\int_0^{2\pi}[U_m^{\,i}][\sin n\theta]Rd\theta=\pi R(\frac{n(\nu-1)-2(\nu+1)}{n}\frac{\rho^n}{R^n}+(1-\nu)\frac{\rho^{n-2}}{R^{n-2}})\sin n\phi,\ R>\rho$		$\int_0^{2\pi}[U_m^{\,e}][1]Rd\theta=2\pi R((3+\nu)+(\nu-1)\frac{R^2}{\rho^2}+2\ln\rho(\nu+1)),\ \rho>R$ $\int_0^{2\pi}[U_m^{\,e}][\cos\theta]Rd\theta=\pi R((\nu-1)\frac{R^3}{\rho^3}-2(\nu+1)\frac{R}{\rho})\cos\phi,\ \rho>R$ $\int_0^{2\pi}[U_m^{\,e}][\sin\theta]Rd\theta=\pi R((\nu-1)\frac{R^3}{\rho^3}-2(\nu+1)\frac{R}{\rho})\sin\phi,\ \rho>R$ $\int_0^{2\pi}[U_m^{\,e}][\cos n\theta]Rd\theta=\pi R(\frac{n(1-\nu)-2(\nu+1)}{n}\frac{R^n}{\rho^n}-n(1-\nu)\frac{R^{n+2}}{\rho^{n+2}})\cos n\phi,\ \rho>R$ $\int_0^{2\pi}[U_m^{\,e}][\sin n\theta]Rd\theta=\pi R(\frac{n(1-\nu)-2(\nu+1)}{n}\frac{R^n}{\rho^n}-n(1-\nu)\frac{R^{n+2}}{\rho^{n+2}})\sin n\phi,\ \rho>R$
	Limiting behavior across the boundary	$\lim_{\rho\to R}2\pi R(2(1+\nu)(1+\ln R))=4\pi R(1+\nu)(1+\ln R)$ $-\lim_{\rho\to R}\pi R((\nu+3)\frac{\rho}{R})\cos\phi=-\pi R(3+\nu)\cos\phi$ $-\lim_{\rho\to R}\pi R((\nu+3)\frac{\rho}{R})\sin\phi=-\pi R(3+\nu)\sin\phi$ $\lim_{\rho\to R}\pi R(\frac{n(\nu-1)-2(\nu+1)}{n}\frac{\rho^n}{R^n}+(1-\nu)\frac{\rho^{n-2}}{R^{n-2}})\cos n\phi$ $=-\frac{2\pi R(\nu+1)}{n}\cos n\phi$ $\lim_{\rho\to R}\pi R(\frac{n(\nu-1)-2(\nu+1)}{n}\frac{\rho^n}{R^n}+(1-\nu)\frac{\rho^{n-2}}{R^{n-2}})\sin n\phi$ $=-\frac{2\pi R(\nu+1)}{n}\sin n\phi$	Discontinuous $(\rho^-\to R\leftarrow\rho^+)$	$\lim_{\rho\to R}2\pi R((3+\nu)+(\nu-1)\frac{R^2}{\rho^2}+2\ln\rho(\nu+1))=4\pi R(1+\nu)(1+\ln R)$ $\lim_{\rho\to R}\pi R((\nu-1)\frac{R^3}{\rho^3}-2(\nu+1)\frac{R}{\rho})\cos\phi=-\pi R(\nu+3)\cos\phi$ $\lim_{\rho\to R}\pi R((\nu-1)\frac{R^3}{\rho^3}-2(\nu+1)\frac{R}{\rho})\sin\phi=-\pi R(\nu+3)\sin\phi$ $\lim_{\rho\to R}\pi R(\frac{n(1-\nu)-2(\nu+1)}{n}\frac{R^n}{\rho^n}-n(1-\nu)\frac{R^{n+2}}{\rho^{n+2}})\cos n\phi$ $=-\frac{2\pi R(\nu+1)}{n}\cos n\phi$ $\lim_{\rho\to R}\pi R(\frac{n(1-\nu)-2(\nu+1)}{n}\frac{R^n}{\rho^n}-n(1-\nu)\frac{R^{n+2}}{\rho^{n+2}})\sin n\phi$ $=-\frac{2\pi R(\nu+1)}{n}\sin n\phi$

Continue

$\Theta_m(s,x)$		Interior		Exterior
	Degenerate kernel	$\Theta_m{}^i(R,\theta;\rho,\phi)=\frac{2(1+\nu)}{R}$ $+(3+\nu)\frac{\rho}{R^2}\cos(\theta-\phi)$ $+\sum_{m=2}^{\infty}\left[\left(m(1-\nu)+2(1+\nu)\right)\frac{\rho^m}{R^{m+1}}-(1-\nu)(m-2)\frac{\rho^{m-2}}{R^{m-1}}\right]\cos m(\theta-\phi),\ R>\rho$		$\Theta_m{}^e(R,\theta;\rho,\phi)=\frac{2(\nu-1)R}{\rho^2}$ $+\left[\frac{-2(1+\nu)}{\rho}+\frac{3R^2}{\rho^3}(\nu-1)\right]\cos(\theta-\phi)$ $+\sum_{m=2}^{\infty}\left[\left(m(1-\nu)-2(1+\nu)\right)\frac{R^{m-1}}{\rho^m}-(1-\nu)(m+2)\frac{R^{m+1}}{\rho^{m+2}}\right]\cos m(\theta-\phi),\ \rho>R$
	Orthogonal process	$\int_0^{2\pi}[\Theta_m{}^i][1]Rd\theta=2\pi R(\frac{2(1+\nu)}{R}),\ R>\rho$ $\int_0^{2\pi}[\Theta_m{}^i][\cos\theta]Rd\theta=\pi R((3+\nu)\frac{\rho}{R^2})\cos\phi,\ R>\rho$ $\int_0^{2\pi}[\Theta_m{}^i][\sin\theta]Rd\theta=\pi R((3+\nu)\frac{\rho}{R^2})\sin\phi,\ R>\rho$ $\int_0^{2\pi}[\Theta_m{}^i][\cos n\theta]Rd\theta=\pi R(\left(n(1-\nu)+2(1+\nu)\right)\frac{\rho^n}{R^{n+1}}-(1-\nu)(n-2)\frac{\rho^{n-2}}{R^{n-1}})\cos n\phi,\ R>\rho$ $\int_0^{2\pi}[\Theta_m{}^i][\sin n\theta]Rd\theta=\pi R(\left(n(1-\nu)+2(1+\nu)\right)\frac{\rho^n}{R^{n+1}}-(1-\nu)(n-2)\frac{\rho^{n-2}}{R^{n-1}})\sin n\phi,\ R>\rho$		$\int_0^{2\pi}[\Theta_m{}^e][1]Rd\theta=2\pi R(\frac{2(\nu-1)R}{\rho^2}),\ \rho>R$ $\int_0^{2\pi}[\Theta_m{}^e][\cos\theta]Rd\theta=\pi R(\frac{-2(1+\nu)}{\rho}+\frac{3R^2}{\rho^3}(\nu-1))\cos\phi,\ \rho>R$ $\int_0^{2\pi}[\Theta_m{}^e][\sin\theta]Rd\theta=\pi R(\frac{-2(1+\nu)}{\rho}+\frac{3R^2}{\rho^3}(\nu-1))\sin\phi,\ \rho>R$ $\int_0^{2\pi}[\Theta_m{}^e][\cos n\theta]Rd\theta=\pi R(\left(n(1-\nu)-2(1+\nu)\right)\frac{R^{n-1}}{\rho^m}-(1-\nu)(n+2)\frac{R^{n+1}}{\rho^{n+2}})\cos n\phi,\ \rho>R$ $\int_0^{2\pi}[\Theta_m{}^e][\sin n\theta]Rd\theta=\pi R(\left(n(1-\nu)-2(1+\nu)\right)\frac{R^{n-1}}{\rho^n}-(1-\nu)(n+2)\frac{R^{n+1}}{\rho^{n+2}})\sin n\phi,\ \rho>R$
	Limiting behavior across the boundary	$\lim_{\rho\to R}2\pi R(\frac{2(1+\nu)}{R})=4\pi(1+\nu)$ $\lim_{\rho\to R}\pi R((3+\nu)\frac{\rho}{R^2})\cos\phi=\pi(3+\nu)\cos\phi$ $\lim_{\rho\to R}\pi R((3+\nu)\frac{\rho}{R^2})\sin\phi=\pi(3+\nu)\sin\phi$ $\lim_{\rho\to R}\pi R(\left(n(1-\nu)+2(1+\nu)\right)\frac{\rho^n}{R^{n+1}}-(1-\nu)(n-2)\frac{\rho^{n-2}}{R^{n-1}})\cos n\phi=4\pi\cos n\phi$ $\lim_{\rho\to R}\pi R(\left(n(1-\nu)+2(1+\nu)\right)\frac{\rho^n}{R^{n+1}}-(1-\nu)(n-2)\frac{\rho^{n-2}}{R^{n-1}})\sin n\phi=4\pi\sin n\phi$	Discontinuous $(\rho^-\to R\leftarrow\rho^+)$	$\lim_{\rho\to R}2\pi R(\frac{2(\nu-1)R}{\rho^2})=4\pi(\nu-1)$ $\lim_{\rho\to R}\pi R(\frac{-2(1+\nu)}{\rho}+\frac{3R^2}{\rho^3}(\nu-1))\cos\phi=\pi(\nu-5)\cos\phi$ $\lim_{\rho\to R}\pi R(\frac{-2(1+\nu)}{\rho}+\frac{3R^2}{\rho^3}(\nu-1))\sin\phi=\pi(\nu-5)\sin\phi$ $\lim_{\rho\to R}\pi R(\left(n(1-\nu)-2(1+\nu)\right)\frac{R^{n-1}}{\rho^m}-(1-\nu)(n+2)\frac{R^{n+1}}{\rho^{n+2}})\cos n\phi=-4\pi\cos n\phi$ $\lim_{\rho\to R}\pi R(\left(n(1-\nu)-2(1+\nu)\right)\frac{R^{n-1}}{\rho^m}-(1-\nu)(n+2)\frac{R^{n+1}}{\rho^{n+2}})\sin n\phi=-4\pi\sin n\phi$

Continue

$M_m(s,x)$		Interior	Exterior
	Degenerate kernel	$M_m^{\,i}(R,\theta;\rho,\phi)=\frac{2(\nu^2-1)}{R^2}$ $+2(\nu-1)(\nu+3)\frac{\rho}{R^3}\cos(\theta-\phi)$ $+\sum_{m=2}^{\infty}\frac{[(m(1-\nu)-2(1+\nu))(m-1)(1-\nu)\frac{\rho^{m-2}}{R^m}}{+[m(1-\nu)+2(1+\nu)](m+1)(\nu-1)\frac{\rho^m}{R^{m+2}}]}\cos m(\theta-\phi),\ R>\rho$	$M_m^{\,e}(R,\theta;\rho,\phi)=\frac{2(\nu^2-1)}{\rho^2}$ $+2(\nu-1)(\nu+3)\frac{R}{\rho^3}\cos(\theta-\phi)$ $+\sum_{m=2}^{\infty}\frac{[(m(\nu-1)+2(1+\nu))(m-1)(\nu-1)\frac{R^{m-2}}{\rho^m}}{-(m+1)(\nu-1)(m(\nu-1)-2(1+\nu))\frac{R^m}{\rho^{m+2}}]}\cos m(\theta-\phi),\ \rho>R$
	Orthogonal process	$\int_0^{2\pi}[M_m^{\,i}][1]Rd\theta=2\pi R(\frac{2(\nu^2-1)}{R^2}),\ R>\rho$ $\int_0^{2\pi}[M_m^{\,i}][\cos\theta]Rd\theta=\pi R(2(\nu-1)(\nu+3)\frac{\rho}{R^3})\cos\phi,\ R>\rho$ $\int_0^{2\pi}[M_m^{\,i}][\sin\theta]Rd\theta=\pi R(2(\nu-1)(\nu+3)\frac{\rho}{R^3})\sin\phi,\ R>\rho$ $\int_0^{2\pi}[M_m^{\,i}][\cos n\theta]Rd\theta=\pi R((n(1-\nu)-2(1+\nu))(n-1)(1-\nu)\frac{\rho^{n-2}}{R^n}$ $+[n(1-\nu)+2(1+\nu)](n+1)(\nu-1)\frac{\rho^n}{R^{n+2}})\cos n\phi,\ R>\rho$ $\int_0^{2\pi}[M_m^{\,i}][\sin n\theta]Rd\theta=\pi R((n(1-\nu)-2(1+\nu))(n-1)(1-\nu)\frac{\rho^{n-2}}{R^n}$ $+[n(1-\nu)+2(1+\nu)](n+1)(\nu-1)\frac{\rho^n}{R^{n+2}})\sin n\phi,\ R>\rho$	$\int_0^{2\pi}[M_m^{\,e}][1]Rd\theta=2\pi R(\frac{2(\nu^2-1)}{\rho^2}),\ \rho>R$ $\int_0^{2\pi}[M_m^{\,e}][\cos\theta]Rd\theta=\pi R(2(\nu-1)(\nu+3)\frac{R}{\rho^3})\cos\phi,\ \rho>R$ $\int_0^{2\pi}[M_m^{\,e}][\sin\theta]Rd\theta=\pi R(2(\nu-1)(\nu+3)\frac{R}{\rho^3})\sin\phi,\ \rho>R$ $\int_0^{2\pi}[M_m^{\,e}][\cos n\theta]Rd\theta=\pi R((n(\nu-1)+2(1+\nu))(n-1)(\nu-1)\frac{R^{n-2}}{\rho^n}$ $-(n+1)(\nu-1)(n(\nu-1)-2(1+\nu))\frac{R^n}{\rho^{n+2}})\cos n\phi,\ \rho>R$ $\int_0^{2\pi}[M_m^{\,e}][\sin n\theta]Rd\theta=\pi R((n(\nu-1)+2(1+\nu))(n-1)(\nu-1)\frac{R^{n-2}}{\rho^n}$ $-(n+1)(\nu-1)(n(\nu-1)-2(1+\nu))\frac{R^n}{\rho^{n+2}})\cos n\phi\sin n\phi,\ \rho>R$
	Limiting behavior across the boundary	$\lim_{\rho\to R}2\pi R(\frac{2(\nu^2-1)}{R^2})=4\pi\frac{(\nu^2-1)}{R}$ $\lim_{\rho\to R}\pi R(2(\nu-1)(\nu+3)\frac{\rho}{R^3})\cos\phi=\frac{2\pi(\nu-1)(\nu+3)}{R}\cos\phi$ $\lim_{\rho\to R}\pi R(2(\nu-1)(\nu+3)\frac{\rho}{R^3})\sin\phi=\frac{2\pi(\nu-1)(\nu+3)}{R}\sin\phi$ $\lim_{\rho\to R}\pi R((n(1-\nu)-2(1+\nu))(n-1)(1-\nu)\frac{\rho^{n-2}}{R^n}$ $+[n(1-\nu)+2(1+\nu)](n+1)(\nu-1)\frac{\rho^n}{R^{n+2}})\cos n\phi=\frac{2n\pi(\nu-1)(\nu+3)}{R}\cos n\phi$ $\lim_{\rho\to R}\pi R((n(1-\nu)-2(1+\nu))(n-1)(1-\nu)\frac{\rho^{n-2}}{R^n}$ $+[n(1-\nu)+2(1+\nu)](n+1)(\nu-1)\frac{\rho^n}{R^{n+2}})\sin n\phi=\frac{2n\pi(\nu-1)(\nu+3)}{R}\sin n\phi$	Pseudo-continuous $(\rho^-\to R\leftarrow\rho^+)$
			$\lim_{\rho\to R}2\pi R(\frac{2(\nu^2-1)}{\rho^2})=\frac{4\pi(\nu^2-1)}{R}$ $\lim_{\rho\to R}\pi R(2(\nu-1)(\nu+3)\frac{R}{\rho^3})\cos\phi=\frac{2\pi(\nu-1)(\nu+3)}{R}\cos\phi$ $\lim_{\rho\to R}\pi R(2(\nu-1)(\nu+3)\frac{R}{\rho^3})\sin\phi=\frac{2\pi(\nu-1)(\nu+3)}{R}\sin\phi$ $\lim_{\rho\to R}\pi R((n(\nu-1)+2(1+\nu))(n-1)(\nu-1)\frac{R^{n-2}}{\rho^n}$ $-(n+1)(\nu-1)(n(\nu-1)-2(1+\nu))\frac{R^n}{\rho^{n+2}})\cos n\phi=\frac{2n\pi(\nu-1)(\nu+3)}{R}\cos n\phi$ $\lim_{\rho\to R}\pi R((n(\nu-1)+2(1+\nu))(n-1)(\nu-1)\frac{R^{n-2}}{\rho^n}$ $-(n+1)(\nu-1)(n(\nu-1)-2(1+\nu))\frac{R^n}{\rho^{n+2}})\sin n\phi=\frac{2n\pi(\nu-1)(\nu+3)}{R}\sin n\phi$

$V_m(s,x)$		Interior		Exterior
	Degenerate kernel	$V_m^{\,i}(R,\theta;\rho,\phi)=$ $2(\nu-1)(\nu+3)\frac{\rho}{R^4}\cos(\theta-\phi)$ $+\sum_{m=2}^{\infty}[m(m+1)(\nu-1)\big(m(1-\nu)+2(1+\nu)\big)\frac{\rho^m}{R^{m+3}}$ $+m(m-1)(1-\nu)\big(4+m(1-\nu)\big)\frac{\rho^{m-2}}{R^{m+1}}]\cos m(\theta-\phi),\ R>\rho$		$V_m^{\,e}(R,\theta;\rho,\phi)=$ $\frac{2(\nu-1)(\nu+3)}{\rho^3}\cos(\theta-\phi)$ $+\sum_{m=2}^{\infty}[m(m-1)(\nu-1)\big(m(1-\nu)-2(1+\nu)\big)\frac{R^{m-3}}{\rho^m}$ $+m(m+1)(1-\nu)\big(m(1-\nu)-4\big)\frac{R^{m-1}}{\rho^{m+2}}]\cos m(\theta-\phi),\ \rho>R$
	Orthogonal process	$\int_0^{2\pi}[V_m^{\,i}][1]Rd\theta=0,\ R>\rho$ $\int_0^{2\pi}[V_m^{\,i}][\cos\theta]Rd\theta=\pi R(2(\nu-1)(\nu+3)\frac{\rho}{R^4})\cos\phi,\ R>\rho$ $\int_0^{2\pi}[V_m^{\,i}][\sin\theta]Rd\theta=\pi R(2(\nu-1)(\nu+3)\frac{\rho}{R^4})\sin\phi,\ R>\rho$ $\int_0^{2\pi}[V_m^{\,i}][\cos n\theta]Rd\theta=\pi R(n(n+1)(\nu-1)\big(n(1-\nu)+2(1+\nu)\big)\frac{\rho^n}{R^{n+3}}$ $+n(n-1)(1-\nu)\big(4+n(1-\nu)\big)\frac{\rho^{n-2}}{R^{n+1}})\cos n\phi,\ R>\rho$ $\int_0^{2\pi}[V_m^{\,i}][\sin n\theta]Rd\theta=\pi R(n(n+1)(\nu-1)\big(n(1-\nu)+2(1+\nu)\big)\frac{\rho^n}{R^{n+3}}$ $+n(n-1)(1-\nu)\big(4+n(1-\nu)\big)\frac{\rho^{n-2}}{R^{n+1}})\sin n\phi,\ R>\rho$		$\int_0^{2\pi}[V_m^{\,e}][1]Rd\theta=0,\ \rho>R$ $\int_0^{2\pi}[V_m^{\,e}][\cos\theta]Rd\theta=\pi R(\frac{2(\nu-1)(\nu+3)}{\rho^3})\cos\phi,\ \rho>R$ $\int_0^{2\pi}[V_m^{\,e}][\sin\theta]Rd\theta=\pi R(\frac{2(\nu-1)(\nu+3)}{\rho^3})\sin\phi,\ \rho>R$ $\int_0^{2\pi}[V_m^{\,e}][\cos n\theta]Rd\theta=\pi R(n(n-1)(\nu-1)\big(n(1-\nu)-2(1+\nu)\big)\frac{R^{n-3}}{\rho^n}$ $+n(n+1)(1-\nu)\big(n(1-\nu)-4\big)\frac{R^{n-1}}{\rho^{n+2}})\cos n\phi,\ \rho>R$ $\int_0^{2\pi}[V_m^{\,e}][\sin n\theta]Rd\theta=\pi R(n(n-1)(\nu-1)\big(n(1-\nu)-2(1+\nu)\big)\frac{R^{n-3}}{\rho^n}$ $+n(n+1)(1-\nu)\big(n(1-\nu)-4\big)\frac{R^{n-1}}{\rho^{n+2}})\cos n\phi\sin n\phi,\ \rho>R$
	Limiting behavior across the boundary	$\lim_{\rho\to R}0=0$ $\lim_{\rho\to R}\pi R(2(\nu-1)(\nu+3)\frac{\rho}{R^4})\cos\phi=\frac{2\pi(\nu-1)(\nu+3)}{R^2}\cos\phi$ $\lim_{\rho\to R}\pi R(2(\nu-1)(\nu+3)\frac{\rho}{R^4})\sin\phi=\frac{2\pi(\nu-1)(\nu+3)}{R^2}\sin\phi$ $\lim_{\rho\to R}\pi R(n(n+1)(\nu-1)\big(n(1-\nu)+2(1+\nu)\big)\frac{\rho^n}{R^{n+3}}$ $+n(n-1)(1-\nu)\big(4+n(1-\nu)\big)\frac{\rho^{n-2}}{R^{n+1}})\cos n\phi=\frac{2n\pi(\nu-1)(\nu+3)}{R^2}\cos n\phi$ $\lim_{\rho\to R}\pi R(n(n+1)(\nu-1)\big(n(1-\nu)+2(1+\nu)\big)\frac{\rho^n}{R^{n+3}}$ $+n(n-1)(1-\nu)\big(4+n(1-\nu)\big)\frac{\rho^{n-2}}{R^{n+1}})\sin n\phi=\frac{2n\pi(\nu-1)(\nu+3)}{R^2}\sin n\phi$	Pseudo-continuous $(\rho^-\to R\leftarrow\rho^+)$	$\lim_{\rho\to R}0=0$ $\lim_{\rho\to R}\pi R(\frac{2(\nu-1)(\nu+3)}{\rho^3})\cos\phi=\frac{2\pi(\nu-1)(\nu+3)}{R^2}\cos\phi$ $\lim_{\rho\to R}\pi R(\frac{2(\nu-1)(\nu+3)}{\rho^3})\sin\phi=\frac{2\pi(\nu-1)(\nu+3)}{R^2}\sin\phi$ $\lim_{\rho\to R}\pi R(n(n-1)(\nu-1)\big(n(1-\nu)-2(1+\nu)\big)\frac{R^{n-3}}{\rho^n}$ $+n(n+1)(1-\nu)\big(n(1-\nu)-4\big)\frac{R^{n-1}}{\rho^{n+2}})\cos n\phi=\frac{2n\pi(\nu-1)(\nu+3)}{R^2}\cos n\phi$ $\lim_{\rho\to R}\pi R(n(n-1)(\nu-1)\big(n(1-\nu)-2(1+\nu)\big)\frac{R^{n-3}}{\rho^n}$ $+n(n+1)(1-\nu)\big(n(1-\nu)-4\big)\frac{R^{n-1}}{\rho^{n+2}})\sin n\phi=\frac{2n\pi(\nu-1)(\nu+3)}{R^2}\sin n\phi$

Continue

		Interior		Exterior
$U_v(s,x)$	Degenerate kernel	$U_v^{\,i}(R,\theta;\rho,\phi)=$ $-\frac{(3+\nu)}{R}\cos(\theta-\phi)$ $+\sum_{m=2}^{\infty}\left[\left(-4+m(1-\nu)\right)\frac{\rho^{m-1}}{R^m}-m(1-\nu)\frac{\rho^{m-3}}{R^{m-2}}\right]\cos m(\theta-\phi),\ R>\rho$		$U_v^{\,e}(R,\theta;\rho,\phi)=\frac{4}{\rho}$ $+\left[(3-\nu)\frac{2R}{\rho^2}-(1-\nu)\frac{R^3}{\rho^4}\right]\cos(\theta-\phi)$ $+\sum_{m=2}^{\infty}\left[\left(4+m(1-\nu)\right)\frac{R^m}{\rho^{m+1}}-m(1-\nu)\frac{R^{m+2}}{\rho^{m+3}}\right]\cos m(\theta-\phi),\ \rho>R$
	Orthogonal process	$\int_0^{2\pi}[U_v^{\,i}][1]Rd\theta=0,\ R>\rho$ $\int_0^{2\pi}[U_v^{\,i}][\cos\theta]Rd\theta=-\pi R(\frac{(3+\nu)}{R})\cos\phi,\ R>\rho$ $\int_0^{2\pi}[U_v^{\,i}][\sin\theta]Rd\theta=-\pi R(\frac{(3+\nu)}{R})\sin\phi,\ R>\rho$ $\int_0^{2\pi}[U_v^{\,i}][\cos n\theta]Rd\theta=\pi R(\left(-4+n(1-\nu)\right)\frac{\rho^{n-1}}{R^n}-n(1-\nu)\frac{\rho^{n-3}}{R^{n-2}})\cos n\phi,\ R>\rho$ $\int_0^{2\pi}[U_v^{\,i}][\sin n\theta]Rd\theta=\pi R(\left(-4+n(1-\nu)\right)\frac{\rho^{n-1}}{R^n}-n(1-\nu)\frac{\rho^{n-3}}{R^{n-2}})\sin n\phi,\ R>\rho$		$\int_0^{2\pi}[U_v^{\,e}][1]Rd\theta=2\pi R(\frac{4}{\rho}),\ \rho>R$ $\int_0^{2\pi}[U_v^{\,e}][\cos\theta]Rd\theta=\pi R((3-\nu)\frac{2R}{\rho^2}-(1-\nu)\frac{R^3}{\rho^4})\cos\phi,\ \rho>R$ $\int_0^{2\pi}[U_v^{\,e}][\sin\theta]Rd\theta=\pi R((3-\nu)\frac{2R}{\rho^2}-(1-\nu)\frac{R^3}{\rho^4})\sin\phi,\ \rho>R$ $\int_0^{2\pi}[U_v^{\,e}][\cos n\theta]Rd\theta=\pi R(\left(4+n(1-\nu)\right)\frac{R^n}{\rho^{n+1}}-n(1-\nu)\frac{R^{n+2}}{\rho^{n+3}})\cos n\phi,\ \rho>R$ $\int_0^{2\pi}[U_v^{\,e}][\sin n\theta]Rd\theta=\pi R(\left(4+n(1-\nu)\right)\frac{R^n}{\rho^{n+1}}-n(1-\nu)\frac{R^{n+2}}{\rho^{n+3}})\cos n\phi\sin n\phi,\ \rho>R$
	Limiting behavior across the boundary	$\lim_{\rho\to R}0=0$ $-\lim_{\rho\to R}\pi R((\frac{(3+\nu)}{R}))\cos\phi=-\pi(\nu+3)\cos\phi$ $-\lim_{\rho\to R}\pi R((\frac{(3+\nu)}{R}))\sin\phi=-\pi(\nu+3)\sin\phi$ $\lim_{\rho\to R}\pi R(\left(-4+n(1-\nu)\right)\frac{\rho^{n-1}}{R^n}-n(1-\nu)\frac{\rho^{n-3}}{R^{n-2}})\cos n\phi=-4\pi\cos n\phi$ $\lim_{\rho\to R}\pi R(\left(-4+n(1-\nu)\right)\frac{\rho^{n-1}}{R^n}-n(1-\nu)\frac{\rho^{n-3}}{R^{n-2}})\sin n\phi=-4\pi\sin n\phi$	Discontinuous $(\rho^-\to R\leftarrow\rho^+)$	$\lim_{\rho\to R}2\pi R(\frac{4}{\rho})=8\pi$ $\lim_{\rho\to R}\pi R((3-\nu)\frac{2R}{\rho^2}-(1-\nu)\frac{R^3}{\rho^4})\cos\phi=\pi(5-\nu)\cos\phi$ $\lim_{\rho\to R}\pi R((3-\nu)\frac{2R}{\rho^2}-(1-\nu)\frac{R^3}{\rho^4})\sin\phi=\pi(5-\nu)\sin\phi$ $\lim_{\rho\to R}\pi R(\left(4+n(1-\nu)\right)\frac{R^n}{\rho^{n+1}}-n(1-\nu)\frac{R^{n+2}}{\rho^{n+3}})\cos n\phi=4\pi\cos n\phi$ $\lim_{\rho\to R}\pi R(\left(4+n(1-\nu)\right)\frac{R^n}{\rho^{n+1}}-n(1-\nu)\frac{R^{n+2}}{\rho^{n+3}})\sin n\phi=4\pi\sin n\phi$

Continue

$\Theta_v(s,x)$		Interior		Exterior
	Degenerate kernel	$\Theta_v^{\,i}(R,\theta;\rho,\phi)=$ $\frac{(\nu+3)}{R^2}\cos(\theta-\phi)$ $+\sum_{m=2}^{\infty}\left[m\left(4+m(\nu-1)\right)\frac{\rho^{m-1}}{R^{m+1}}+m(m-2)(1-\nu)\frac{\rho^{m-3}}{R^{m-1}}\right]\cos m(\theta-\phi),\ R>\rho$		$\Theta_v^{\,e}(R,\theta;\rho,\phi)=$ $\left[(3-\nu)\frac{2}{\rho^2}+3(\nu-1)\frac{R^2}{\rho^4}\right]\cos(\theta-\phi)$ $+\sum_{m=2}^{\infty}\left[m\left(4+m(1-\nu)\right)\frac{R^{m-1}}{\rho^{m+1}}-m(m+2)(1-\nu)\frac{R^{m+1}}{\rho^{m+3}}\right]\cos m(\theta-\phi),\ \rho>R$
	Orthogonal process	$\int_0^{2\pi}[\Theta_v^{\,i}][1]Rd\theta=0,\ R>\rho$ $\int_0^{2\pi}[\Theta_v^{\,i}][\cos\theta]Rd\theta=\pi R(\frac{(\nu+3)}{R^2})\cos\phi,\ R>\rho$ $\int_0^{2\pi}[\Theta_v^{\,i}][\sin\theta]Rd\theta=\pi R(\frac{(\nu+3)}{R^2})\sin\phi,\ R>\rho$ $\int_0^{2\pi}[\Theta_v^{\,i}][\cos n\theta]Rd\theta=\pi R(n\left(4+n(\nu-1)\right)\frac{\rho^{n-1}}{R^{n+1}}+n(n-2)(1-\nu)\frac{\rho^{n-3}}{R^{n-1}})\cos n\phi,\ R>\rho$ $\int_0^{2\pi}[\Theta_v^{\,i}][\sin n\theta]Rd\theta=\pi R(n\left(4+n(\nu-1)\right)\frac{\rho^{n-1}}{R^{n+1}}+n(n-2)(1-\nu)\frac{\rho^{n-3}}{R^{n-1}})\sin n\phi,\ R>\rho$		$\int_0^{2\pi}[\Theta_v^{\,e}][1]Rd\theta=0,\ \rho>R$ $\int_0^{2\pi}[\Theta_v^{\,e}][\cos\theta]Rd\theta=\pi R((3-\nu)\frac{2}{\rho^2}+3(\nu-1)\frac{R^2}{\rho^4})\cos\phi,\ \rho>R$ $\int_0^{2\pi}[\Theta_v^{\,e}][\sin\theta]Rd\theta=\pi R((3-\nu)\frac{2}{\rho^2}+3(\nu-1)\frac{R^2}{\rho^4})\sin\phi,\ \rho>R$ $\int_0^{2\pi}[\Theta_v^{\,e}][\cos n\theta]Rd\theta=\pi R(n\left(4+n(1-\nu)\right)\frac{R^{n-1}}{\rho^{n+1}}-n(n+2)(1-\nu)\frac{R^{n+1}}{\rho^{n+3}})\cos n\phi,\ \rho>R$ $\int_0^{2\pi}[\Theta_v^{\,e}][\sin n\theta]Rd\theta=\pi R(n\left(4+n(1-\nu)\right)\frac{R^{n-1}}{\rho^{n+1}}-n(n+2)(1-\nu)\frac{R^{n+1}}{\rho^{n+3}})\cos n\phi\sin n\phi,\ \rho>R$
	Limiting behavior across the boundary	$\lim_{\rho\to R}0=0$ $\lim_{\rho\to R}\pi R\frac{(\nu+3)}{R^2}\cos\phi=\frac{\pi(\nu+3)}{R}\cos\phi$ $\lim_{\rho\to R}\pi R\frac{(\nu+3)}{R^2}\sin\phi=\frac{\pi(\nu+3)}{R}\sin\phi$ $\lim_{\rho\to R}\pi R(n\left(4+n(\nu-1)\right)\frac{\rho^{n-1}}{R^{n+1}}+n(n-2)(1-\nu)\frac{\rho^{n-3}}{R^{n-1}})\cos n\phi=\frac{2n\pi(1+\nu)}{R}\cos n\phi$ $\lim_{\rho\to R}\pi R(n\left(4+n(\nu-1)\right)\frac{\rho^{n-1}}{R^{n+1}}+n(n-2)(1-\nu)\frac{\rho^{n-3}}{R^{n-1}})\sin n\phi=\frac{2n\pi(1+\nu)}{R}\sin n\phi$	Pseudo-continuous $(\rho^-\to R\leftarrow\rho^+)$	$\lim_{\rho\to R}0=0$ $\lim_{\rho\to R}\pi R((3-\nu)\frac{2}{\rho^2}+3(\nu-1)\frac{R^2}{\rho^4})\cos\phi=\frac{\pi(\nu+3)}{R}\cos\phi$ $\lim_{\rho\to R}\pi R((3-\nu)\frac{2}{\rho^2}+3(\nu-1)\frac{R^2}{\rho^4})\sin\phi=\frac{\pi(\nu+3)}{R}\sin\phi$ $\lim_{\rho\to R}\pi R(n\left(4+n(1-\nu)\right)\frac{R^{n-1}}{\rho^{n+1}}-n(n+2)(1-\nu)\frac{R^{n+1}}{\rho^{n+3}})\cos n\phi=\frac{2n\pi(1+\nu)}{R}\cos n\phi$ $\lim_{\rho\to R}\pi R(n\left(4+n(1-\nu)\right)\frac{R^{n-1}}{\rho^{n+1}}-n(n+2)(1-\nu)\frac{R^{n+1}}{\rho^{n+3}})\sin n\phi=\frac{2n\pi(1+\nu)}{R}\sin n\phi$

Continue

$M_v(s,x)$		***Interior***		***Exterior***
	Degenerate kernel	$M_v^{\,i}(R,\theta;\rho,\phi)=$ $\frac{2(\nu+3)(\nu-1)}{R^3}\cos(\theta-\phi)$ $+\sum_{m=2}^{\infty}[m(m+1)(\nu-1)(4-m(1-\nu))\frac{\rho^{m-1}}{R^{m+2}}$ $-(m(1-\nu)-2(1+\nu))(1-\nu)m(m-1)\frac{\rho^{m-3}}{R^m}]\cos m(\theta-\phi),\ R>\rho$		$M_v^{\,e}(R,\theta;\rho,\phi)=$ $2(\nu-1)(\nu+3)\frac{R}{\rho^4}\cos(\theta-\phi)$ $+\sum_{m=2}^{\infty}[-m(m-1)(\nu-1)(4+m(1-\nu))\frac{R^{m-2}}{\rho^{m+1}}$ $+(m(\nu-1)-2(\nu+1))m(m+1)(1-\nu)\frac{R^m}{\rho^{m+3}}]\cos m(\theta-\phi),\ \rho>R$
	Orthogonal process	$\int_0^{2\pi}[M_v^{\,i}][1]Rd\theta=0,\ R>\rho$ $\int_0^{2\pi}[M_v^{\,i}][\cos\theta]Rd\theta=\pi R(\frac{2(\nu+3)(\nu-1)}{R^3})\cos\phi,\ R>\rho$ $\int_0^{2\pi}[M_v^{\,i}][\sin\theta]Rd\theta=\pi R(\frac{2(\nu+3)(\nu-1)}{R^3})\sin\phi,\ R>\rho$ $\int_0^{2\pi}[M_v^{\,i}][\cos n\theta]Rd\theta=\pi R(n(n+1)(\nu-1)(4-n(1-\nu))\frac{\rho^{n-1}}{R^{n+2}}$ $-(n(1-\nu)-2(1+\nu))(1-\nu)n(n-1)\frac{\rho^{n-3}}{R^n})\cos n\phi,\ R>\rho$ $\int_0^{2\pi}[M_v^{\,i}][\sin n\theta]Rd\theta=\pi R(n(n+1)(\nu-1)(4-n(1-\nu))\frac{\rho^{n-1}}{R^{n+2}}$ $-(n(1-\nu)-2(1+\nu))(1-\nu)n(n-1)\frac{\rho^{n-3}}{R^n})\sin n\phi,\ R>\rho$		$\int_0^{2\pi}[M_v^{\,e}][1]Rd\theta=0,\ \rho>R$ $\int_0^{2\pi}[M_v^{\,e}][\cos\theta]Rd\theta=\pi R(2(\nu-1)(\nu+3)\frac{R}{\rho^4})\cos\phi,\ \rho>R$ $\int_0^{2\pi}[M_v^{\,e}][\sin\theta]Rd\theta=\pi R(2(\nu-1)(\nu+3)\frac{R}{\rho^4})\sin\phi,\ \rho>R$ $\int_0^{2\pi}[M_v^{\,e}][\cos n\theta]Rd\theta=\pi R(-n(n-1)(\nu-1)(4+n(1-\nu))\frac{R^{n-2}}{\rho^{n+1}}$ $+(n(\nu-1)-2(\nu+1))n(n+1)(1-\nu)\frac{R^n}{\rho^{n+3}})\cos n\phi,\ \rho>R$ $\int_0^{2\pi}[M_v^{\,e}][\sin n\theta]Rd\theta=\pi R(-n(n-1)(\nu-1)(4+n(1-\nu))\frac{R^{n-2}}{\rho^{n+1}}$ $+(n(\nu-1)-2(\nu+1))n(n+1)(1-\nu)\frac{R^n}{\rho^{n+3}})\cos n\phi\sin n\phi,\ \rho>R$
	Limiting behavior across the boundary	$\lim_{\rho\to R}0=0$ $\lim_{\rho\to R}\pi R(\frac{2(\nu+3)(\nu-1)}{R^3})\cos\phi=\frac{2\pi(\nu+3)(\nu-1)}{R^2}\cos\phi$ $\lim_{\rho\to R}\pi R(\frac{2(\nu+3)(\nu-1)}{R^3})\sin\phi=\frac{2\pi(\nu+3)(\nu-1)}{R^2}\sin\phi$ $\lim_{\rho\to R}\pi R(n(n+1)(\nu-1)(4-n(1-\nu))\frac{\rho^{n-1}}{R^{n+2}}$ $-(n(1-\nu)-2(1+\nu))(1-\nu)n(n-1)\frac{\rho^{n-3}}{R^n})\cos n\phi=\frac{2n\pi(\nu-1)(\nu+3)}{R^2}\cos n\phi$ $\lim_{\rho\to R}\pi R(n(n+1)(\nu-1)(4-n(1-\nu))\frac{\rho^{n-1}}{R^{n+2}}$ $-(n(1-\nu)-2(1+\nu))(1-\nu)n(n-1)\frac{\rho^{n-3}}{R^n})\sin n\phi=\frac{2n\pi(\nu-1)(\nu+3)}{R^2}\sin n\phi$	Pseudo-continuous $(\rho^-\to R\leftarrow\rho^+)$	$\lim_{\rho\to R}0=0$ $\lim_{\rho\to R}\pi R(2(\nu-1)(\nu+3)\frac{R}{\rho^4})\cos\phi=\frac{2\pi(\nu-1)(\nu+3)}{R^2}\cos\phi$ $\lim_{\rho\to R}\pi R(2(\nu-1)(\nu+3)\frac{R}{\rho^4})\sin\phi=\frac{2\pi(\nu-1)(\nu+3)}{R^2}\sin\phi$ $\lim_{\rho\to R}\pi R(-n(n-1)(\nu-1)(4+n(1-\nu))\frac{R^{n-2}}{\rho^{n+1}}$ $+(n(\nu-1)-2(\nu+1))n(n+1)(1-\nu)\frac{R^n}{\rho^{n+3}})\cos n\phi=\frac{2n\pi(\nu-1)(\nu+3)}{R^2}\cos n\phi$ $\lim_{\rho\to R}\pi R(-n(n-1)(\nu-1)(4+n(1-\nu))\frac{R^{n-2}}{\rho^{n+1}}$ $+(n(\nu-1)-2(\nu+1))n(n+1)(1-\nu)\frac{R^n}{\rho^{n+3}})\sin n\phi=\frac{2n\pi(\nu-1)(\nu+3)}{R^2}\sin n\phi$

Continue

		Interior		Exterior
$V_v(s,x)$	Degenerate kernel	$V_v^i(R,\theta;\rho,\phi)=$ $\frac{2(\nu-1)(\nu+3)}{R^4}\cos(\theta-\phi)$ $+\sum_{m=2}^{\infty}[m^2(m+1)(\nu-1)(4+m(\nu-1))\frac{\rho^{m-1}}{R^{m+3}}$ $-m^2(m-1)(1-\nu)(4+m(1-\nu))\frac{\rho^{m-3}}{R^{m+1}}]\cos m(\theta-\phi),\ R>\rho$		$V_v^e(R,\theta;\rho,\phi)=$ $\frac{2(\nu-1)(3+\nu)}{\rho^4}\cos(\theta-\phi)$ $+\sum_{m=2}^{\infty}[m^2(m-1)(\nu-1)(4+m(1-\nu))\frac{R^{m-3}}{\rho^{m+1}}$ $+m^2(m+1)(1-\nu)(m(1-\nu)-4)\frac{R^{m-1}}{\rho^{m+3}}]\cos m(\theta-\phi),\ \rho>R$
	Orthogonal process	$\int_0^{2\pi}[V_v^i][1]Rd\theta=0,\ \rho>R$ $\int_0^{2\pi}[V_v^i][\cos\theta]Rd\theta=\pi R\frac{2(\nu-1)(3+\nu)}{R^4}\cos\phi,\ \rho>R$ $\int_0^{2\pi}[V_v^i][\sin\theta]Rd\theta=\pi R\frac{2(\nu-1)(3+\nu)}{R^4}\sin\phi,\ \rho>R$ $\int_0^{2\pi}[V_v^i][\cos n\theta]Rd\theta=\pi R(n^2(n+1)(\nu-1)(4+n(\nu-1))\frac{\rho^{n-1}}{R^{n+3}}$ $-n^2(n-1)(1-\nu)(4+n(1-\nu))\frac{\rho^{n-3}}{R^{n+1}})\cos n\phi,\ \rho>R$ $\int_0^{2\pi}[V_v^i][\sin n\theta]Rd\theta=\pi R(n^2(n+1)(\nu-1)(4+n(\nu-1))\frac{\rho^{n-1}}{R^{n+3}}$ $-n^2(n-1)(1-\nu)(4+n(1-\nu))\frac{\rho^{n-3}}{R^{n+1}})\sin n\phi,\ \rho>R$		$\int_0^{2\pi}[V_v^e][1]Rd\theta=0,\ \rho>R$ $\int_0^{2\pi}[V_v^e][\cos\theta]Rd\theta=\pi R\frac{2(\nu-1)(3+\nu)}{\rho^4}\cos\phi,\ \rho>R$ $\int_0^{2\pi}[V_v^e][\sin\theta]Rd\theta=\pi R\frac{2(\nu-1)(3+\nu)}{\rho^4}\sin\phi,\ \rho>R$ $\int_0^{2\pi}[V_v^e][\cos n\theta]Rd\theta=\pi R(n^2(n-1)(\nu-1)(4+n(1-\nu))\frac{R^{n-3}}{\rho^{n+1}}$ $+n^2(n+1)(1-\nu)(n(1-\nu)-4)\frac{R^{n-1}}{\rho^{n+3}})\cos n\phi,\ \rho>R$ $\int_0^{2\pi}[V_v^e][\sin n\theta]Rd\theta=\pi R(n^2(n-1)(\nu-1)(4+n(1-\nu))\frac{R^{n-3}}{\rho^{n+1}}$ $+n^2(n+1)(1-\nu)(n(1-\nu)-4)\frac{R^{n-1}}{\rho^{n+3}})\cos n\phi\sin n\phi,\ \rho>R$
	Limiting behavior across the boundary	$\lim_{\rho\to R}0=0$ $\lim_{\rho\to R}\pi R(\frac{2(\nu-1)(3+\nu)}{R^4})\cos\phi=\frac{2\pi(\nu+3)(\nu-1)}{R^3}\cos\phi$ $\lim_{\rho\to R}\pi R(\frac{2(\nu-1)(3+\nu)}{R^4})\sin\phi=\frac{2\pi(\nu+3)(\nu-1)}{R^3}\sin\phi$ $\lim_{\rho\to R}\pi R((n^2(n+1)(\nu-1)(4+n(\nu-1))\frac{\rho^{n-1}}{R^{n+3}}$ $-n^2(n-1)(1-\nu)(4+n(1-\nu))\frac{\rho^{n-3}}{R^{n+1}})\cos n\phi=\frac{2n^3\pi(\nu-1)(\nu+3)}{R^3}\cos n\phi$ $\lim_{\rho\to R}\pi R((n^2(n+1)(\nu-1)(4+n(\nu-1))\frac{\rho^{n-1}}{R^{n+3}}$ $-n^2(n-1)(1-\nu)(4+n(1-\nu))\frac{\rho^{n-3}}{R^{n+1}})\sin n\phi=\frac{2n^3\pi(\nu-1)(\nu+3)}{R^3}\sin n\phi$	Pseudo-continuous $(\rho^-\to R\leftarrow\rho^+)$	$\lim_{\rho\to R}0=0$ $\lim_{\rho\to R}\pi R(\frac{2(\nu-1)(3+\nu)}{\rho^4})\cos\phi=\frac{2\pi(\nu-1)(\nu+3)}{R^3}\cos\phi$ $\lim_{\rho\to R}\pi R(\frac{2(\nu-1)(3+\nu)}{\rho^4})\sin\phi=\frac{2\pi(\nu-1)(\nu+3)}{R^3}\sin\phi$ $\lim_{\rho\to R}\pi R(n^2(n-1)(\nu-1)(4+n(1-\nu))\frac{R^{n-3}}{\rho^{n+1}}$ $+n^2(n+1)(1-\nu)(n(1-\nu)-4)\frac{R^{n-1}}{\rho^{n+3}})\cos n\phi=\frac{2n^3\pi(\nu-1)(\nu+3)}{R^3}\cos n\phi$ $\lim_{\rho\to R}\pi R(n^2(n-1)(\nu-1)(4+n(1-\nu))\frac{R^{n-3}}{\rho^{n+1}}$ $+n^2(n+1)(1-\nu)(n(1-\nu)-4)\frac{R^{n-1}}{\rho^{n+3}})\sin n\phi=\frac{2n^3\pi(\nu-1)(\nu+3)}{R^3}\sin n\phi$

Table 3-3 The definitions of the moment and shear force (a) Szilard, (b) Leissa, (c) Chen et al. and (d) Adewale.

	(a) Szilard	(b) Leissa	(c) Chen et al.	(d) Adewale
Displacement	u	u	u	$R_m(r)\cos m\theta$
Moment	$-D\left[\frac{\partial^2 u}{\partial r^2}+\nu\left(\frac{1}{r^2}\frac{\partial^2 u}{\partial \varphi^2}+\frac{1}{r}\frac{\partial u}{\partial r}\right)\right]$	$-D\left[\frac{\partial^2 u}{\partial r^2}+\nu\left(\frac{1}{r^2}\frac{\partial^2 u}{\partial \theta^2}+\frac{1}{r}\frac{\partial u}{\partial r}\right)\right]$	$\nu\nabla_x^2 u+(1-\nu)\frac{\partial^2 u}{\partial n_x^2}$	$\frac{\partial^2 R_m}{\partial r^2}+\nu\left(\frac{1}{r}\frac{\partial R_m}{\partial r}-\frac{m^2}{r^2}R_m\right)$
Shear	$-D\left[\frac{\partial}{\partial r}\nabla_r^2 u+\frac{1-\nu}{r}\frac{\partial}{\partial \varphi}\left(\frac{1}{r}\frac{\partial^2 u}{\partial r\partial \varphi}-\frac{1}{r^2}\frac{\partial u}{\partial \varphi}\right)\right]$	$-D\frac{\partial}{\partial r}\left(\nabla^2 u\right)+\frac{1}{r}\frac{\partial}{\partial \theta}\left[-D(1-\nu)\frac{\partial}{\partial r}\left(\frac{1}{r}\frac{\partial u}{\partial \theta}\right)\right]$	$\frac{\partial \nabla_x^2 u}{\partial n_x}+(1-\nu)\frac{\partial}{\partial t_x}\left[\frac{\partial}{\partial n_x}\left(\frac{\partial u}{\partial t_x}\right)\right]$	$\frac{\partial^3 R_m}{\partial r^3}-\frac{1}{r^2}\frac{\partial R_m}{\partial r}+\frac{1}{r}\frac{\partial^2 R_m}{\partial r^2}-\frac{m^2}{r^2}\frac{\partial R_m}{\partial r}$
Derivation of the moment according to the Adewale's form	$\nu\left(\frac{\partial^2(R_m\cos m\theta)}{\partial r^2}+\frac{1}{r}\frac{\partial(R_m\cos m\theta)}{\partial r}+\frac{1}{r^2}\frac{\partial^2(R_m\cos m\theta)}{\partial \theta^2}\right)+(1-\nu)\frac{\partial^2(R_m\cos m\theta)}{\partial r^2}=\frac{\partial^2 R_m}{\partial r^2}+\nu\left(\frac{1}{r}\frac{\partial R_m}{\partial r}-\frac{m^2}{r^2}R_m\right)$			
Derivation of the shear according to the Adewale's form	$\frac{\partial}{\partial r}\left[\frac{\partial^2(R_m\cos m\theta)}{\partial r^2}+\frac{1}{r}\frac{\partial(R_m\cos m\theta)}{\partial r}+\frac{1}{r^2}\frac{\partial^2(R_m\cos m\theta)}{\partial \theta^2}\right]+(1-\nu)\frac{1}{r}\frac{\partial}{\partial \theta}\left[\frac{\partial}{\partial r}\left(\frac{1}{r}\frac{\partial(R_m\cos m\theta)}{\partial \theta}\right)\right]$ $=\frac{\partial}{\partial r}\left[\frac{\partial^2 R_m}{\partial r^2}+\frac{1}{r}\frac{\partial R_m}{\partial r}-\frac{m^2}{r^2}R_m\right]+(1-\nu)\frac{1}{r}\frac{\partial}{\partial \theta}\left[\frac{\partial}{\partial r}\left(-\frac{m}{r}R_m\sin m\theta\right)\right]$ $=\frac{\partial^3 R_m}{\partial r^3}-\frac{1}{r^2}\frac{\partial R_m}{\partial r}+\frac{1}{r}\frac{\partial^2 R_m}{\partial r^2}+\frac{2m^2}{r^3}R_m-\frac{m^2}{r^2}\frac{\partial R_m}{\partial r}+(1-\nu)\left[\frac{m^2}{r^3}R_m-\frac{m^2}{r^2}\frac{\partial R_m}{\partial r}\right]$			

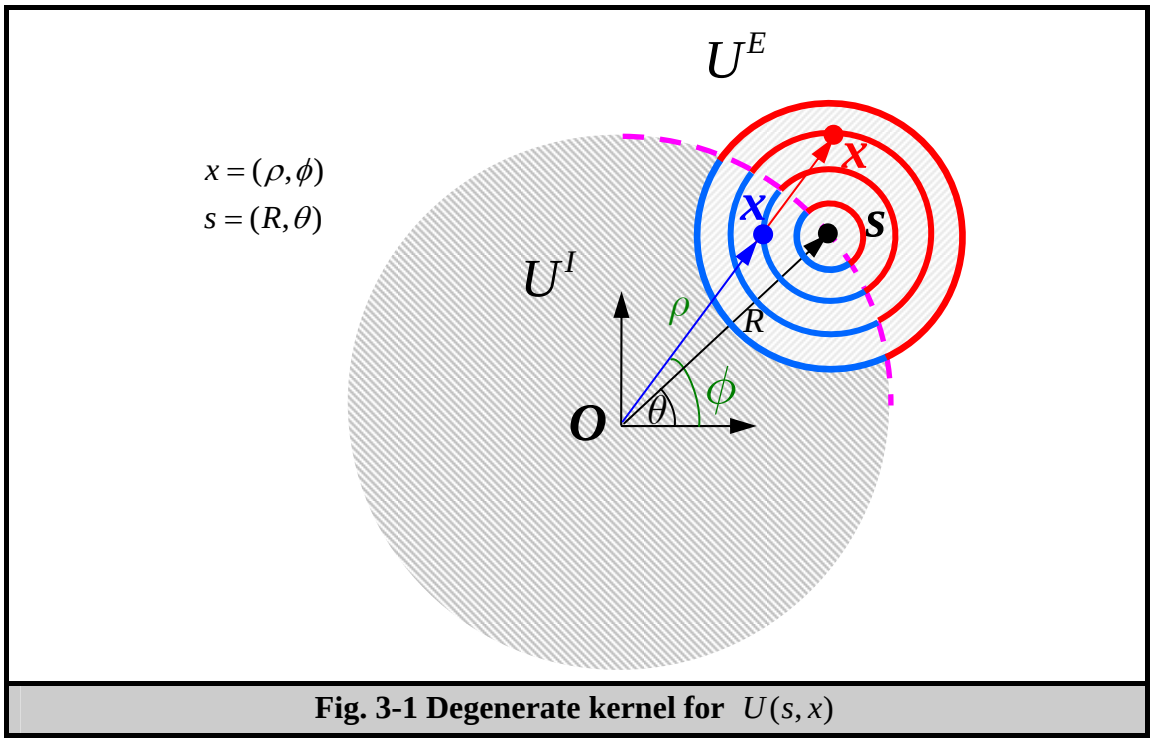

Fig. 3-1 Degenerate kernel for $U(s,x)$

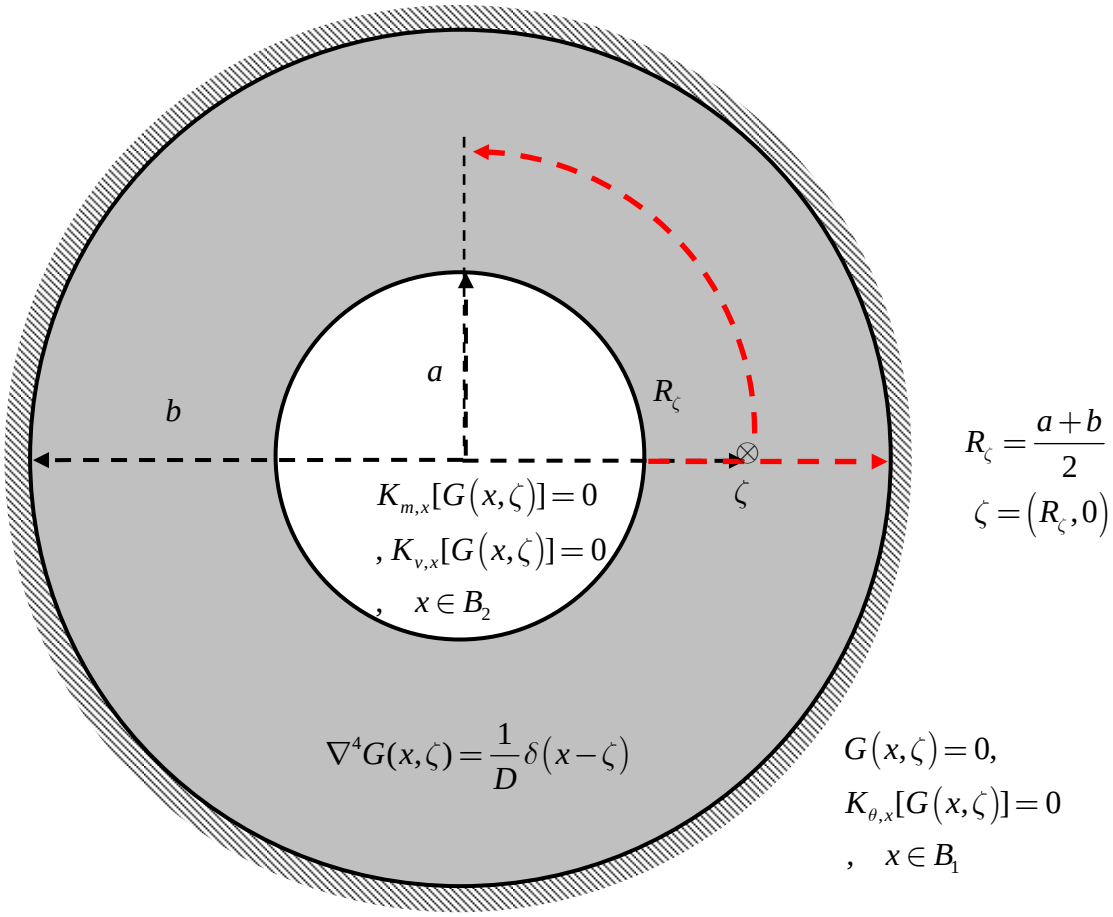

Fig. 3-2 Green's function of the biharmonic equation for the annular plate problem

R_ζ **is the distance between the source and the center of the circle.**

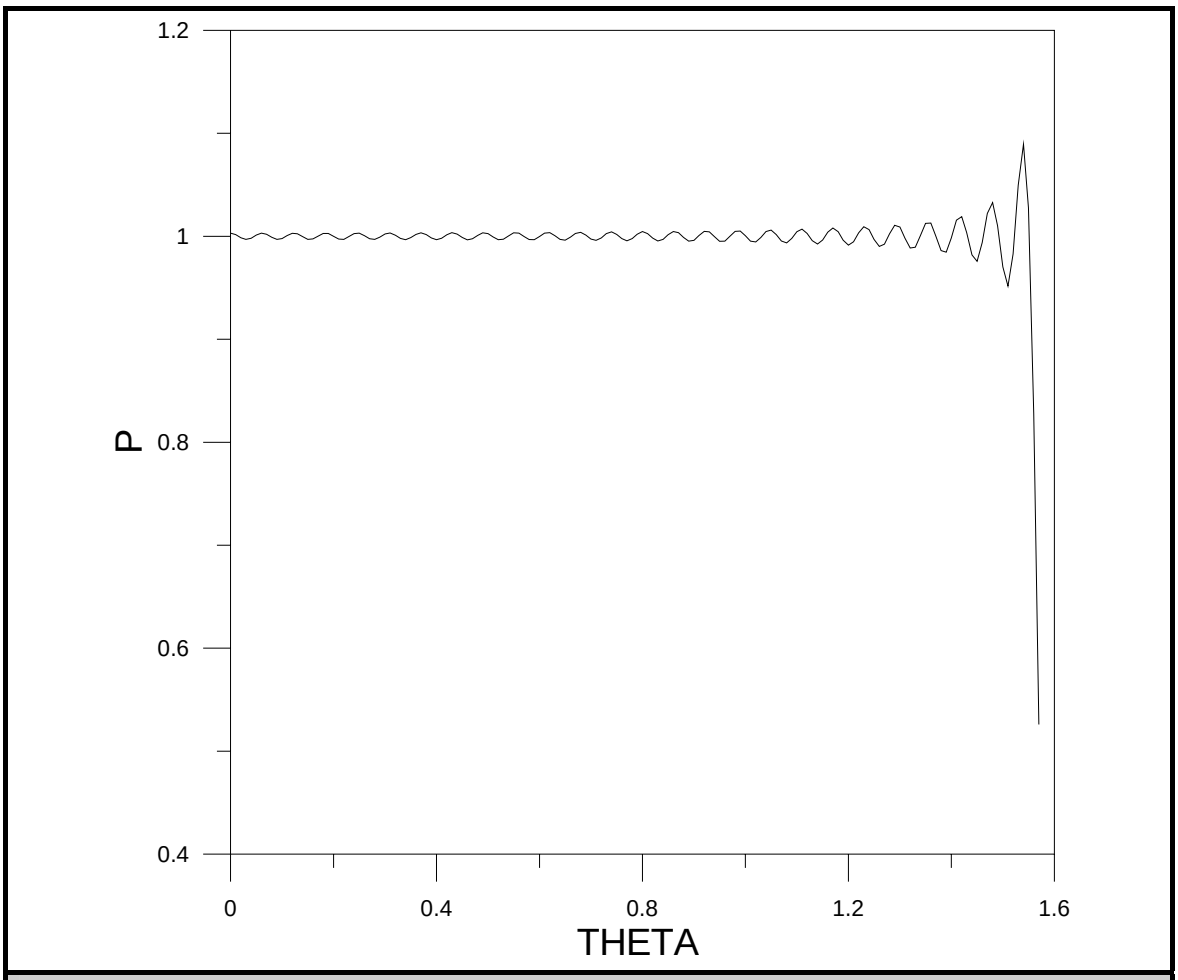

Fig. 3-3 Simulation of a concentrated force by Adewale [1] ($M = 101$)

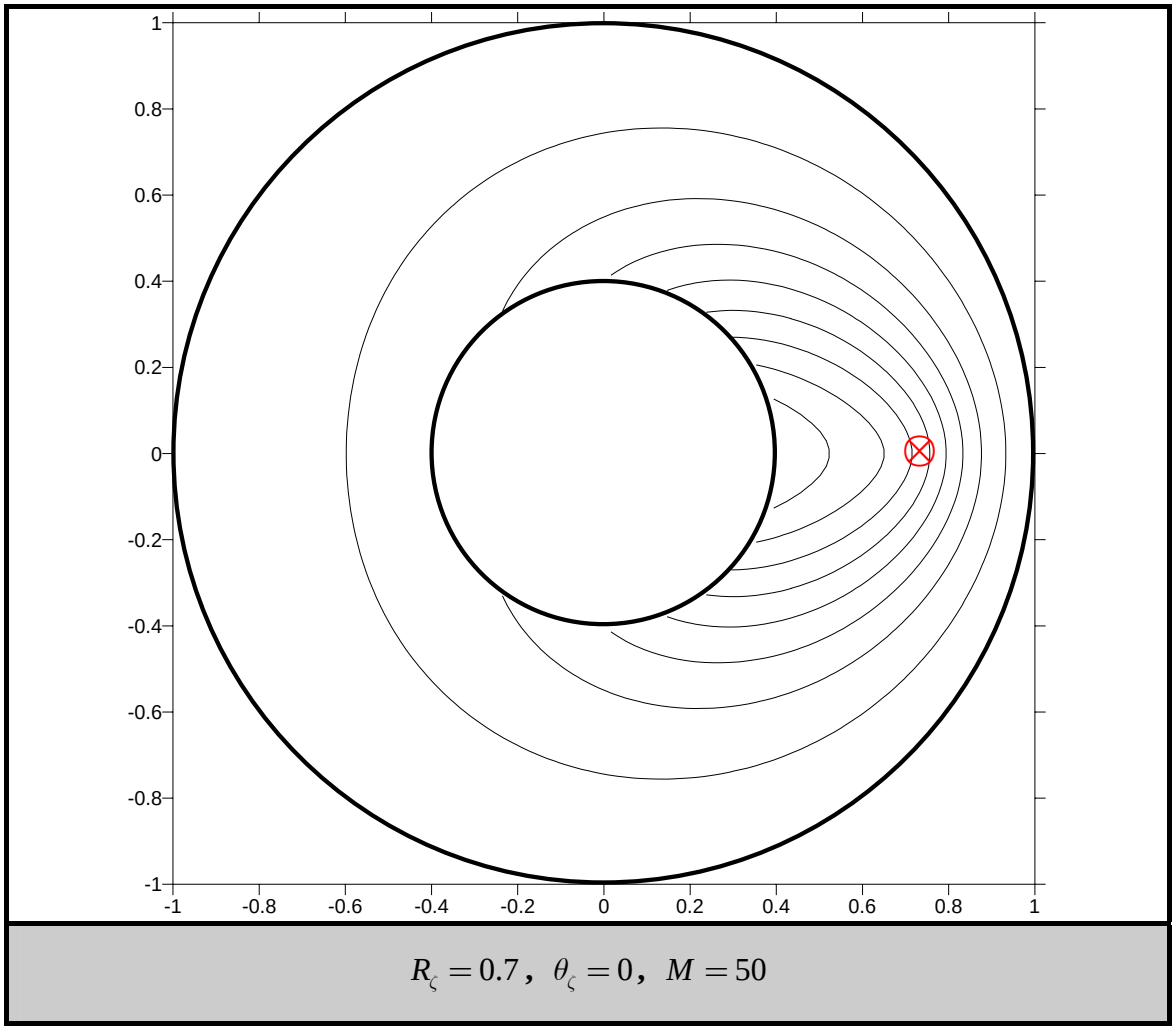

Fig. 3-4 Displacement contour of the Green's function of the biharmonic equation for the fixed-free plate problem using the present method

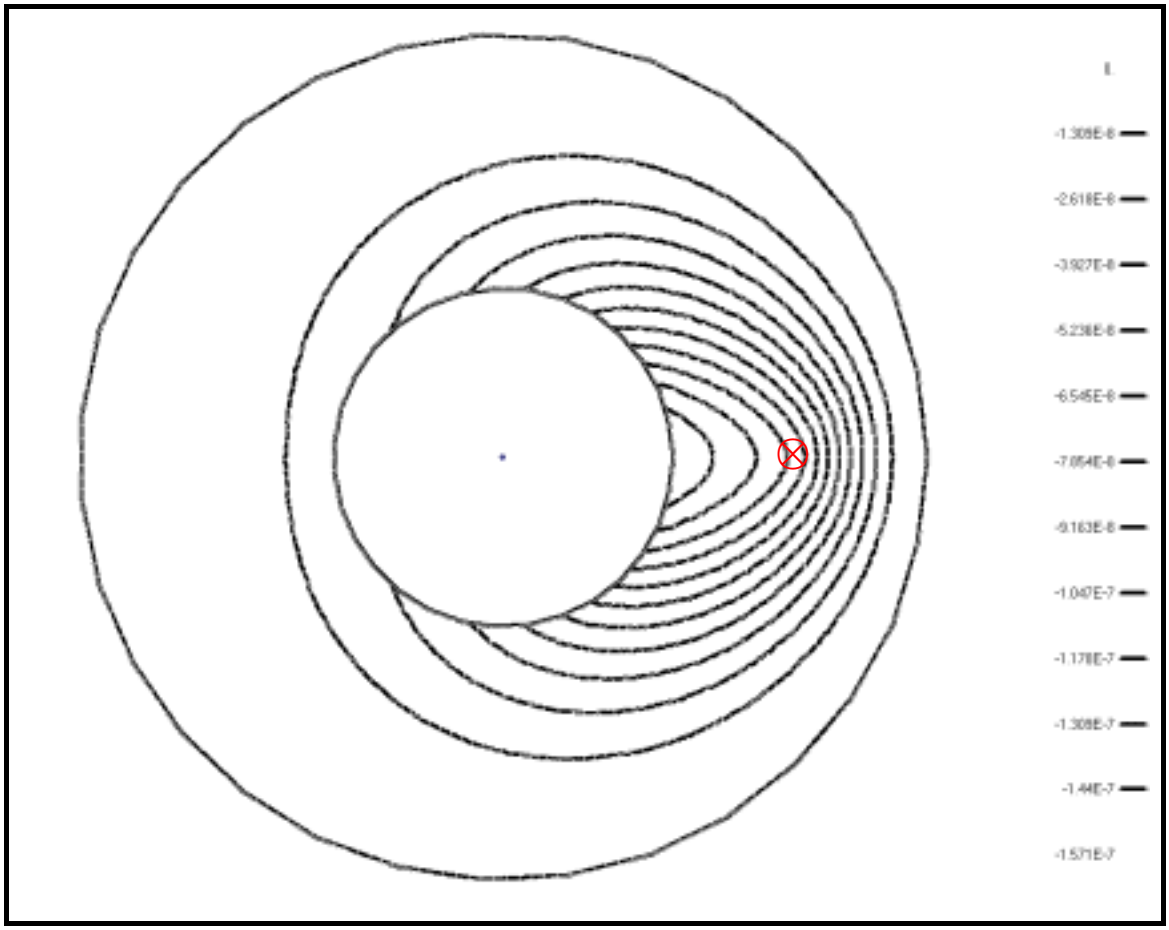

Fig. 3-5 Displacement contour of Green's function of the biharmonic equation for fixed-free plate problem using the ABAQUS program

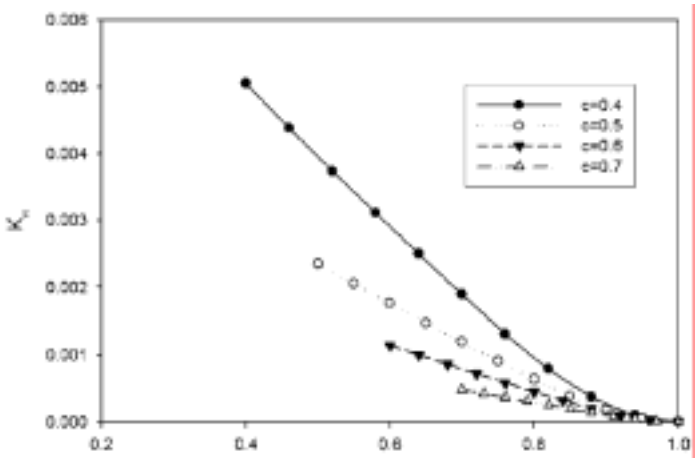

(a) Adewale's result

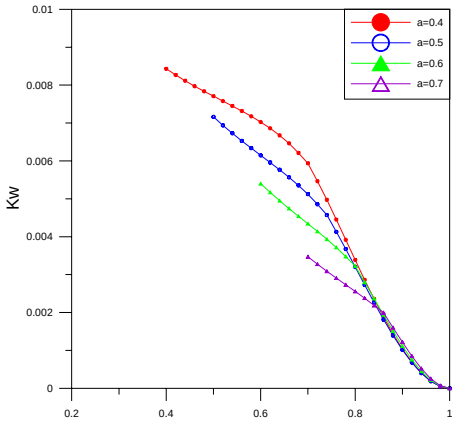

(b) FEM (ABAQUS)

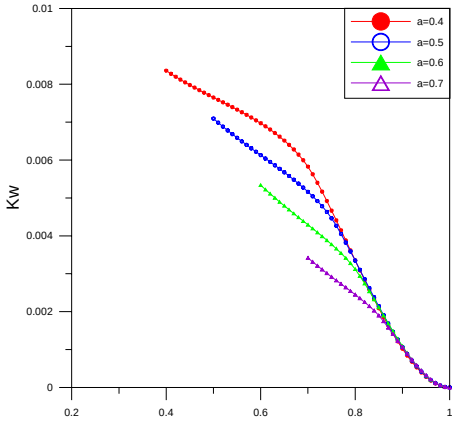

(c) Present method $(M=50)$

Fig. 3-6 Variation of deflection coefficients versus radial position

$(a=0.4,\ b=1.0,\ R_\zeta=0.7,\ D=1,\ \nu=0.3,\ k_w=\dfrac{wD}{P})$

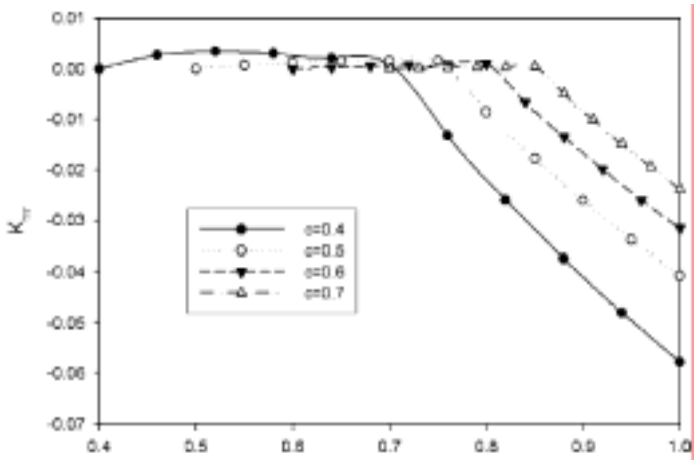

(a) Adewale's result

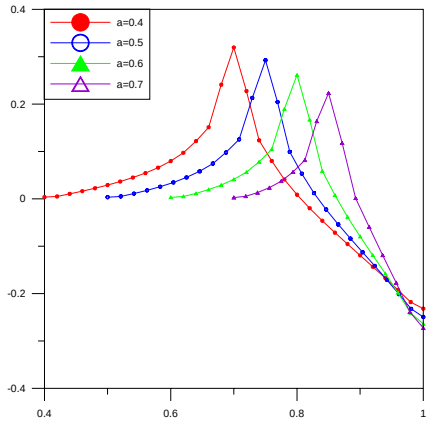

(b) FEM (ABAQUS)

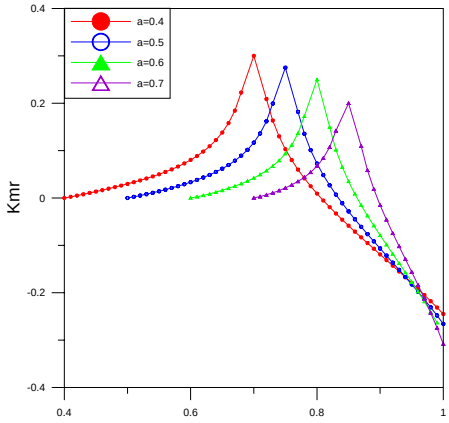

(c) Present method $(M=50)$

Fig. 3-7 Variation of moment coefficient versus radial position

$(a=0.4,\ b=1.0,\ R_{\zeta}=0.7,\ D=1,\ \nu=0.3,\ k_{mr}=\dfrac{M_r D}{P})$

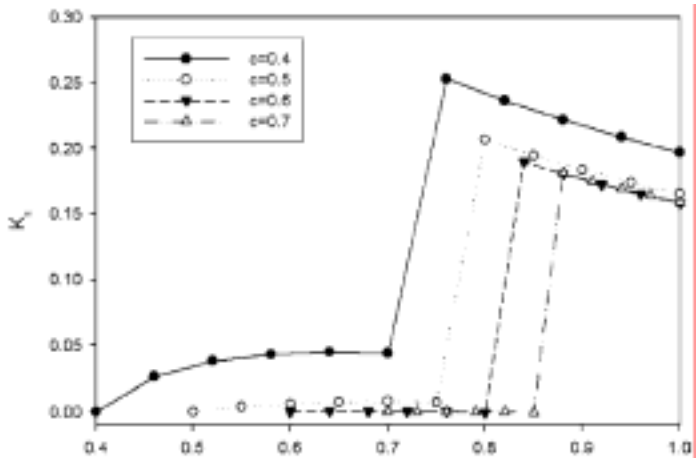

(a) Adewale's result

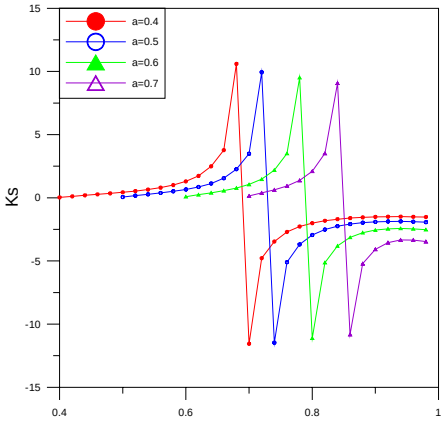

(b) FEM (ABAQUS)

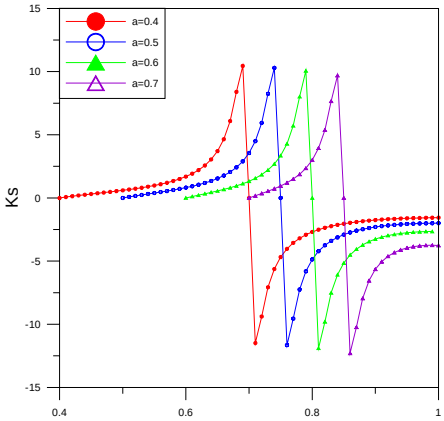

(c) Present method $(M=50)$

Fig. 3-8 Variation of shear force coefficient versus radial position

$(a=0.4,\ b=1.0,\ R_{\zeta}=0.7,\ D=1,\ \nu=0.3,\ k_s=\dfrac{M_s D}{P})$

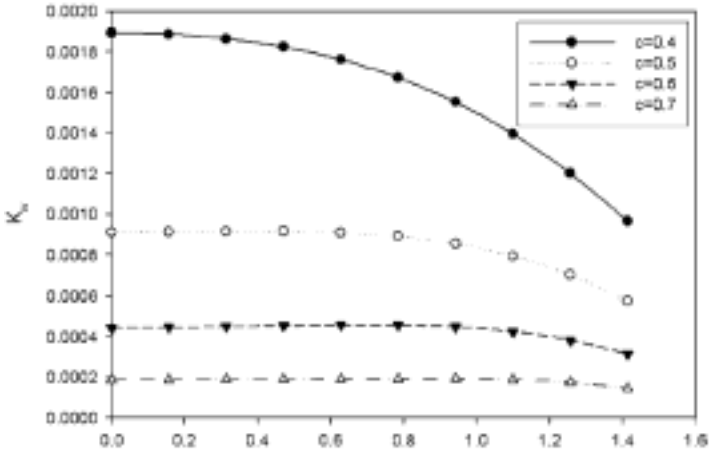

(a) Adewale's result

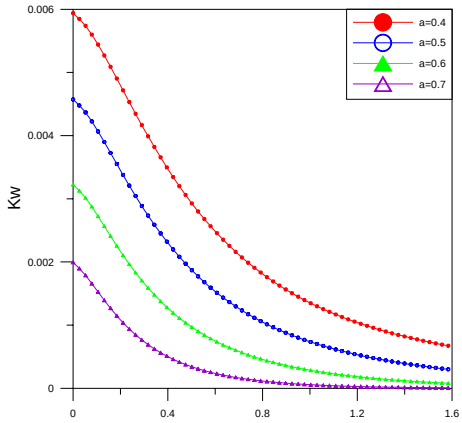

(b) FEM (ABAQUS) (Rad)

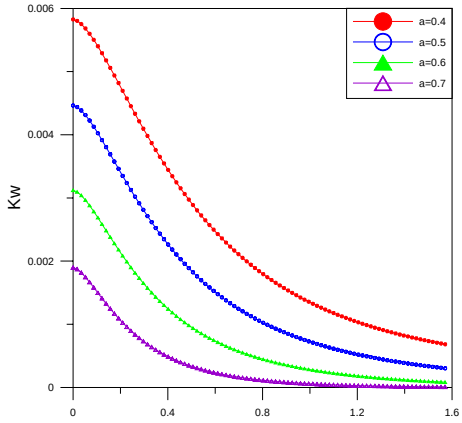

(c) Present method $(M=50)$ (Rad)

Fig. 3-9 Variation of deflection coefficient versus radial angle

($a=0.4$, $b=1.0$, $R_\zeta=0.7$, $D=1$, $\nu=0.3$, $k_w=\dfrac{wD}{P}$)

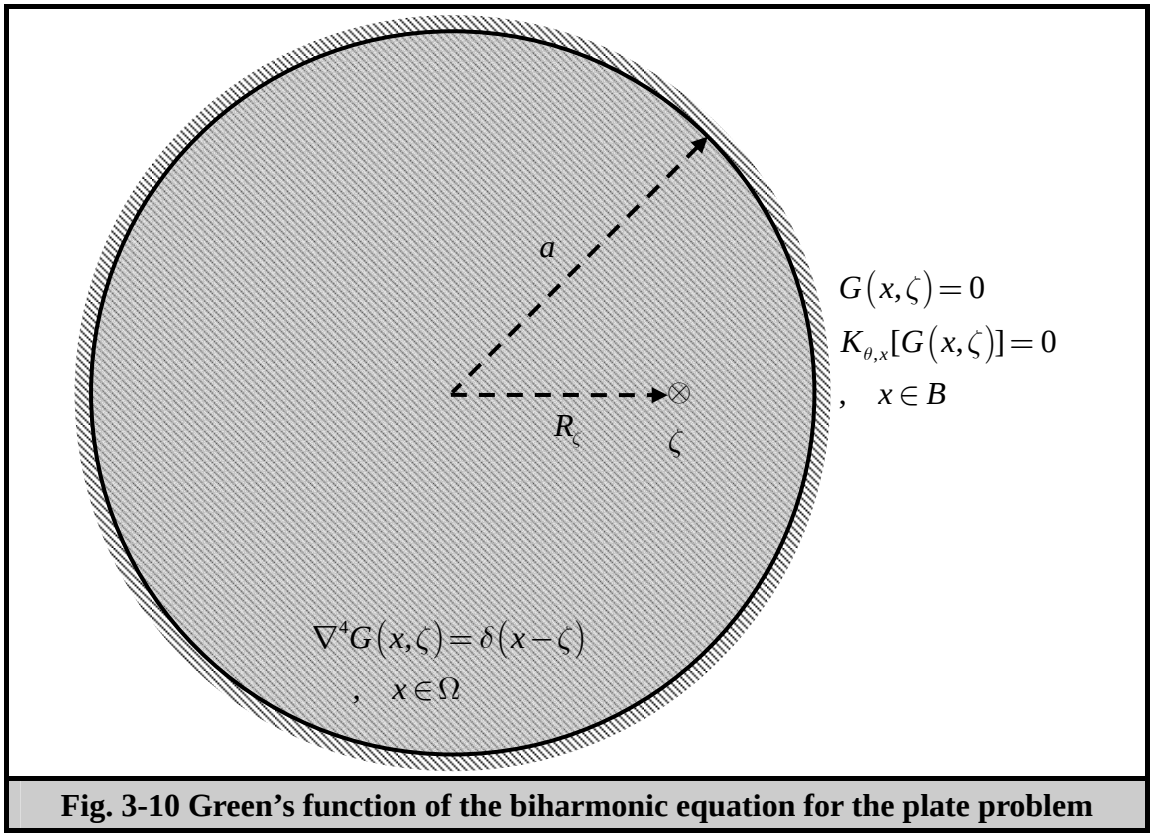

Fig. 3-10 Green's function of the biharmonic equation for the plate problem

R_s **is the distance between the source and the center of the circle.**

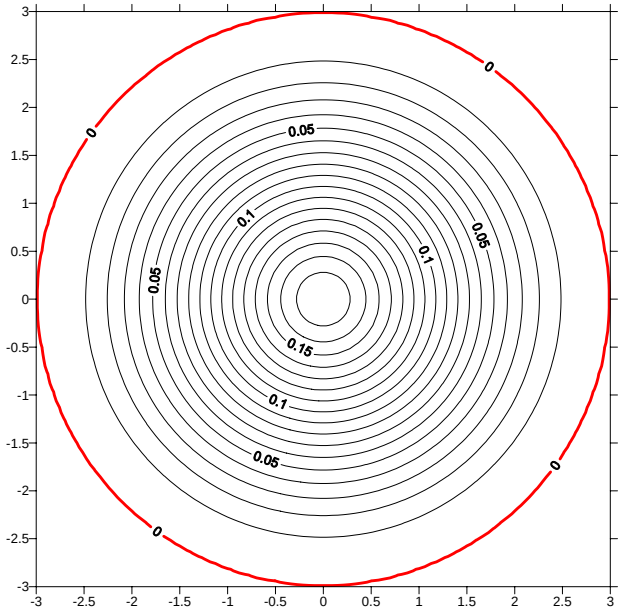

(a) Present method ($M = 1$)

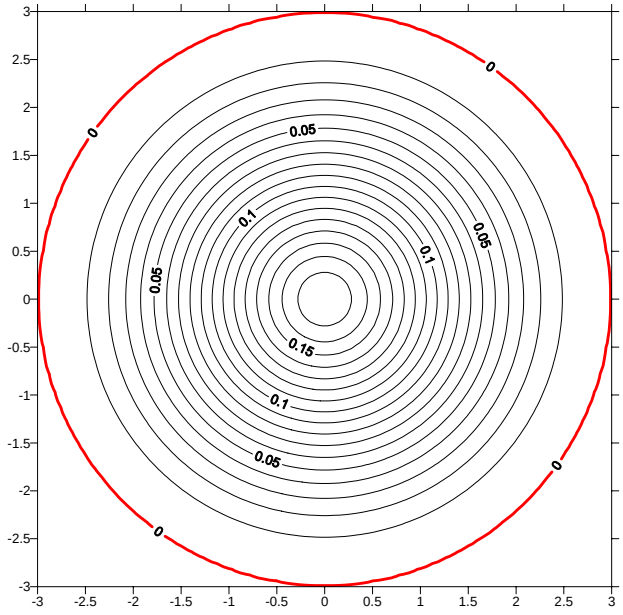

(b) Szilard's approach

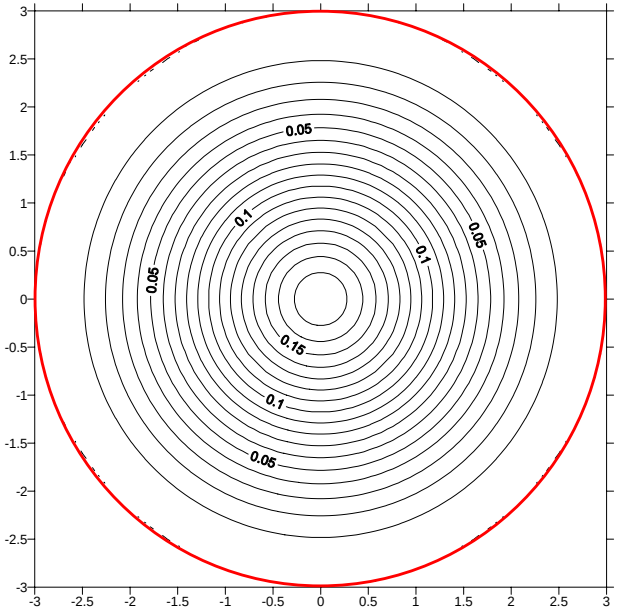

(c) Melnikov's approach

Fig. 3-11 Displacement contour of the Green's function of the biharmonic equation for the circular plate problem ($a = 3$)

Present method (Source at different directions)

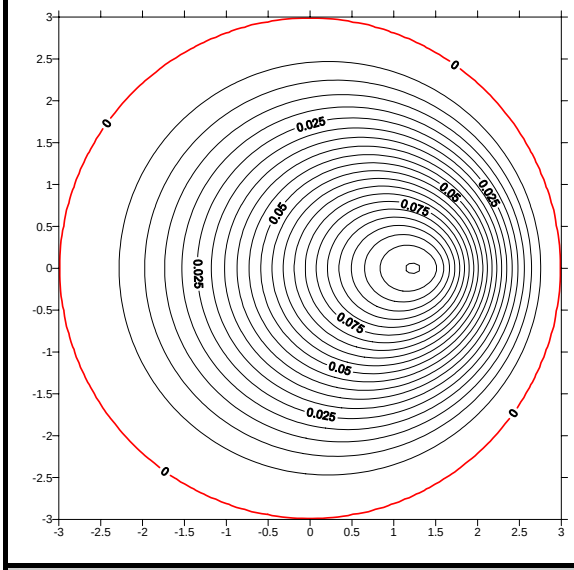

(a) $\theta_\zeta = 0$

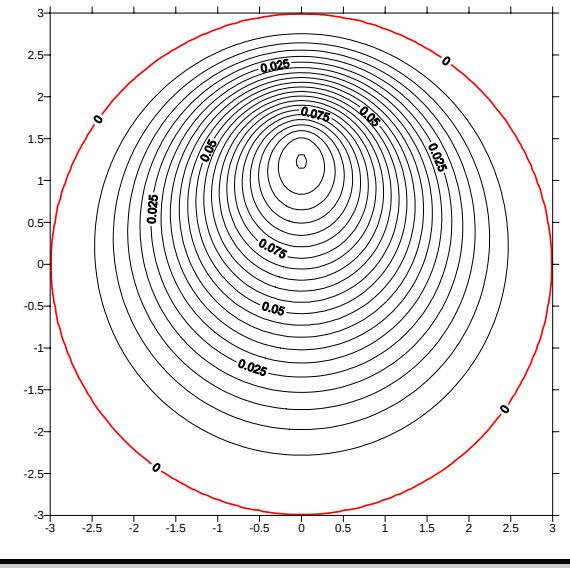

(b) $\theta_\zeta = \dfrac{\pi}{2}$

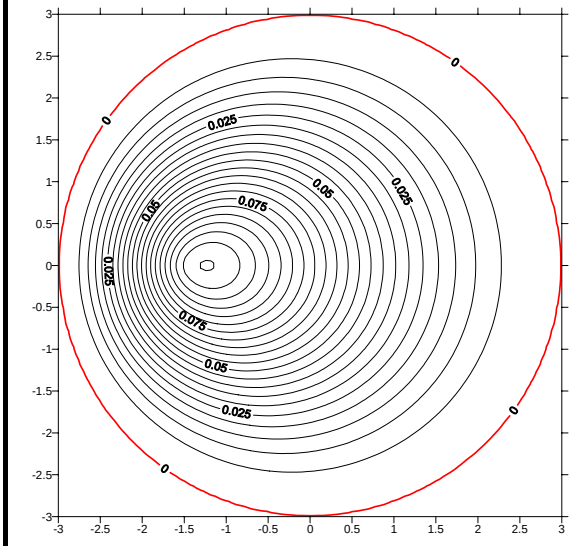

(c) $\theta_\zeta = \pi$

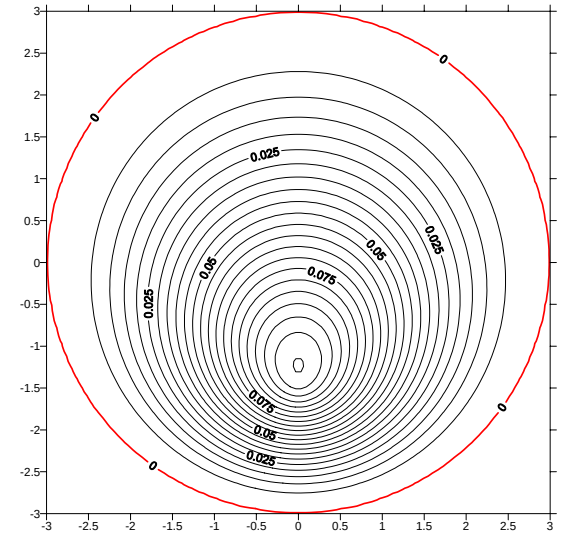

(d) $\theta_\zeta = \dfrac{3\pi}{2}$

Fig. 3-12 Displacement contour of the Green's function of the biharmonic equation for the circular problem using the present method ($a = 3$, $R_s = 1.5$ and $M = 50$)

Melnikov's approach (Source at different directions)

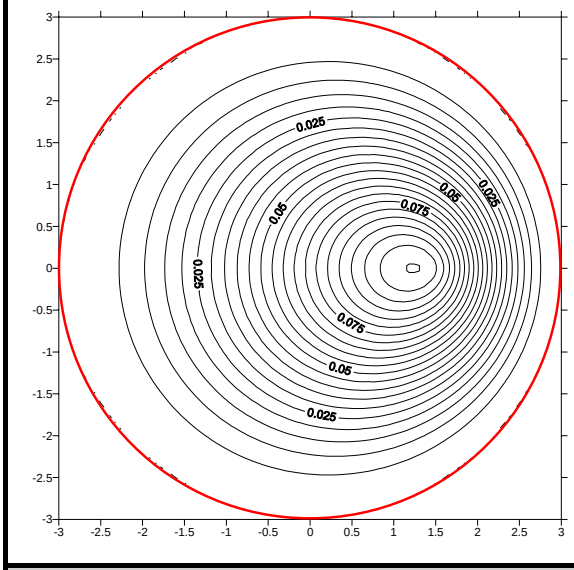

$\theta_\zeta = 0$

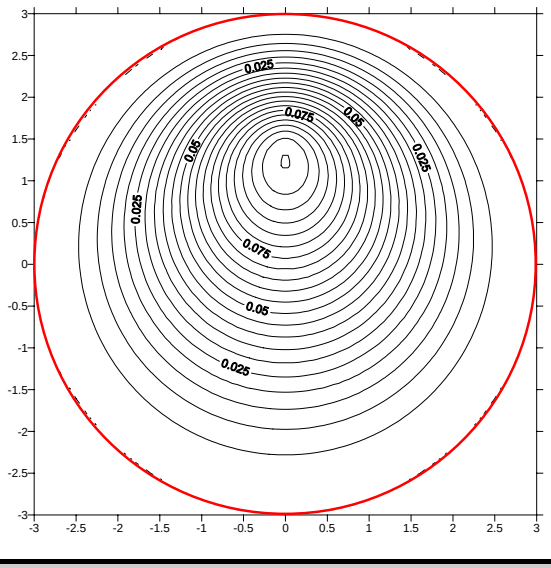

$\theta_\zeta = \frac{\pi}{2}$

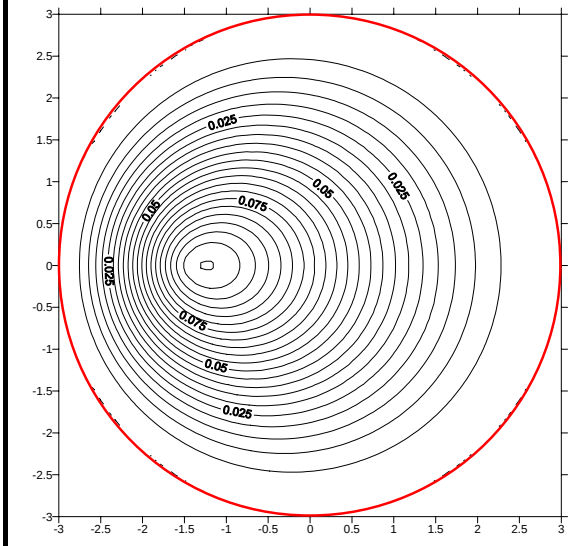

$\theta_\zeta = \pi$

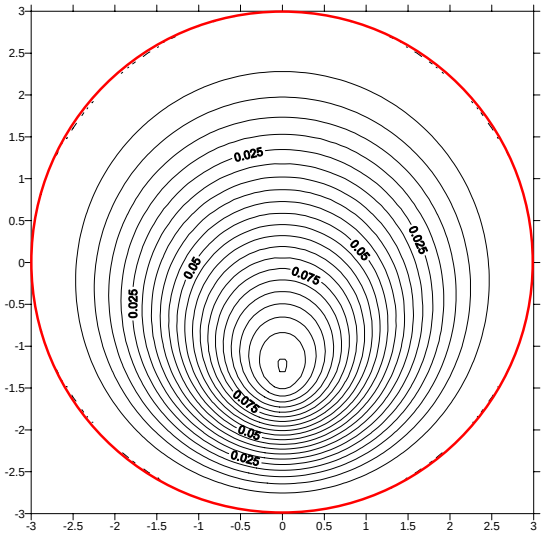

$\theta_\zeta = \frac{3\pi}{2}$

Fig. 3-13 Displacement contour of the Green's function of the biharmonic equation for the circular plate problem using the Melnikov's approach ($a = 3$ and $R_\zeta = 1.5$)

Present method (Source at different radial positions)

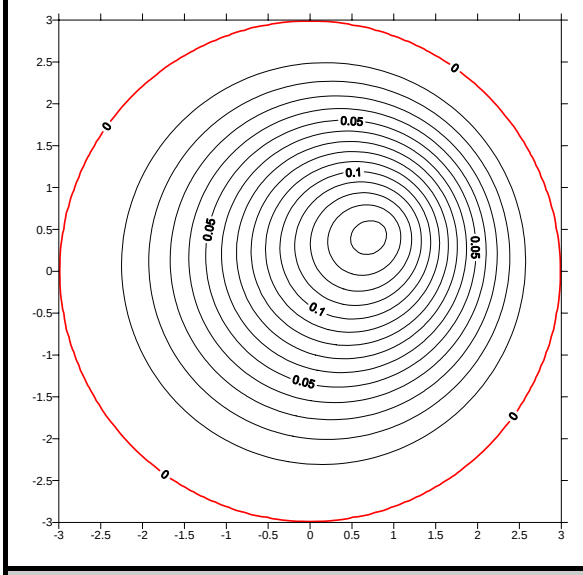

$R_\zeta = 1$

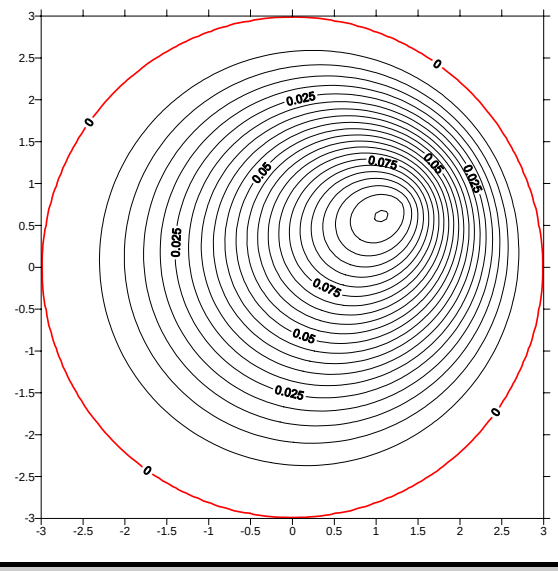

$R_\zeta = 1.5$

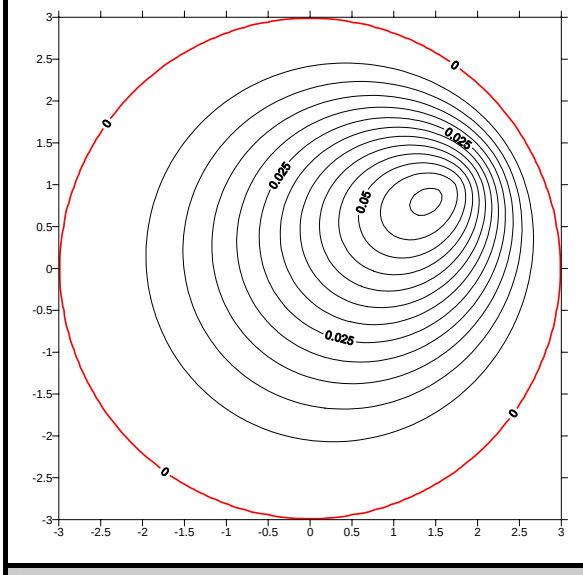

$R_\zeta = 2$

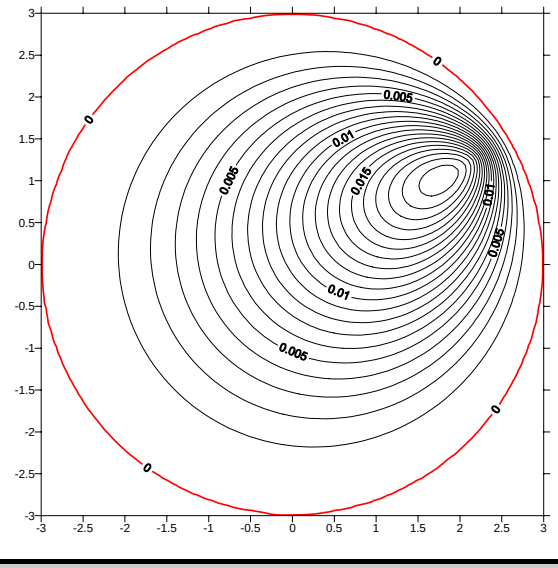

$R_\zeta = 2.5$

Fig. 3-14 Potential contour of the Green's function of the biharmonic equation for the circular plate problem using the present method ($a = 3, \theta_\zeta = \frac{\pi}{6}$ and $M = 50$)

Melnikov's approach (Source at different radial positions)

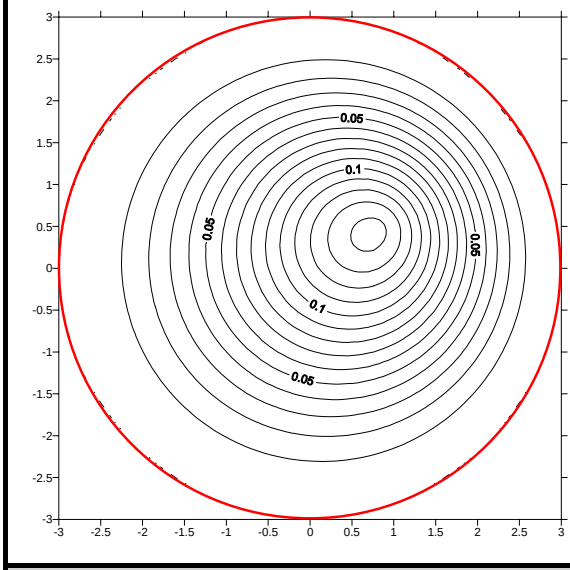

$R_\zeta = 1$

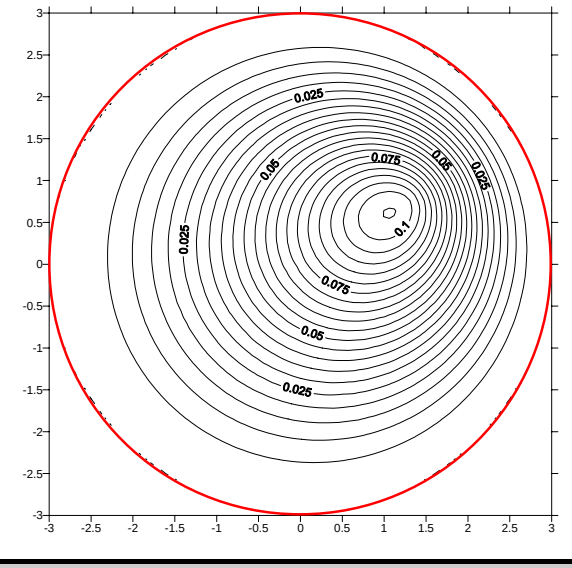

$R_\zeta = 1.5$

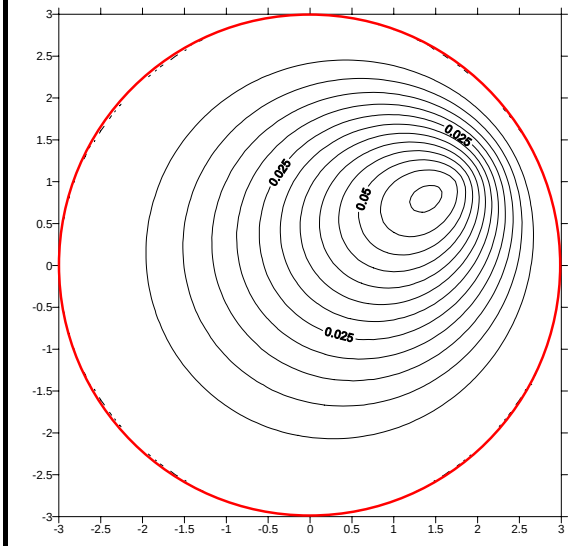

$R_\zeta = 2$

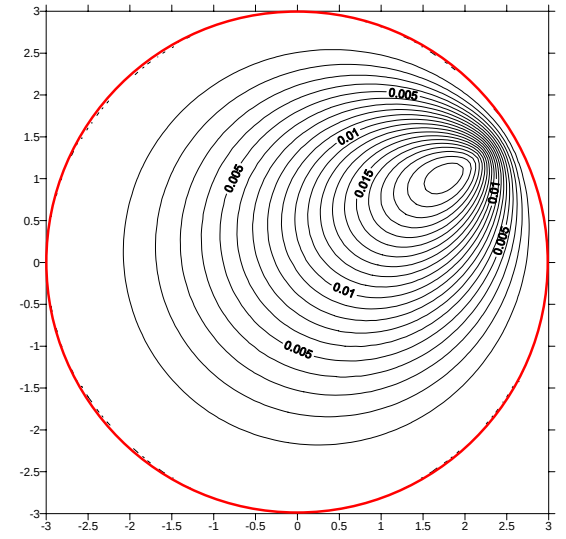

$R_\zeta = 2.5$

Fig. 3-15 Potential contour of the Green's function of the biharmonic equation for the circular plate problem using the Melnikov's approach ($a = 3$ and $\theta_\zeta = \frac{\pi}{6}$)

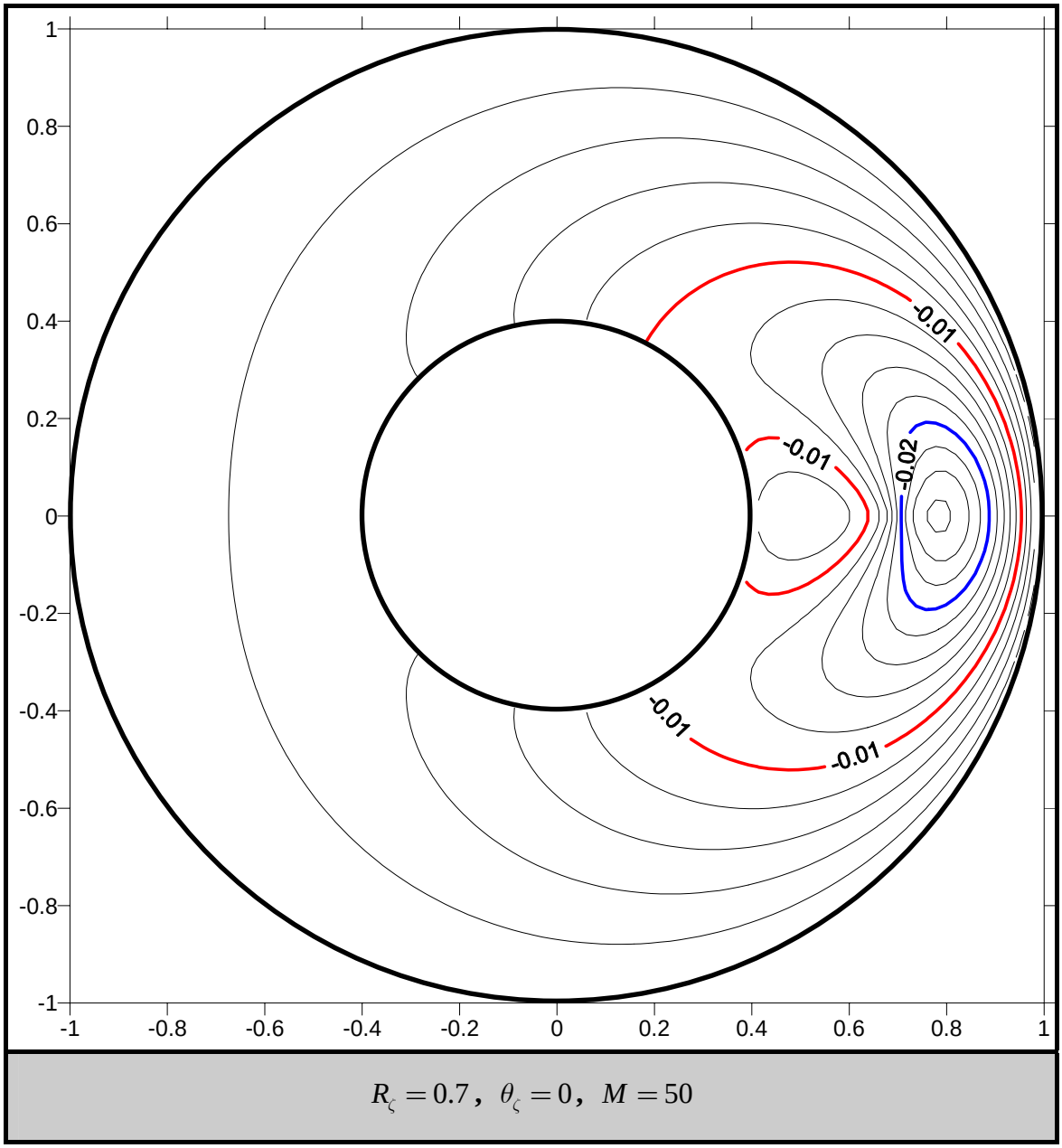

Fig. 3-16 Radial slope contour of the Green's function of the biharmonic equation for the fixed-free annular plate using the present method

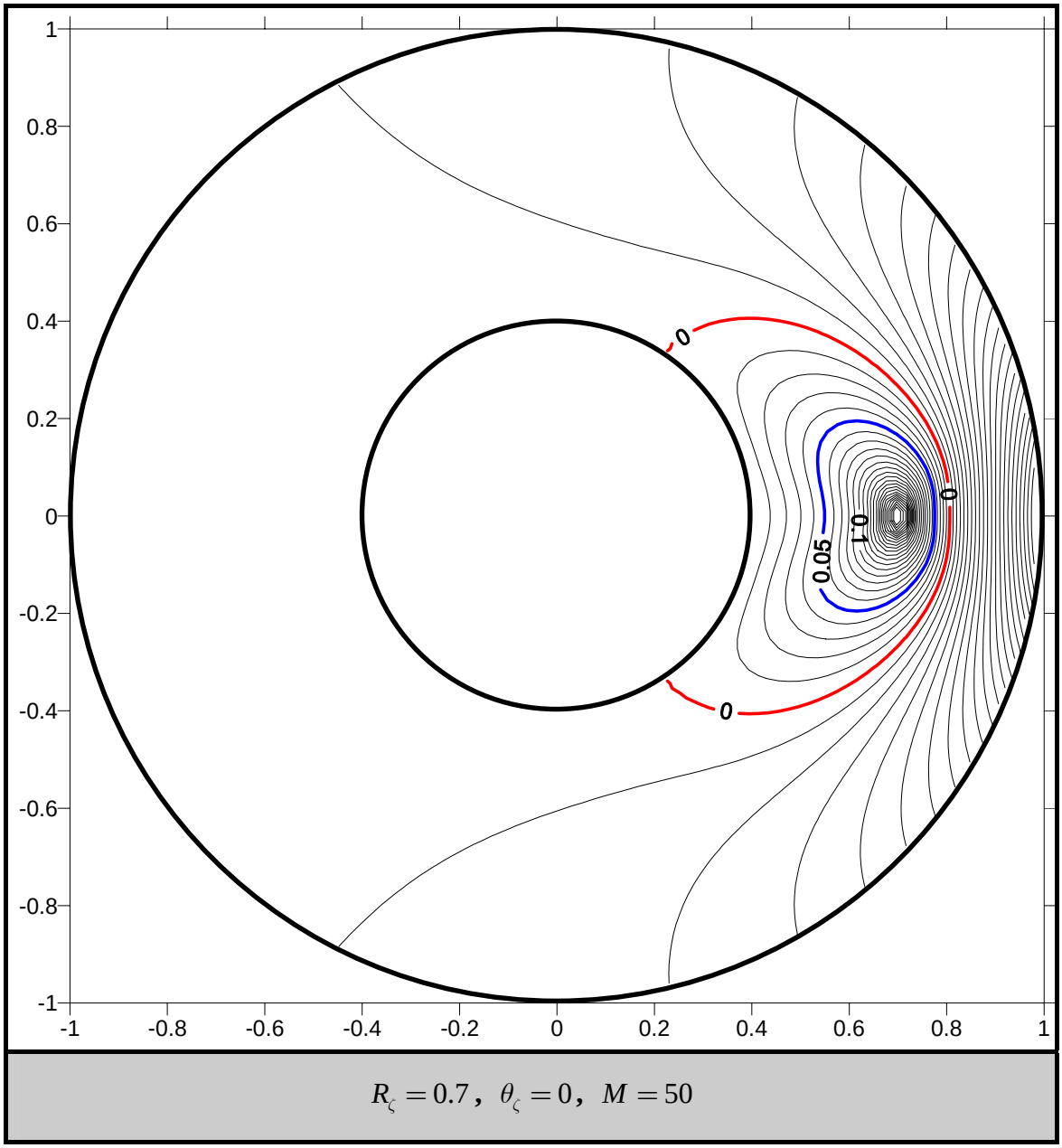

Fig. 3-17 Normal moment contour of the Green's function of the biharmonic equation for the fixed-free annular plate using the present method

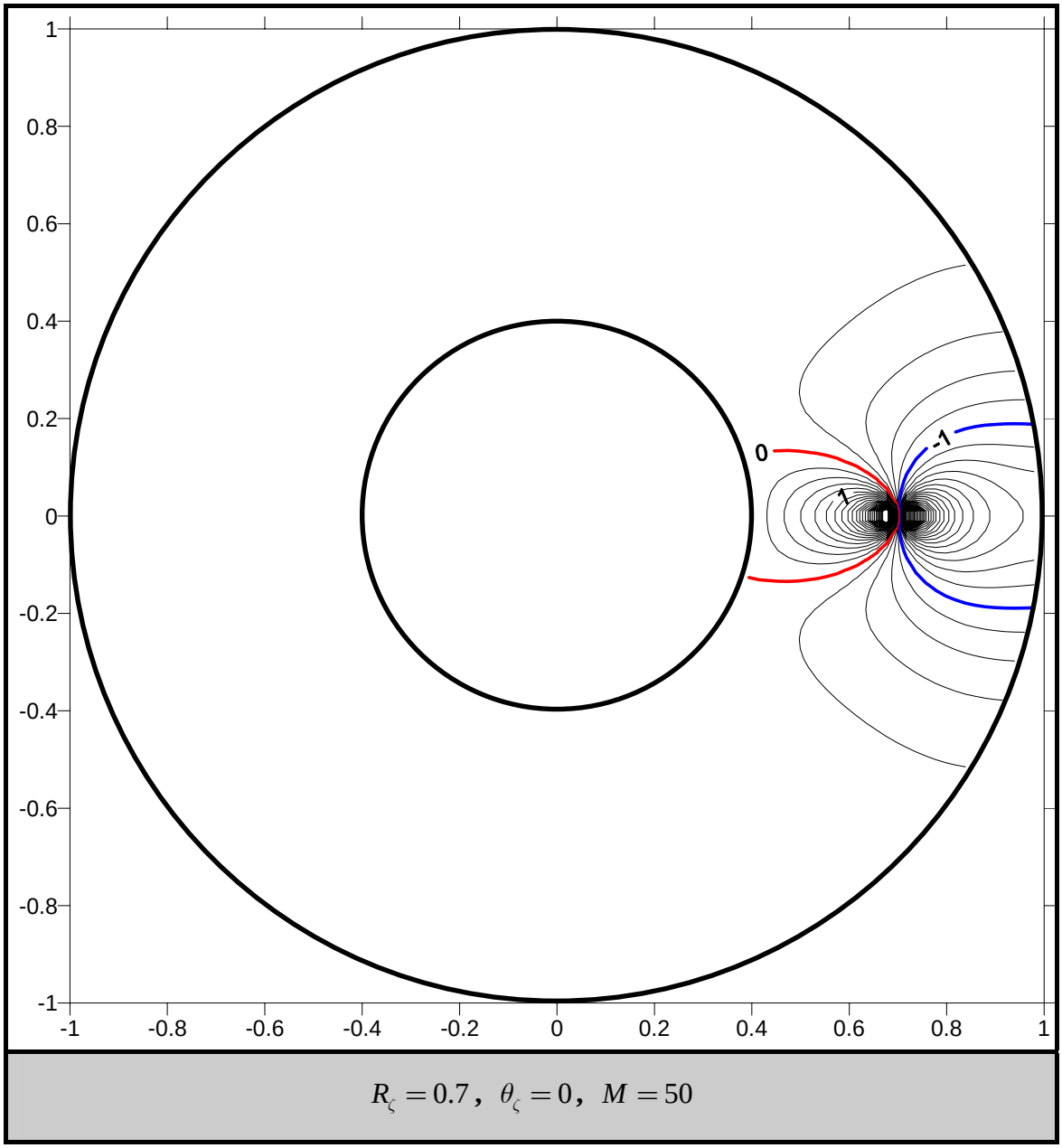

Fig. 3-18 Shear force contour of the Green's function of the biharmonic equation for the fixed-free annular plate using the present method

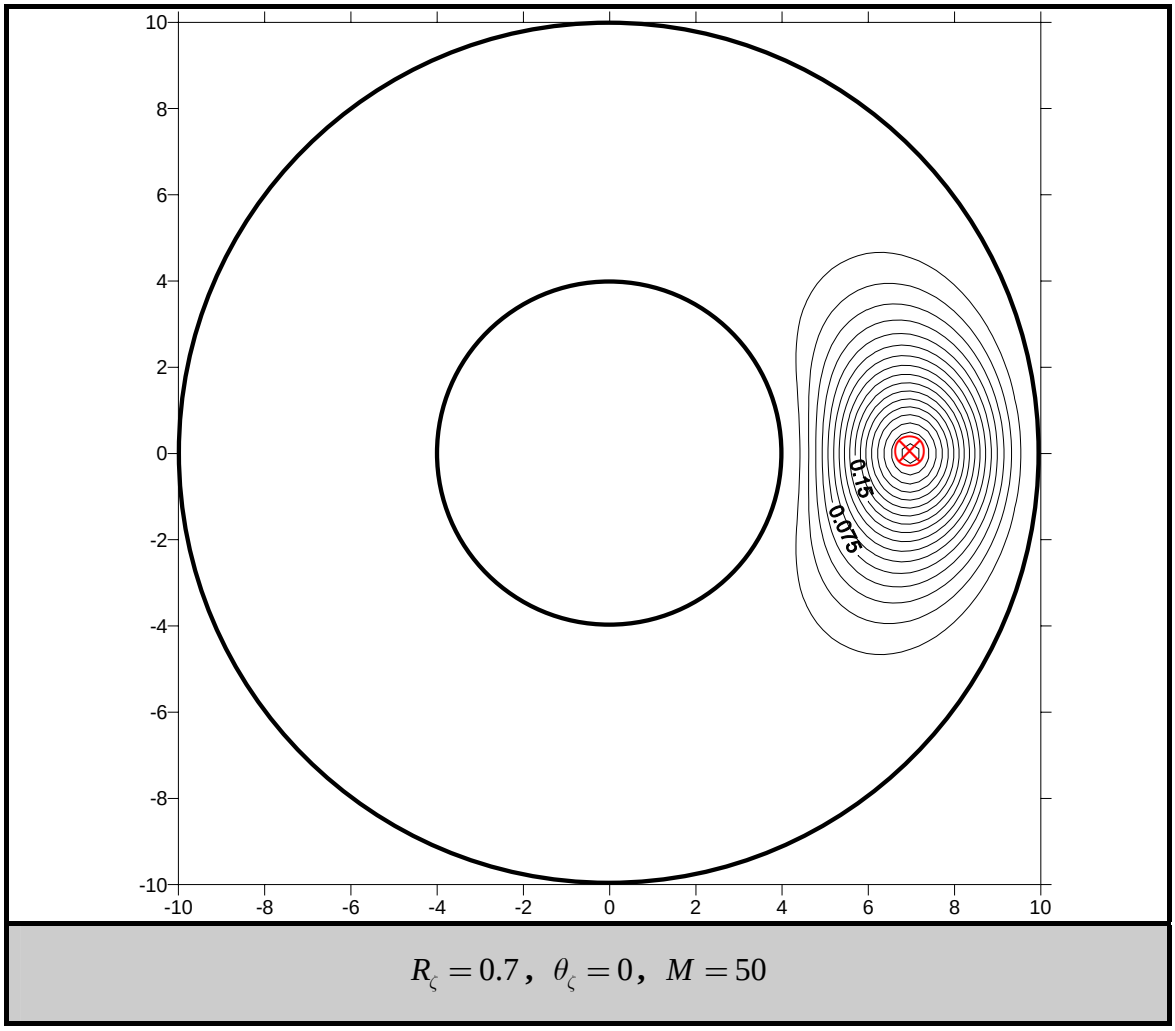

Fig. 3-19 Displacement contour of the Green's function of the biharmonic equation for the fixed-fixed annular plate using the present method

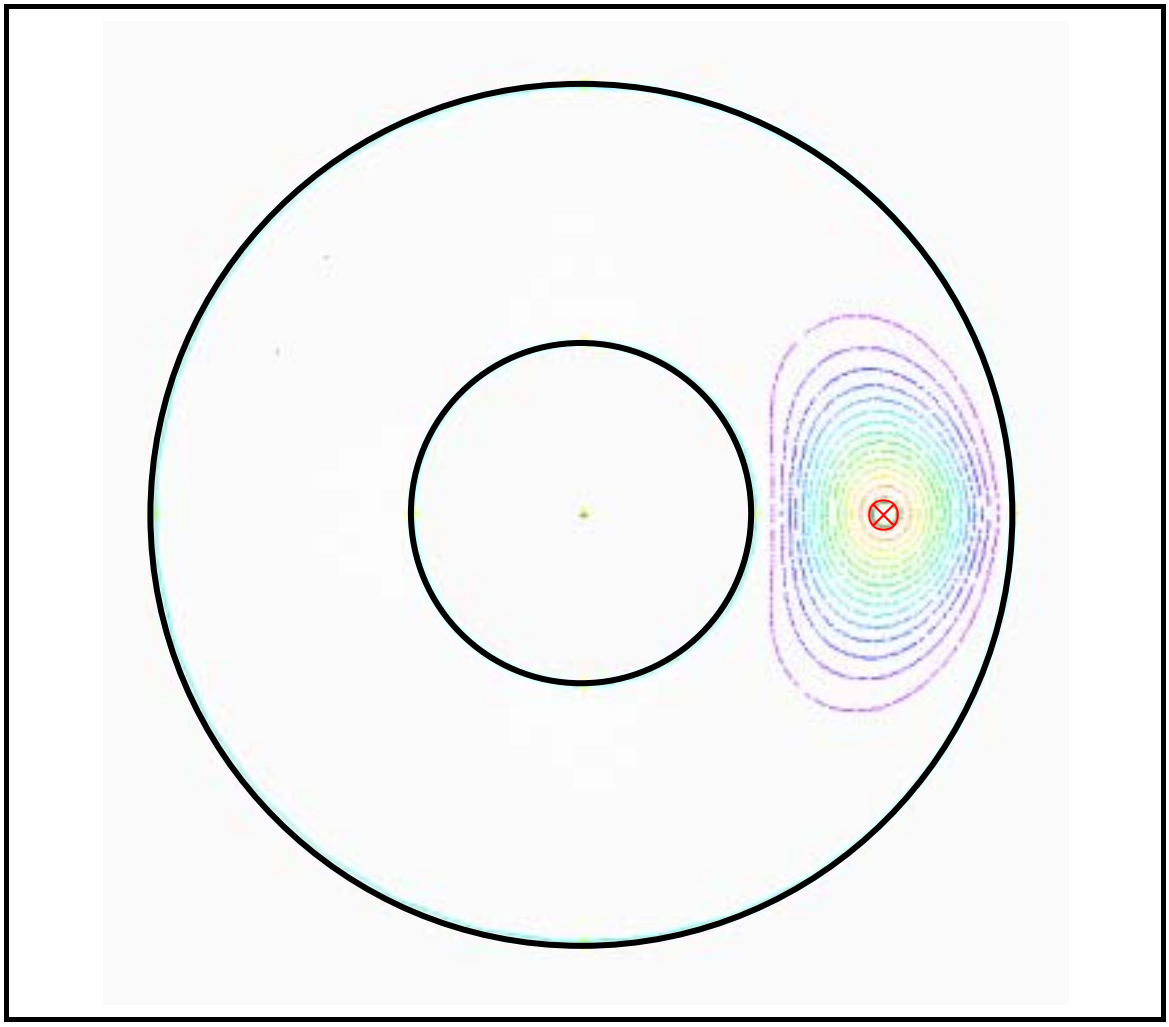

Fig. 3-20 Displacement contour of Green's function of the biharmonic equation for the fixed-fixed annular plate using the ABAQUS program

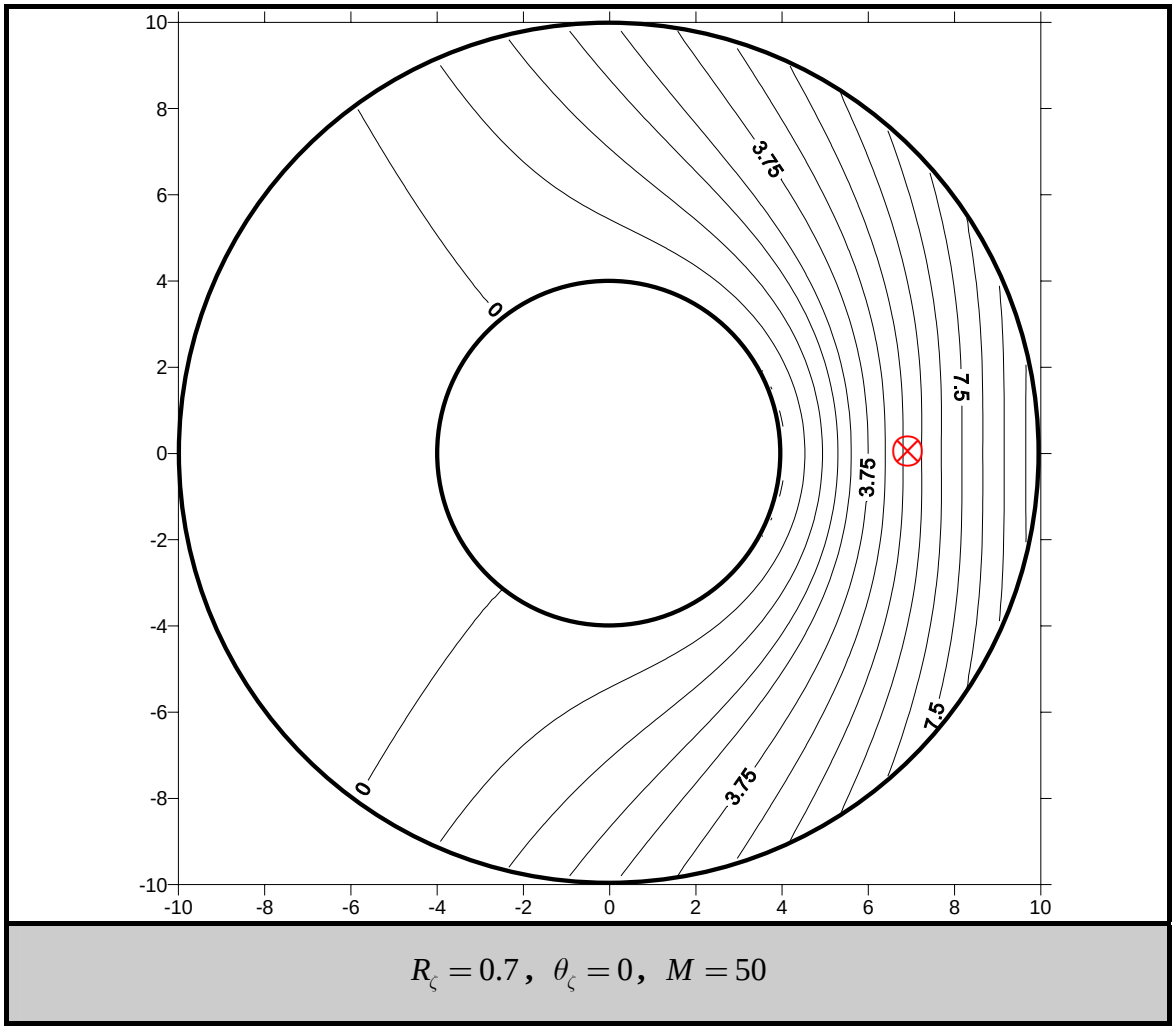

Fig. 3-21 Displacement contour of the Green's function of the biharmonic equation for the free-simply supported annular plate using the present method

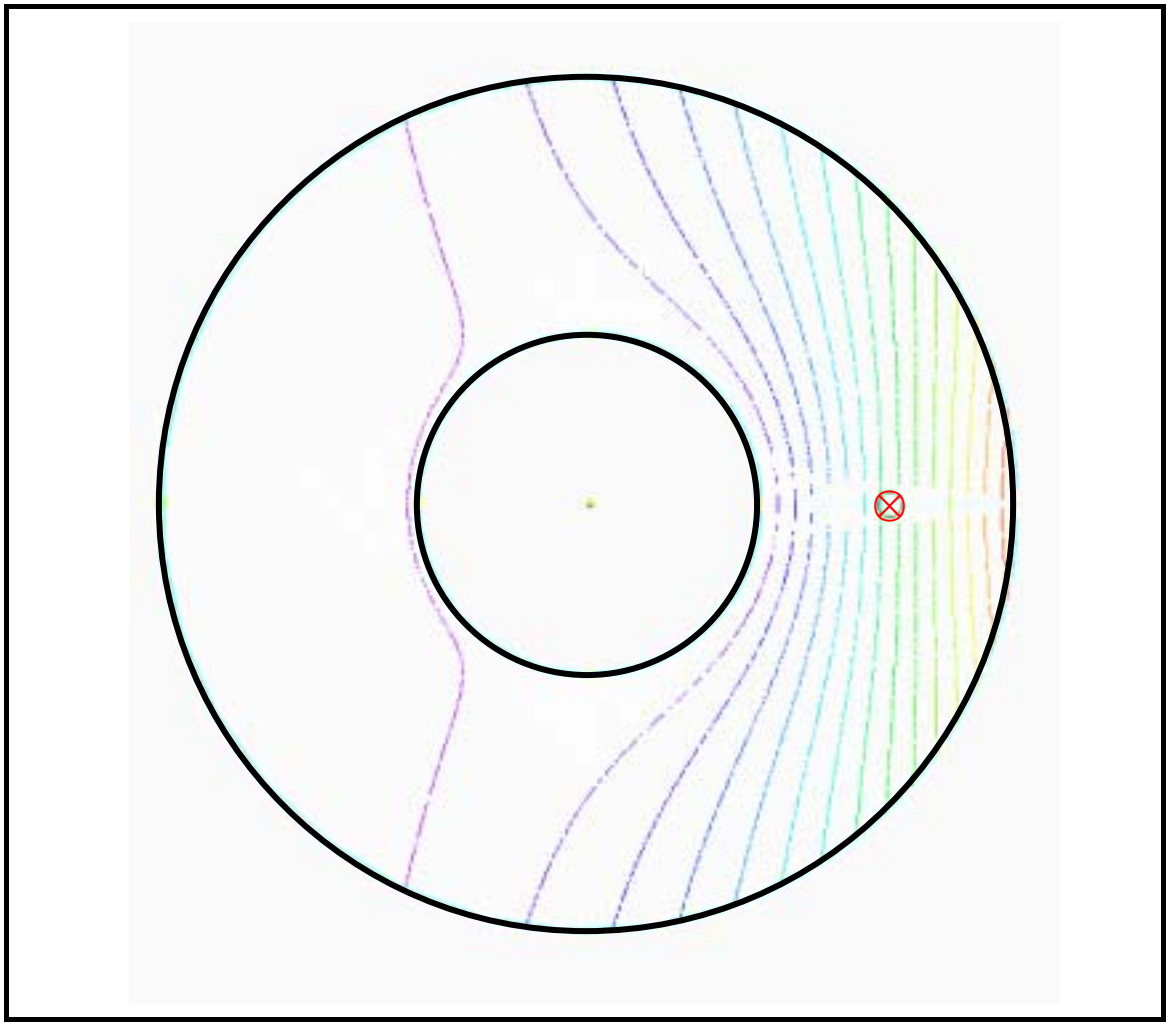

Fig. 3-22 Displacement contour of Green's function of the biharmonic equation for the free-simply supported annular plate using the ABAQUS program

Chapter 4 Conclusions and further research

4.1. Conclusions

The Green's function for Laplace and biharmonic equation of the circular and annular plate problems is the main concern in this thesis. From the study, some conclusions are made item by item as follows:

1. The Green's functions for the Laplace and biharmonic problems have been solved analytically in this thesis by using the null-field BIEs in conjunction with Fourier series and degenerate kernels. The singularity and hypersingularity were avoided due to the introduction of degenerate kernels for interior and exterior regions separated by the circular boundary. The limiting behaviors across the boundary for potential were also examined as shown in Table 3-2. Instead of directly calculating principal values, all the boundary integrals can be performed analytically by using the degenerate kernels and Fourier expansion. Therefore, the present approach is seen as an "analytical" approach in the circular or annular situation since error only ascribes to the truncated Fourier terms.

2. For the Robin problem of Laplace equation, we have proposed an analytical approach to construct the Green's function by using degenerate kernels and Fourier series. The mathematical equivalence between our result and Melnikov's [37] analytical solution has been proved successfully as shown in Appendix 1.

3. The Green's function not only the circular plate but also the annular problems have been solved analytically by using the present method which are compared with available exact solutions and FEM results. For the circular plate, Appendix 2 also shows the mathematical equivalence between our result and Melnikov's [42] closed form solution. For the annular case, the Adewale's [1] result was examined. ABAQUS data are used to compare with Adewale's [1] result and our result. Annular plates subject to different boundary conditions (fixed-fixed, simply supported-free and free-simply supported) are also verified with ABAQUS. Good agreements are made.

4. Five goals of singularity free, boundary-layer effect free, exponential convergence, well-posed model and mesh free are achieved.

4.2. Further research

Problems with circular boundaries were studied by using the direct BIEM. However, several works needs further conduction as follows:

1. From the viewpoint of geometry, only circular boundary was considered in this thesis. Degenerate kernels for ellipse or crack or square shape with BIEM need to be developed.

2. In this thesis, Green's function of the circular plate problems was solved by using the present method. The image method with degenerate kernel seems more convenient in constructing the Green's function. It is worthy of further investigate.

3. It is well known that the BIEM is a better approach for solving multiply-connected problems. Following the success of this thesis, extension to the Green's function of circular plate with multiple holes or inclusions can be considered.

4. The BIEM for solving three dimensional problems can be constructed in the further research.

References

[1] Adewale A. O., 2006, Isotropic Clamped-Free Thin Annular Circular Plate Subjected to a Concentrated Load, *Journal of Applied Mechanics*, Vol. **73,** pp. 658-663.

[2] Barone M. R. and Caulk D. A., 1981, Special boundary integral equations for approximate solution of Laplace's equation in two-dimensional regions with circular holes, *Quarterly Journal of Mechanics and Applied Mathematics*, Vol. **34**, pp. 265-286.

[3] Barone M. R. and Caulk D. A., 1982, Optimal arrangement of holes in a two-dimensional heat conductor by a special boundary integral method, *International Journal for Numerical Methods in Engineering*, Vol. **18**, pp. 675-685.

[4] Barone M. R. and Caulk D. A., 1985, Special boundary integral equations for approximate solution of potential problems in three-dimensional regions with slender cavities of circular cross-section, *IMA Journal of Applied Mathematics*, Vol. **35**, pp. 311-325.

[5] Barone M. R. and Caulk D. A., 2000, Analysis of liquid metal flow in die casting, *International Journal of Engineering Science*, Vol. **38**, pp. 1279-1302.

[6] Bates R. H. T., 1968, Modal expansions for electromagnetic scattering from perfectly conducting cylinders of arbitrary cross-section, *Proceedings of the Institution of Electrical Engineers*, Vol. **115**, pp. 1443-1445.

[7] Bates R. H. T. and Wall D. J. N, 1977, Null field approach to scalar diffraction, I. General method, *Philosophical Transactions of the Royal Society of London*, Vol. **287**, pp. 45-78.

[8] Beskos D. E., (edited), 1991. Boundary Element Analysis of Plates and Shells, Springer-Verlag Berlin, *Heidelberg*.

[9] Bird M. D. and Steele C. R., 1991, Separated solution procedure for bending of circular plates with circular holes, *ASME Applied Mechanics Reviews*, Vol. **44**, pp. 27-35.

[10] Bird M. D. and Steele C. R., 1992, A solution procedure for Laplace's equation on multiply-connected circular domains, *ASME Journal of Applied Mechanics*, Vol. **59**, pp. 398-404.

[11] Bonnet M., 1995. Boundary Integral Equation Methods for Solids and Fluids, John Wiley & Sons Ltd, *Chichester*.

[12] Boström A., 1982, Time-dependent scattering by a bounded obstacle in three

dimensions, *Journal of Mathematical Physics*, Vol. **23**, pp. 1444-1450.

[13] Boykov I. V., Boykova A. I. and Ventsel E. S., 2004, Fundamental solutions for thick sandwich plates, *Engineering Analysis with Boundary Elements*, Vol.**28,** pp. 1437-1444.

[14] Carrier G. F., 1944, The Bending of the Cylindrically Aeolotropic Plate, *Journal of Applied Mechanics*, Vol. **66**, pp. 129-133.

[15] Chen C. T., 2005, Null-field integral equation approach for Helmholtz (interior and exterior acoustic) problems with circular boundaries, Master Thesis, *Department of Harbor and River Engineering, National Taiwan Ocean University*, Keelung, Taiwan.

[16] Chen H. B., Lu P. and Schnack E., 2001, Regularized algorithms for the calculation of values on and near boundaries in 2D elastic BEM, *Engineering Analysis with Boundary Elements*, Vol. **25**, pp. 851-876.

[17] Chen J. T. and Hong H. K., 1994, Dual boundary integral equations at a corner using contour approach around singularity, *Advances in Engineering Software*, Vol. **21**, pp. 169-178.

[18] Chen J. T. and Hong H. K., 1999, Review of dual boundary element methods with emphasis on hypersingular integrals and divergent series, *ASME Applied Mechanics Reviews*, Vol. **52**, pp. 17-33.

[19] Chen J. T. and Chiu Y. P., 2002, On the pseudo-differential operators in the dual boundary integral equations using degenerate kernels and circulants, *Engineering Analysis with Boundary Elements*, Vol. **26**, pp. 41-35.

[20] Chen, J. T., Wu, C. S. and Chen, K. H., 2005, A study of free terms for plate problems in the dual boundary integral equations, *Engineering Analysis with Boundary Elements*, Vol. **29**, pp. 435-446.

[21] Chen J. T., Hsiao C. C. and Leu S. Y., 2006, Null-field integral approach for plate problems with circular boundaries, *Journal of Applied Mechanics.*, Vol. **73**, pp. 679-693.

[22] Chen J. T., Wu C. S. and Lee Y. T., 2007, On the equivalence of the Trefftz method and method of fundamental solutions for Laplace and Biharmonic Equations, *Computers and Mathematics with Applications*, Vol. **53**, pp. 851-879.

[23] Conway H. D., 1948, *Journal of Applied Mechanics*, Vol. **15**, pp. 1-5.

[24] Crouch S. L. and Mogilevskaya S. G., 2003, On the use of Somigliana's formula and Fourier series for elasticity problems with circular boundaries, *International Journal for Numerical Methods in Engineering*, Vol. **58**, pp.

537-578.

[25] Gray L. J. and Manne L. L., 1993, Hypersingular integrals at a corner, *Engineering Analysis with Boundary Elements*, Vol. **11**, pp. 327-334.

[26] Guiggiani M, 1995, Hypersingular boundary integral equations have an additional free term, *Computational Mechanics*, Vol. **16**, pp. 245-248.

[27] Hsiao C. C., 2005, A semi-analytical approach for Stokes flow and plate problems with circular boundaries, Master Thesis, *Department of Harbor and River Engineering, National Taiwan Ocean University*, Taiwan.

[28] Huang Q. and Cruse T. A., 1993, Some notes on singular integral techniques in boundary element analysis, *International Journal for Numerical Methods in Engineering*, Vol. **36**, pp. 2643-2659.

[29] Kisu H. and Kawahara T., 1988, Boundary element analysis system based on a formulation with relative quantity, Boundary Elements X, Brebbia CA, eds., *Springer-Verlag*, Vol. **1**, pp. 111-121.

[30] Kress R., 1989, Linear integral equations, *Springer-Verlag*, Berlin.

[31] Leissa A., 1993, Vibration of plates, *Acoustical Society of American*.

[32] Leitão V. M. A., 1994, Boundary elements in nonlinear fracture mechanics, Computational mechanics publications *Southampton UK and Boston USA*.

[33] Martin P. A., 1980, On the null-field equations for the exterior problems of acoustics, *Quarterly Journal of Mechanics and Applied Mathematics*, Vol. **33**, pp. 385-396.

[34] Martin P. A., 1981, On the null-field equations for water-wave radiation problems, *Journal of Fluid Mechanics*, Vol. **113**, pp. 315-332.

[35] Melnikov Y. A., 2001, Green's function of a thin circular plate with elastically supported edge, *Engineering analysis with Boundary Elements*, **Vol. 36**, pp. 669-676.

[36] Melnikov Y. A. and Arman A. S., 2001, The fields of potential generated by a point source in the ring-shaped region, *Mathematical Engineering in Industry*, Vol.**8,** pp.223-238.

[37] Melnikov Y. A. and Melnikov M. Y., 2001, Modified potential as a tool for computing Green's functions in continuum mechanics, *Computer Modeling in Engineering & Science*, Vol. **2**, pp. 391-305.

[38] Melnikov Y. A. and Melnikov M. Y., 2006, Green's function for mixed boundary value problems in Regions of irregular shape, *Electronic Journal of Boundary Elements*, Vol. **4**, pp. 82-104.

[39] Melnikov Y. A. and Sheremet V. D., 2001, Some new results on the bending of a circular plate subject to a transverse point force, *Mathematics and*

Mechanics of Solids, Vol. **6 ,** pp. 29-45.

[40] Melnikov Y. A., 2004, Influence functions of a point force for multiply connected Kirchhoff Plates, *Mathematics and Mechanics of Solids*, **Vol. 9,** pp.419-43**7**.

[41] Melnikov Y. A., 2004, Influence functions of a point source for perforated compound plates with facial convection, *Journal of Engineering Mathematics.*, Vol.**49,** pp.253-270.

[42] Melnikov Y. A., 2004, Influence functions of a point force for Kirchhoff plates with rigid inclusions, *Journal of Mechanics*, Vol. **20**, pp. 249-256.

[43] Mogilevskaya S. G. and Crouch S. L., 2001, A Galerkin boundary integral method for multiple circular elastic inclusions, *International Journal for Numerical Methods in Engineering*, Vol. **52**, pp. 1069-1106.

[44] Norbert O. and Peter W., 1990, Green's functions of clamped semi-infinite vibrating beams and plates, *International Journal of Solids and Structures*, Vol. **26,** pp. 237-249.

[45] Olsson P., 1984, Elastostatics as a limit of elastodynamics – a matrix formulation, *Applied Scientific Research,* Vol. **41**, pp. 125-151.

[46] Panton, Ronald L, 1933. Incompressible Flow, *A Wiley-Interscience* publication, New York.

[47] Sen Gupta A. M., 1952, Bending of a cylindrically aeolotropic circular plate with eccentric load, *Journal of Applied Mechanics*, Vol. **72,** pp. 9-12.

[48] Sharafutdinov G. Z., 2004, Stress and Concentrated Forces in Thin Annular Plates, *Journal of Applied Mathematics and Mechanics*, Vol. **68,** pp. 39-51.

[49] Shen WC, 2005, Null-field approach for Laplace problems with circular boundaries using degenerate kernels, Master Thesis, *Department of Harbor and River Engineering*, *National Taiwan Ocean University*, Keelung, Taiwan.

[50] Sladek V. and Sladek J., 1991, Elimination of the boundary layer effect in BEM computation of stresses, *Communications in Applied Numerical Methods*, Vol. **7**, pp. 539-550.

[51] Sladek V., Sladek J. and Tanaka M, 1993, Regularization of hypersingular and nearly singular integrals in the potential theory and elasticity, *International Journal for Numerical Methods in Engineering*, Vol. **36**, pp. 1609-1628.

[52] Szilard R., 1974, Theory and analysis of plates classical and numerical methods, *Englewood Cliffs*, New Jersey.

[53] Telles J. C. F., 1987, A self-adaptative coordinate transformation for efficient

numerical evaluation of general boundary element integrals, *International Journal for Numerical Methods in Engineering*, Vol. **24**, pp. 959-973.

[54] Varatharajulu V. and Pao Y. H., 1976, Scattering matrix for elastic waves, I. Theory, *Journal of Acoustical Society of America*, Vol. **60**, pp. 556-566.

[55] Wang J., Mogilevskaya S. G. and Crouch S. L., 2002, A numerical procedure for multiple circular holes and elastic inclusions in a finite domain with a circular boundary, *Computational Mechanics*, Vol. **32**, pp. 250-258.

[56] Wang X. and Sudak L. J., 2007, Antiplane time-harmonic Green's functions for a circular inhomogeneity with an imperfect interface, *Mechanics Research Communications*, Vol. **34**, pp. 352-358.

[57] Waterman P. C., 1965, Matrix formulation of electromagnetic scattering, *Proceedings of the IEEE*, Vol. **53**, pp. 805-812.

[58] Waterman P. C., 1976, Matrix theory of elastic wave scattering, *Journal of Acoustical Society of America*, Vol. **60**, pp. 567-580.

[59] Wu A. C., 2006, Null-field approach for multiple circular inclusion problems in anti-plane piezoelectricity, Master Thesis, *Department of Harbor and River Engineering, National Taiwan Ocean University*, Taiwan.

[60] Wu C. S., 2004, Degenerate scale analysis for membrane and plate problems using the meshless method and boundary element method, Master Thesis, *Department of Harbor and River Engineering, National Taiwan Ocean University*, Taiwan.

[61] Wu K. C., 2004, A new boundary integral equation method for analysis of cracked linear elastic bodies, *Journal of the Chinese Institute of Engineers*, Vol. **27**, pp. 935-939.

[62] 陳正宗，洪宏基，1992。邊界元素法，第二版，新世界出版社，台北。

Appendix 1. Equivalence between the present solution and Melnikov's solution

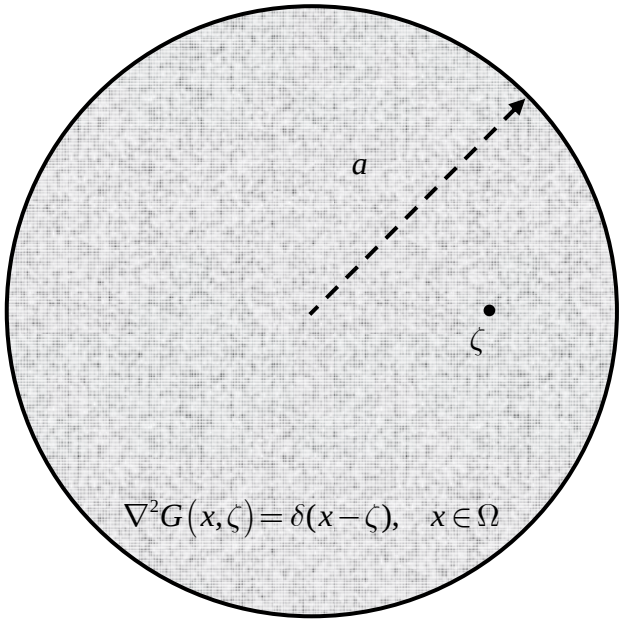

Fig. A-1 Green's function for the Laplace problem subject to the Robin boundary condition

For the Green's function of Laplace problem subject to the Robin boundary condition solved by Melnikov [37], the closed-form and series-form solutions are shown below:

$$G(x,\zeta)=\frac{1}{2\pi}\left\{\frac{1}{\beta}+\ln\frac{\left|x\bar{\zeta}-1\right|}{\left|x-\zeta\right|}+2\,\mathrm{Re}\left[\omega^{-\beta}\int_0^{\omega}\frac{t^{\beta-1}}{1-t}dt\right]\right\},\ \text{Closed-form} \tag{A1-1}$$

$$G(x,\zeta)=\frac{1}{2\pi}\left[\frac{1}{a\beta}+\ln\frac{a^3}{\left|x-\zeta\right|\left|x\bar{\zeta}-a^2\right|}-\sum_{m=1}^{\infty}\frac{2a\beta}{m(m+a\beta)}\left(\frac{\rho R_\zeta}{a^2}\right)^m\cos m\left(\phi-\theta_\zeta\right)\right], \tag{A1-2}$$

Series-form

where Re is the real part of a function of a complex variable, a is the radius, β is the impedance coefficient, $\omega=\rho R_\zeta e^{i(\theta_\zeta-\phi)}$ in which $x=\rho e^{i\phi}$ and $\zeta=R_\zeta e^{i\theta_\zeta}$ represent the field and force points, respectively. Based on the null-field integral equation approach, we have

$$G(x,\zeta)=(1+a\beta\ln a)\,p_0+\sum_{m=1}^{\infty}\frac{\rho^m}{a^m}\frac{m-a\beta}{2m}\left(p_m\cos m\phi+q_m\sin m\phi\right)+\frac{\ln\left|x-\zeta\right|}{2\pi} \tag{A1-3}$$

where $p_0=-\dfrac{1}{2\pi a\beta}$, $p_m=-\dfrac{R_\zeta^m}{\pi(m+a\beta)a^m}\cos m\theta_\zeta$, $q_m=-\dfrac{R_\zeta^m}{\pi(m+a\beta)a^m}\sin m\theta_\zeta$. First, we rearrange Eq. (A1-2) to

$$G(x,\zeta)=\frac{1}{2\pi}[\frac{1}{a\beta}+\ln\frac{a}{|x-\zeta|}-\ln\left|1-\frac{x\bar{\zeta}}{a^2}\right|-\sum_{m=1}^{\infty}\frac{2a\beta}{m(m+a\beta)}(\frac{\rho R_\zeta}{a^2})^m\cos(m\phi-m\theta_\zeta)] \qquad \text{(A1-4)}$$

where $\ln\left|1-\frac{x\bar{\zeta}}{a^2}\right|$ is expanded by using the degenerate kernel as shown below

$$\ln\left|1-\frac{x\bar{\zeta}}{a^2}\right|=-\sum_{m=1}^{\infty}\frac{1}{m}\left(\frac{\rho R_\zeta}{a^2}\right)^m\cos m(\theta_s-\phi),\ a^2>\rho R_\zeta, \qquad \text{(A1-5)}$$

After substituting Eq. (A1-5) into Eq. (A1-4), we can derive another series-form solution as shown below:

$$G(x,\zeta)=\frac{1}{2\pi}[\frac{1}{a\beta}+\ln\frac{a}{|x-\zeta|}+\sum_{m=1}^{\infty}\frac{m-a\beta}{m(m+a\beta)}(\frac{\rho R_\zeta}{a^2})^m\cos(m\phi-m\theta_\zeta)], \qquad \text{(A1-6)}$$

Second, we substitute the Fourier coefficients into Eq. (A1-3) to obtain

$$G(x,\zeta)=-\frac{1}{2\pi}[\frac{1}{a\beta}+\ln\frac{a}{|x-\zeta|}+\sum_{m=1}^{\infty}\frac{m-a\beta}{m(m+a\beta)}(\frac{\rho R_\zeta}{a^2})^m\cos(m\phi-m\theta_\zeta)], \qquad \text{(A1-7)}$$

Eqs. (A1-6) and (A1-7) only differ by a sign due to the opposite loading. The two solutions are proved to be equivalence.

Appendix 2. Equivalence between the present solution and the Melnikov's result

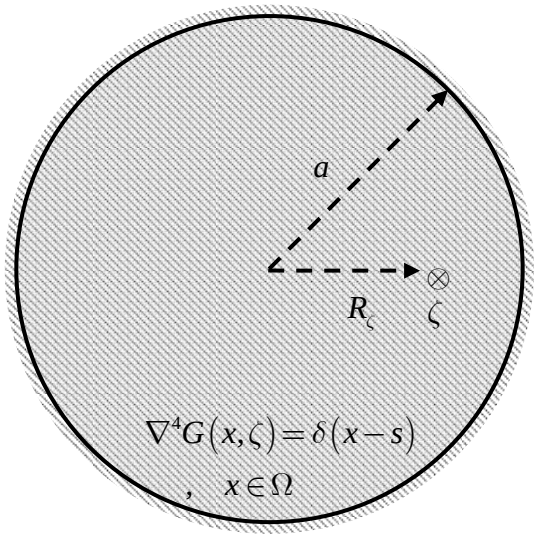

Fig. A-2 Green's function for the biharmonic equation

For the circular plate subject to a concentrated load solved by Melnikov [42], the closed-form solution is shown below:

$$G(x,\zeta)=\frac{1}{8\pi D}\left[\frac{1}{2a^2}\left(a^2-|z|^2\right)\left(a^2-|\zeta|^2\right)-(z-\zeta)^2\ln\frac{\left|a^2-z\bar{\zeta}\right|}{a|z-\zeta|}\right], \tag{A2-1}$$

where D is the flexural rigidity, a is the radius, $z=\rho e^{i\phi}$ and $\zeta=R_\zeta e^{i\theta_\zeta}$ denote the field and the force point, respectively. The problem is also solved by using the present method. Also, we have a series-form solution as shown below:

$$\begin{aligned}
8\pi G(x,\zeta)=&-2\pi a\rho^2(1+\ln a)a_0-2\pi a^3\ln a a_0+\left[a\rho(1+2\ln a)+\frac{1}{2}\frac{\rho^3}{a}\right]\pi a\left(a_1\cos\phi+b_1\sin\phi\right)\\
&+\sum_{n=2}^{\infty}\left[\frac{1}{n(n+1)}\frac{\rho^{n+2}}{a^n}-\frac{1}{n(n-1)}\frac{\rho^n}{a^{n-2}}\right]\pi a\left(a_n\cos n\phi+b_n\sin n\phi\right)\\
&+2\pi\rho^2 p_0+2\pi a^2(1+2\ln a)p_0-\left[\rho(3+2\ln a)-\frac{1}{2}\frac{\rho^3}{a^2}\right]\pi a\left(p_1\cos\phi+q_1\sin\phi\right)\\
&+\sum_{n=2}^{\infty}\left[\frac{1}{n+1}\frac{\rho^{n+2}}{a^{n+1}}-\frac{n-2}{n(n-1)}\frac{\rho^n}{a^{n-1}}\right]\pi a\left(p_n\cos n\phi+q_n\sin n\phi\right)\\
&+(x-\zeta)^2\ln|x-\zeta|,\quad x\in\Omega,
\end{aligned} \tag{A2-2}$$

where $\begin{Bmatrix}a_0\\p_0\end{Bmatrix}=\begin{Bmatrix}\frac{1}{2\pi a}\\ \frac{a^2-R_\zeta^2}{4\pi a^2}\end{Bmatrix}$, $\begin{Bmatrix}a_1\\p_1\end{Bmatrix}=\begin{Bmatrix}\frac{-\cos\theta_\zeta R_\zeta\left(R_\zeta^2-3a^2\right)}{2\pi a^4}\\ \frac{\cos\theta_\zeta R_\zeta\left(a^2-R_\zeta^2\right)}{2\pi a^3}\end{Bmatrix}$, $\begin{Bmatrix}b_1\\q_1\end{Bmatrix}=\begin{Bmatrix}\frac{-\sin\theta_\zeta R_\zeta\left(R_\zeta^2-3a^2\right)}{2\pi a^4}\\ \frac{\sin\theta_\zeta R_\zeta\left(a^2-R_\zeta^2\right)}{2\pi a^3}\end{Bmatrix}$,

$$\begin{Bmatrix} a_n \\ p_n \end{Bmatrix} = \begin{Bmatrix} \dfrac{a^{-n-3}\cos n\theta_\zeta R_\zeta^n\left[(n+2)a^2 - nR_\zeta^2\right]}{2\pi} \\ \dfrac{a^{-n-2}\cos n\theta_\zeta R_\zeta^n\left[a^2 - R_\zeta^2\right]}{2\pi} \end{Bmatrix}, \quad \begin{Bmatrix} b_n \\ q_n \end{Bmatrix} = \begin{Bmatrix} \dfrac{a^{-n-3}\sin n\theta_\zeta R_\zeta^n\left[(n+2)a^2 - nR_\zeta^2\right]}{2\pi} \\ \dfrac{a^{-n-2}\sin n\theta_\zeta R_\zeta^n\left[a^2 - R_\zeta^2\right]}{2\pi} \end{Bmatrix}.$$

By rearranging Eq. (A2-1), we have

$$G(x,\zeta) = \frac{1}{8\pi D}\left[\frac{1}{2a^2}\left(a^2-\rho^2\right)\left(a^2-R_\zeta{}^2\right) - \left[\rho^2 + R_\zeta^2 - 2\rho R_\zeta\cos\left(\theta_\zeta-\phi\right)\right]\left[\ln\left|1-\frac{z\bar{\zeta}}{a^2}\right| + \ln a\right]\right. \\ \left. + \left(x-\zeta\right)^2\ln\left|x-\zeta\right|\right] \tag{A2-3}$$

where $\ln\left|1-\dfrac{x\bar{\zeta}}{a^2}\right|$ can be expanded by using the degenerate kernel as shown below:

$$\ln\left|1-\frac{x\bar{\zeta}}{a^2}\right| = -\sum_{m=1}^{\infty}\frac{1}{m}\left(\frac{\rho R_\zeta}{a^2}\right)^m\cos m\left(\theta_\zeta-\phi\right),\ a^2 > \rho R_\zeta \tag{A2-4}$$

After substituting Eq. (A2-4) into Eq. (A2-3), we can have another series-form solution as shown below

$$G(x,\zeta) = \frac{1}{8\pi D}\left[\frac{\left(a^2-\rho^2\right)\left(a^2-R_\zeta{}^2\right)}{2a^2} - \left(\rho^2+R_\zeta^2\right)\ln a\right. \\ + 2\rho R_\zeta\ln a\cos\left(\theta_\zeta-\phi\right) + \sum_{m=1}^{\infty}\frac{\rho^2+R_\zeta^2}{m}\left(\frac{\rho R_\zeta}{a^2}\right)^m\cos m\left(\theta_s-\phi\right) \\ - \sum_{m=1}^{\infty}\frac{\rho R_\zeta}{m}\left(\frac{\rho R_\zeta}{a^2}\right)^m\cos\left(m+1\right)\left(\theta_\zeta-\phi\right) - \sum_{m=1}^{\infty}\frac{\rho R_\zeta}{m}\left(\frac{\rho R_\zeta}{a^2}\right)^m\cos\left(m-1\right)\left(\theta_\zeta-\phi\right) \\ \left. + \left(x-\zeta\right)^2\ln\left|x-\zeta\right|\right] \tag{A2-5}$$

Eq. (A2-5) can be rearranged to

$$G(x,\zeta) = \frac{1}{8\pi D}\left[\frac{\left(a^2-\rho^2\right)\left(a^2-R_\zeta{}^2\right)}{2a^2} - \left(\rho^2+R_\zeta^2\right)\ln a - \rho R_\zeta\frac{\rho R_\zeta}{a^2}\right. \\ + \left[2\rho R_\zeta\ln a + \left(\rho^2+R_\zeta^2\right)\frac{\rho R_\zeta}{a^2} - \frac{\rho R_\zeta}{2}\left(\frac{\rho R_\zeta}{a^2}\right)^2\right]\cos\left(\theta_\zeta-\phi\right) \\ + \sum_{m=2}^{\infty}\left[\frac{\rho^2+R_\zeta^2}{m}\left(\frac{\rho R_\zeta}{a^2}\right)^m - \frac{\rho R_\zeta}{m-1}\left(\frac{\rho R_\zeta}{a^2}\right)^{m-1} - \frac{\rho R_\zeta}{m+1}\left(\frac{\rho R_\zeta}{a^2}\right)^{m+1}\right]\cos m\left(\theta_\zeta-\phi\right) \\ \left. + \left(x-\zeta\right)^2\ln\left|x-\zeta\right|\right] \tag{A2-6}$$

By substituting the Fourier coefficients into Eq. (A2-2), we have

$$
\begin{aligned}
8\pi G(x,\zeta) = & -\rho^2\left(1+\ln a\right)-a^2\ln a+\rho^2\frac{a^2-R_\zeta^2}{2a^2}+\left(1+2\ln a\right)\frac{a^2-R_\zeta^2}{2} \\
& +\left[a\rho\left(1+2\ln a\right)+\frac{1}{2}\frac{\rho^3}{a}\right]\frac{R_\zeta\left(3a^2-R_\zeta^2\right)}{2a^3}\cos\left(\theta_\zeta-\phi\right) \\
& -\left[\rho\left(3+2\ln a\right)-\frac{1}{2}\frac{\rho^3}{a^2}\right]\frac{R_\zeta\left(a^2-R_\zeta^2\right)}{2a^2}\cos\left(\theta_\zeta-\phi\right) \\
& +\sum_{n=2}^{\infty}\left[\frac{1}{n\left(n+1\right)}\frac{\rho^{n+2}}{a^n}-\frac{1}{n\left(n-1\right)}\frac{\rho^n}{a^{n-2}}\right]\frac{a^{-n-2}R_\zeta^n\left[\left(n+2\right)a^2-nR_\zeta^2\right]}{2}\cos n\left(\theta_\zeta-\phi\right) \\
& +\sum_{n=2}^{\infty}\left[\frac{1}{n+1}\frac{\rho^{n+2}}{a^{n+1}}-\frac{n-2}{n\left(n-1\right)}\frac{\rho^n}{a^{n-1}}\right]\frac{a^{-n-1}R_\zeta^n\left[a^2-R_\zeta^2\right]}{2}\cos n\left(\theta_\zeta-\phi\right)
\end{aligned}
\tag{A2-7}
$$

Although Eqs. (A2-6) and (A2-7) look different, we use Mathematica symbolic software to mathematical prove the equivalence between the two solutions in three aspects, constant term, $\cos(\theta_\zeta-\phi)$ and $\cos m(\theta_\zeta-\phi)$ as shown in Table A2-1.

Table A2-1 Comparison of the Melnikov solution and our solution in three aspects.

	Melnikov term		Present term
constant	$\frac{\left(a^2-\rho^2\right)\left(a^2-R_\zeta^{\,2}\right)}{2a^2}-\left(\rho^2+R_\zeta^2\right)\ln a-\rho R_\zeta\frac{\rho R_\zeta}{a^2}$	$\equiv$	$-\rho^2\left(1+\ln a\right)-a^2\ln a+\rho^2\frac{a^2-R_\zeta^2}{2a^2}+\left(1+2\ln a\right)\frac{a^2-R_\zeta^2}{2}$
$\cos(\theta_\zeta-\phi)$	$[2\rho R_\zeta\ln a+\left(\rho^2+R_\zeta^2\right)\frac{\rho R_\zeta}{a^2}-\frac{\rho R_\zeta}{2}\left(\frac{\rho R_\zeta}{a^2}\right)^2]\cos\left(\theta_\zeta-\phi\right)$	$\equiv$	$[a\rho\left(1+2\ln a\right)+\frac{1}{2}\frac{\rho^3}{a}]\frac{R_\zeta\left(3a^2-R_\zeta^2\right)}{2a^3}\cos\left(\theta_\zeta-\phi\right)$ $-[\rho\left(3+2\ln a\right)-\frac{1}{2}\frac{\rho^3}{a^2}]\frac{R_\zeta\left(a^2-R_\zeta^2\right)}{2a^2}\cos\left(\theta_\zeta-\phi\right)$
$\cos m(\theta_\zeta-\phi)$	$\sum_{m=2}^{\infty}[\frac{\rho^2+R_\zeta^2}{m}\left(\frac{\rho R_\zeta}{a^2}\right)^m-\frac{\rho R_\zeta}{m-1}\left(\frac{\rho R_\zeta}{a^2}\right)^{m-1}$ $-\frac{\rho R_\zeta}{m+1}\left(\frac{\rho R_\zeta}{a^2}\right)^{m+1}]\cos m\left(\theta_\zeta-\phi\right)$	$\equiv$	$\sum_{n=2}^{\infty}[\frac{1}{n\left(n+1\right)}\frac{\rho^{n+2}}{a^n}-\frac{1}{n\left(n-1\right)}\frac{\rho^n}{a^{n-2}}]\frac{a^{-n-2}R_\zeta^n\left[\left(n+2\right)a^2-nR_\zeta^2\right]}{2}\cos n\left(\theta_\zeta-\phi\right)$ $+\sum_{n=2}^{\infty}[\frac{1}{n+1}\frac{\rho^{n+2}}{a^{n+1}}-\frac{n-2}{n\left(n-1\right)}\frac{\rho^n}{a^{n-1}}]\frac{a^{-n-1}R_\zeta^n\left[a^2-R_\zeta^2\right]}{2}\cos n\left(\theta_\zeta-\phi\right)$

Appendix 3. Degenerate kernels

Degenerate kernels for U, Θ, M, V in the first boundary integral equation

$$U(s,x)=\begin{cases} U^I(s,x)=\rho^2(1+\ln R)+R^2\ln R-\left[R\rho(1+2\ln R)+\frac{1}{2}\frac{\rho^3}{R}\right]\cos(\theta-\phi)-\sum_{m=2}^{\infty}\left[\frac{1}{m(m+1)}\frac{\rho^{m+2}}{R^m}-\frac{1}{m(m-1)}\frac{\rho^m}{R^{m-2}}\right]\cos m(\theta-\phi), & R\ge\rho \\ U^E(s,x)=R^2(1+\ln\rho)+\rho^2\ln\rho-\left[\rho R(1+2\ln\rho)+\frac{1}{2}\frac{R^3}{\rho}\right]\cos(\theta-\phi)-\sum_{m=2}^{\infty}\left[\frac{1}{m(m+1)}\frac{R^{m+2}}{\rho^m}-\frac{1}{m(m-1)}\frac{R^m}{\rho^{m-2}}\right]\cos m(\theta-\phi), & \rho>R \end{cases}$$

$$\Theta(s,x)=\begin{cases} \Theta^I(s,x)=\frac{\rho^2}{R}+R(1+2\ln R)-\left[\rho(3+2\ln R)-\frac{1}{2}\frac{\rho^3}{R^2}\right]\cos(\theta-\phi)+\sum_{m=2}^{\infty}\left[\frac{1}{m+1}\frac{\rho^{m+2}}{R^{m+1}}-\frac{m-2}{m(m-1)}\frac{\rho^m}{R^{m-1}}\right]\cos m(\theta-\phi), & R\ge\rho \\ \Theta^E(s,x)=2R(1+\ln\rho)-\left[\rho(1+2\ln\rho)+\frac{3}{2}\frac{R^2}{\rho}\right]\cos(\theta-\phi)-\sum_{m=2}^{\infty}\left[\frac{m+2}{m(m+1)}\frac{R^{m+1}}{\rho^m}-\frac{1}{m-1}\frac{R^{m-1}}{\rho^{m-2}}\right]\cos m(\theta-\phi), & \rho>R \end{cases}$$

$$M(s,x)=\begin{cases} M^I(s,x)=(\nu-1)\frac{\rho^2}{R^2}+(\nu+3)+2(\nu+1)\ln R-\left[(\nu+1)\frac{2\rho}{R}-(\nu-1)\frac{\rho^3}{R^3}\right]\cos(\theta-\phi)-\sum_{m=2}^{\infty}\left[(\nu-1)\frac{\rho^{m+2}}{R^{m+2}}+\frac{m(1-\nu)-2(1+\nu)}{m}\frac{\rho^m}{R^m}\right]\cos m(\theta-\phi), & R\ge\rho \\ M^E(s,x)=2(1+\nu)(1+\ln\rho)-(\nu+3)\frac{R}{\rho}\cos(\theta-\phi)+\sum_{m=2}^{\infty}\left[\frac{m(\nu-1)-2(\nu+1)}{m}\frac{R^m}{\rho^m}+(1-\nu)\frac{R^{m-2}}{\rho^{m-2}}\right]\cos m(\theta-\phi), & \rho>R \end{cases}$$

$$V(s,x)=\begin{cases} V^I(s,x)=\frac{4}{R}+\left[\frac{2\rho}{R^2}(3-\nu)-\frac{\rho^3}{R^4}(1-\nu)\right]\cos(\theta-\phi)-\sum_{m=2}^{\infty}\left[m(1-\nu)\frac{\rho^{m+2}}{R^{m+3}}-(4+m(1-\nu))\frac{\rho^m}{R^{m+1}}\right]\cos m(\theta-\phi), & R\ge\rho \\ V^E(s,x)=(-3-\nu)\frac{1}{\rho}\cos(\theta-\phi)+\sum_{m=2}^{\infty}\left[(m(1-\nu)-4)\frac{R^{m-1}}{\rho^m}-m(1-\nu)\frac{R^{m-3}}{\rho^{m-2}}\right]\cos m(\theta-\phi), & \rho>R \end{cases}$$

Degenerate kernels for U_θ, Θ_θ, M_θ, V_θ in the second boundary integral equation

$$U_\theta(s,x)=\begin{cases} U_\theta^I(s,x)=2\rho(1+\ln R)-\left[R(1+2\ln R)+\dfrac{3}{2}\dfrac{\rho^2}{R}\right]\cos(\theta-\phi)-\displaystyle\sum_{m=2}^{\infty}\left[\frac{m+2}{m(m+1)}\frac{\rho^{m+1}}{R^m}-\frac{1}{m-1}\frac{\rho^{m-1}}{R^{m-2}}\right]\cos m(\theta-\phi), & R\ge\rho \\ U_\theta^E(s,x)=\dfrac{R^2}{\rho}+\rho(1+2\ln\rho)-\left[R(3+2\ln\rho)-\dfrac{1}{2}\dfrac{R^3}{\rho^2}\right]\cos(\theta-\phi)+\displaystyle\sum_{m=2}^{\infty}\left[\frac{1}{m+1}\frac{R^{m+2}}{\rho^{m+1}}-\frac{m-2}{m(m-1)}\frac{R^m}{\rho^{m-1}}\right]\cos m(\theta-\phi), & \rho>R \end{cases}$$

$$\Theta_\theta(s,x)=\begin{cases} \Theta_\theta^I(s,x)=\dfrac{2\rho}{R}-\left[(3+2\ln R)-\dfrac{3}{2}\dfrac{\rho^2}{R^2}\right]\cos(\theta-\phi)+\displaystyle\sum_{m=2}^{\infty}\left[\frac{m+2}{m+1}\frac{\rho^{m+1}}{R^{m+1}}-\frac{m-2}{m-1}\frac{\rho^{m-1}}{R^{m-1}}\right]\cos m(\theta-\phi), & R\ge\rho \\ \Theta_\theta^E(s,x)=\dfrac{2R}{\rho}-\left[(3+2\ln\rho)-\dfrac{3}{2}\dfrac{R^2}{\rho^2}\right]\cos(\theta-\phi)+\displaystyle\sum_{m=2}^{\infty}\left[\frac{m+2}{m+1}\frac{R^{m+1}}{\rho^{m+1}}-\frac{m-2}{m-1}\frac{R^{m-1}}{\rho^{m-1}}\right]\cos m(\theta-\phi), & \rho>R \end{cases}$$

$$M_\theta(s,x)=\begin{cases} M_\theta^I(s,x)=\dfrac{2\rho}{R^2}(\nu-1)-\left[\dfrac{2}{R}(\nu+1)-3(\nu-1)\dfrac{\rho^2}{R^3}\right]\cos(\theta-\phi)+\displaystyle\sum_{m=2}^{\infty}\left[(m+2)(\nu-1)\frac{\rho^{m+1}}{R^{m+2}}+\big(m(1-\nu)-2(1+\nu)\big)\frac{\rho^{m-1}}{R^m}\right]\cos m(\theta-\phi), & R\ge\rho \\ M_\theta^E(s,x)=\dfrac{2(1+\nu)}{\rho}+(\nu+3)\dfrac{R}{\rho^2}\cos(\theta-\phi)-\displaystyle\sum_{m=2}^{\infty}\left[\big(m(\nu-1)-2(\nu+1)\big)\frac{R^m}{\rho^{m+1}}+(m-2)(1-\nu)\frac{R^{m-2}}{\rho^{m-1}}\right]\cos m(\theta-\phi), & \rho>R \end{cases}$$

$$V_\theta(s,x)=\begin{cases} V_\theta^I(s,x)=\left[\dfrac{2}{R^2}(3-\nu)-3(1-\nu)\dfrac{\rho^2}{R^4}\right]\cos(\theta-\phi)-\displaystyle\sum_{m=2}^{\infty}\left[m(m+2)(1-\nu)\frac{\rho^{m+1}}{R^{m+3}}-m\big(4+m(1-\nu)\big)\frac{\rho^{m-1}}{R^{m+1}}\right]\cos m(\theta-\phi), & R\ge\rho \\ V_\theta^E(s,x)=(3+\nu)\dfrac{1}{\rho^2}\cos(\theta-\phi)-\displaystyle\sum_{m=2}^{\infty}\left[m\big(m(1-\nu)-4\big)\frac{R^{m-1}}{\rho^{m+1}}-m(m-2)(1-\nu)\frac{R^{m-3}}{\rho^{m-1}}\right]\cos m(\theta-\phi), & \rho>R \end{cases}$$

where U_θ, Θ_θ, M_θ, V_θ are equal to $\partial U(s,x)/\partial n_x$, $\partial\Theta(s,x)/\partial n_x$, $\partial M(s,x)/\partial n_x$ and $\partial V(s,x)/\partial n_x$, respectively.

Degenerate kernels for U_m, Θ_m, M_m, V_m in the third boundary integral equation

$$U_m(s,x)=\begin{cases} U_m^I(s,x)=2(1+\nu)(1+\ln R)-(\nu+3)\dfrac{\rho}{R}\cos(\theta-\phi)+\displaystyle\sum_{m=2}^{\infty}\left[\frac{m(\nu-1)-2(\nu+1)}{m}\frac{\rho^m}{R^m}+(1-\nu)\frac{\rho^{m-2}}{R^{m-2}}\right]\cos m(\theta-\phi), & R\ge\rho \\ U_m^E(s,x)=(\nu-1)\dfrac{R^2}{\rho^2}+(\nu+3)+2(\nu+1)\ln\rho-\left[(\nu+1)\dfrac{2R}{\rho}-(\nu-1)\dfrac{R^3}{\rho^3}\right]\cos(\theta-\phi)-\displaystyle\sum_{m=2}^{\infty}\left[(\nu-1)\frac{R^{m+2}}{\rho^{m+2}}+\frac{m(1-\nu)-2(1+\nu)}{m}\frac{R^m}{\rho^m}\right]\cos m(\theta-\phi), & \rho>R \end{cases}$$

$$\Theta_m(s,x)=\begin{cases} \Theta_m^I(s,x)=\dfrac{2(1+\nu)}{R}+(\nu+3)\dfrac{\rho}{R^2}\cos(\theta-\phi)-\displaystyle\sum_{m=2}^{\infty}\left[\big(m(\nu-1)-2(\nu+1)\big)\frac{\rho^m}{R^{m+1}}+(m-2)(1-\nu)\frac{\rho^{m-2}}{R^{m-1}}\right]\cos m(\theta-\phi), & R\ge\rho \\ \Theta_m^E(s,x)=\dfrac{2R}{\rho^2}(\nu-1)-\left[\dfrac{2}{\rho}(\nu+1)-3(\nu-1)\dfrac{R^2}{\rho^3}\right]\cos(\theta-\phi)+\displaystyle\sum_{m=2}^{\infty}\left[(m+2)(\nu-1)\frac{R^{m+1}}{\rho^{m+2}}+\big(m(1-\nu)-2(1+\nu)\big)\frac{R^{m-1}}{\rho^m}\right]\cos m(\theta-\phi), & \rho>R \end{cases}$$

$$M_m(s,x)=\begin{cases} M_m^I(s,x)=\dfrac{2(\nu^2-1)}{R^2}+2(\nu-1)(\nu+3)\dfrac{\rho}{R^3}\cos(\theta-\phi)+\displaystyle\sum_{m=2}^{\infty}\left[(m-1)(\nu-1)\big[m(\nu-1)+2(1+\nu)\big]\frac{\rho^{m-2}}{R^m}+(m+1)(\nu-1)\big[m(1-\nu)+2(1+\nu)\big]\frac{\rho^m}{R^{m+2}}\right]\cos m(\theta-\phi), & R\ge\rho \\ M_m^E(s,x)=\dfrac{2(\nu^2-1)}{\rho^2}+2(\nu-1)(\nu+3)\dfrac{R}{\rho^3}\cos(\theta-\phi)+\displaystyle\sum_{m=2}^{\infty}\left[(m-1)(\nu-1)\big[m(\nu-1)+2(1+\nu)\big]\frac{R^{m-2}}{\rho^m}+(m+1)(\nu-1)\big(m(\nu-1)+2(1+\nu)\big)\frac{R^m}{\rho^{m+2}}\right]\cos m(\theta-\phi), & \rho>R \end{cases}$$

$$V_m(s,x)=\begin{cases} V_m^I(s,x)=2(\nu-1)(\nu+3)\dfrac{\rho}{R^4}\cos(\theta-\phi)+\displaystyle\sum_{m=2}^{\infty}\left[m(m+1)(\nu-1)\big(m(1-\nu)+2(1+\nu)\big)\frac{\rho^m}{R^{m+3}}+m(m-1)(1-\nu)\big(4+m(1-\nu)\big)\frac{\rho^{m-2}}{R^{m+1}}\right]\cos m(\theta-\phi), & R\ge\rho \\ V_m^E(s,x)=\dfrac{2(\nu-1)(\nu+3)}{\rho^3}\cos(\theta-\phi)+\displaystyle\sum_{m=2}^{\infty}\left[m(m-1)(\nu-1)\big(m(1-\nu)-2(1+\nu)\big)\frac{R^{m-3}}{\rho^m}+m(m+1)(1-\nu)\big(m(1-\nu)-4\big)\frac{R^{m-1}}{\rho^{m+2}}\right]\cos m(\theta-\phi), & \rho>R \end{cases}$$

where U_m, Θ_m, M_m, V_m are equal to $\nu\nabla_x^2U(s,x)+(1-\nu)\dfrac{\partial^2U(s,x)}{\partial n_x^2}$, $\nu\nabla_x^2\Theta(s,x)+(1-\nu)\dfrac{\partial^2\Theta(s,x)}{\partial n_x^2}$, $\nu\nabla_x^2M(s,x)+(1-\nu)\dfrac{\partial^2M(s,x)}{\partial n_x^2}$ and

$\nu\nabla_x^2V(s,x)+(1-\nu)\dfrac{\partial^2V(s,x)}{\partial n_x^2}$, respectively.

Degenerate kernels for U_ν, Θ_ν, M_ν, V_ν in the fourth boundary integral equation

$$U_\nu(s,x)=\begin{cases} U_\nu^I(s,x)=(-3-\nu)\dfrac{1}{R}\cos(\theta-\phi)+\displaystyle\sum_{m=2}^{\infty}\left[\left(m(1-\nu)-4\right)\frac{\rho^{m-1}}{R^m}-m(1-\nu)\frac{\rho^{m-3}}{R^{m-2}}\right]\cos m(\theta-\phi), & R\ge\rho \\ U_\nu^E(s,x)=\dfrac{4}{\rho}+\left[\dfrac{2R}{\rho^2}(3-\nu)-\dfrac{R^3}{\rho^4}(1-\nu)\right]\cos(\theta-\phi)-\displaystyle\sum_{m=2}^{\infty}\left[m(1-\nu)\frac{R^{m+2}}{\rho^{m+3}}-\left(4+m(1-\nu)\right)\frac{R^m}{\rho^{m+1}}\right]\cos m(\theta-\phi), & \rho>R \end{cases}$$

$$\Theta_\nu(s,x)=\begin{cases} \Theta_\nu^I(s,x)=(\nu+3)\dfrac{1}{R^2}\cos(\theta-\phi)-\displaystyle\sum_{m=2}^{\infty}\left[m\left(m(1-\nu)-4\right)\frac{\rho^{m-1}}{R^{m+1}}-m(m-2)(1-\nu)\frac{\rho^{m-3}}{R^{m-1}}\right]\cos m(\theta-\phi), & R\ge\rho \\ \Theta_\nu^E(s,x)=\left[\dfrac{2}{\rho^2}(3-\nu)-3(1-\nu)\dfrac{R^2}{\rho^4}\right]\cos(\theta-\phi)-\displaystyle\sum_{m=2}^{\infty}\left[m(m+2)(1-\nu)\frac{R^{m+1}}{\rho^{m+3}}-m\left(4+m(1-\nu)\right)\frac{R^{m-1}}{\rho^{m+1}}\right]\cos m(\theta-\phi), & \rho>R \end{cases}$$

$$M_\nu(s,x)=\begin{cases} M_\nu^I(s,x)=\dfrac{2(\nu-1)(\nu+3)}{R^3}\cos(\theta-\phi)+\displaystyle\sum_{m=2}^{\infty}\left[m(m-1)(\nu-1)\left(m(1-\nu)-2(1+\nu)\right)\frac{\rho^{m-3}}{R^m}+m(m+1)(1-\nu)\left(m(1-\nu)-4\right)\frac{\rho^{m-1}}{R^{m+2}}\right]\cos m(\theta-\phi), & R\ge\rho \\ M_\nu^E(s,x)=2(\nu-1)(\nu+3)\dfrac{R}{\rho^4}\cos(\theta-\phi)+\displaystyle\sum_{m=2}^{\infty}\left[m(m+1)(\nu-1)\left(m(1-\nu)-2(1+\nu)\right)\frac{R^m}{\rho^{m+3}}+m(m-1)(1-\nu)\left(4+m(1-\nu)\right)\frac{R^{m-2}}{\rho^{m+1}}+\right]\cos m(\theta-\phi), & \rho>R \end{cases}$$

$$V_\nu(s,x)=\begin{cases} V_\nu^I(s,x)=\dfrac{2(\nu-1)(\nu+3)}{R^4}\cos(\theta-\phi)+\displaystyle\sum_{m=2}^{\infty}\left[m^2(m+1)(1-\nu)\left(m(1-\nu)-4\right)\frac{\rho^{m-1}}{R^{m+3}}+m^2(m-1)(\nu-1)\left(4+m(1-\nu)\right)\frac{\rho^{m-3}}{R^{m+1}}\right]\cos m(\theta-\phi), & R\ge\rho \\ V_\nu^E(s,x)=\dfrac{2(\nu-1)(\nu+3)}{\rho^4}\cos(\theta-\phi)+\displaystyle\sum_{m=2}^{\infty}\left[m^2(m+1)(1-\nu)\left(m(1-\nu)-4\right)\frac{R^{m-1}}{\rho^{m+3}}+m^2(m-1)(\nu-1)\left(4+m(1-\nu)\right)\frac{R^{m-3}}{\rho^{m+1}}\right]\cos m(\theta-\phi), & \rho>R \end{cases}$$

where U_ν, Θ_ν, M_ν, V_ν are equal to $\dfrac{\partial\nabla_x^2U(s,x)}{\partial n_x}+(1-\nu)\dfrac{\partial}{\partial t_x}\left[\dfrac{\partial}{\partial n_x}\left(\dfrac{\partial U(s,x)}{\partial t_x}\right)\right]$, $\dfrac{\partial\nabla_x^2\Theta(s,x)}{\partial n_x}+(1-\nu)\dfrac{\partial}{\partial t_x}\left[\dfrac{\partial}{\partial n_x}\left(\dfrac{\partial\Theta(s,x)}{\partial t_x}\right)\right]$,

$\dfrac{\partial\nabla_x^2M(s,x)}{\partial n_x}+(1-\nu)\dfrac{\partial}{\partial t_x}\left[\dfrac{\partial}{\partial n_x}\left(\dfrac{\partial M(s,x)}{\partial t_x}\right)\right]$ and $\dfrac{\partial\nabla_x^2V(s,x)}{\partial n_x}+(1-\nu)\dfrac{\partial}{\partial t_x}\left[\dfrac{\partial}{\partial n_x}\left(\dfrac{\partial V(s,x)}{\partial t_x}\right)\right]$, respectively.

Laplacian of the degenerate kernels with respect to U, Θ, M, V

$$U_{\nabla^2}(s,x)=\begin{cases}U^I_{\nabla^2}(s,x)=4(1+\ln R)-4\dfrac{\rho}{R}\cos(\theta-\phi)-\displaystyle\sum_{m=2}^{\infty}\frac{4}{m}\frac{\rho^m}{R^m}\cos m(\theta-\phi), & R\geq\rho\\ U^E_{\nabla^2}(s,x)=4(1+\ln\rho)-4\dfrac{R}{\rho}\cos(\theta-\phi)-\displaystyle\sum_{m=2}^{\infty}\frac{4}{m}\frac{R^m}{\rho^m}\cos m(\theta-\phi), & \rho>R\end{cases}$$

$$\Theta_{\nabla^2}(s,x)=\begin{cases}\Theta^I_{\nabla^2}(s,x)=\dfrac{4}{R}+4\dfrac{\rho}{R^2}\cos(\theta-\phi)+\displaystyle\sum_{m=2}^{\infty}4\frac{\rho^m}{R^{m+1}}\cos m(\theta-\phi), & R\geq\rho\\ \Theta^E_{\nabla^2}(s,x)=-\dfrac{4}{\rho}\cos(\theta-\phi)-\displaystyle\sum_{m=2}^{\infty}4\frac{R^{m-1}}{\rho^m}\cos m(\theta-\phi), & \rho>R\end{cases}$$

$$M_{\nabla^2}(s,x)=\begin{cases}M^I_{\nabla^2}(s,x)=\dfrac{4}{R^2}(\nu-1)+8(\nu-1)\dfrac{\rho}{R^3}\cos(\theta-\phi)+\displaystyle\sum_{m=2}^{\infty}4(m+1)(\nu-1)\frac{\rho^m}{R^{m+2}}\cos m(\theta-\phi), & R\geq\rho\\ M^E_{\nabla^2}(s,x)=\displaystyle\sum_{m=2}^{\infty}4(m-1)(\nu-1)\frac{R^{m-2}}{\rho^m}\cos m(\theta-\phi), & \rho>R\end{cases}$$

$$V_{\nabla^2}(s,x)=\begin{cases}V^I_{\nabla^2}(s,x)=8(\nu-1)\dfrac{\rho}{R^4}\cos(\theta-\phi)+\displaystyle\sum_{m=2}^{\infty}4m(m+1)(\nu-1)\frac{\rho^m}{R^{m+3}}\cos m(\theta-\phi), & R\geq\rho\\ V^E_{\nabla^2}(s,x)=-\displaystyle\sum_{m=2}^{\infty}4m(m-1)(\nu-1)\frac{R^{m-3}}{\rho^m}\cos m(\theta-\phi), & \rho>R\end{cases}$$

Binormal derivative with respect to the field point

$$\frac{\partial^2 U(s,x)}{\partial n_x^2}=\begin{cases} U^I(s,x)=2(1+\ln R)-\dfrac{3\rho}{R}\cos(\theta-\phi)-\displaystyle\sum_{m=2}^{\infty}\left[\frac{m+2}{m}\frac{\rho^m}{R^m}-\frac{\rho^{m-2}}{R^{m-2}}\right]\cos m(\theta-\phi), & R\geq\rho \\ U^E(s,x)=-\dfrac{R^2}{\rho^2}+(3+2\ln\rho)-\left[\dfrac{2R}{\rho}+\dfrac{R^3}{\rho^3}\right]\cos(\theta-\phi)-\displaystyle\sum_{m=2}^{\infty}\left[\frac{R^{m+2}}{\rho^{m+2}}-\frac{m-2}{m}\frac{R^m}{\rho^m}\right]\cos m(\theta-\phi), & \rho>R \end{cases}$$

$$\frac{\partial^2 \Theta(s,x)}{\partial n_x^2}=\begin{cases} \Theta^I(s,x)=\dfrac{2}{R}+\dfrac{3\rho}{R^2}\cos(\theta-\phi)+\displaystyle\sum_{m=2}^{\infty}\left[\frac{(m+2)\rho^m}{R^{m+1}}-\frac{(m-2)\rho^{m-2}}{R^{m-1}}\right]\cos m(\theta-\phi), & R\geq\rho \\ \Theta^E(s,x)=-\dfrac{2R}{\rho^2}-\left[\dfrac{2}{\rho}+\dfrac{3R^2}{\rho^3}\right]\cos(\theta-\phi)-\displaystyle\sum_{m=2}^{\infty}\left[\frac{(m+2)R^{m+1}}{\rho^{m+2}}-\frac{(m-2)R^{m-1}}{\rho^m}\right]\cos m(\theta-\phi), & \rho>R \end{cases}$$

$$\frac{\partial^2 M(s,x)}{\partial n_x^2}=\begin{cases} M^I(s,x)=\dfrac{2(\nu-1)}{R^2}+6(\nu-1)\dfrac{\rho}{R^3}\cos(\theta-\phi)+\displaystyle\sum_{m=2}^{\infty}\left[(m+1)(m+2)(\nu-1)\frac{\rho^m}{R^{m+2}}+\big(m(1-\nu)-2(1+\nu)\big)(m-1)\frac{\rho^{m-2}}{R^m}\right]\cos m(\theta-\phi), & R\geq\rho \\ M^E(s,x)=-\dfrac{2(1+\nu)}{\rho^2}-2(\nu+3)\dfrac{R}{\rho^3}\cos(\theta-\phi)+\displaystyle\sum_{m=2}^{\infty}\left[\big(m(\nu-1)-2(\nu+1)\big)(m+1)\frac{R^m}{\rho^{m+2}}+(m-1)(m-2)(1-\nu)\frac{R^{m-2}}{\rho^m}\right]\cos m(\theta-\phi), & \rho>R \end{cases}$$

$$\frac{\partial^2 V(s,x)}{\partial n_x^2}=\begin{cases} V^I(s,x)=-6(1-\nu)\dfrac{\rho}{R^4}\cos(\theta-\phi)-\displaystyle\sum_{m=2}^{\infty}\left[m(m+1)(m+2)(1-\nu)\frac{\rho^m}{R^{m+3}}-m(m-1)\big(4+m(1-\nu)\big)\frac{\rho^{m-2}}{R^{m+1}}\right]\cos m(\theta-\phi), & R\geq\rho \\ V^E(s,x)=-\dfrac{2(3+\nu)}{\rho^3}\cos(\theta-\phi)+\displaystyle\sum_{m=2}^{\infty}\left[m(m+1)\big(m(1-\nu)-4\big)\frac{R^{m-1}}{\rho^{m+2}}-m(m-1)(m-2)(1-\nu)\frac{R^{m-3}}{\rho^m}\right]\cos m(\theta-\phi), & \rho>R \end{cases}$$

Normal derivative of Laplacian of the degenerate kernels

$$U_{\nabla^2,n}(s,x)=\begin{cases}U^{I}_{\nabla^2,n}(s,x)=-\dfrac{4}{R}\cos(\theta-\phi)-\displaystyle\sum_{m=2}^{\infty}4\frac{\rho^{m-1}}{R^{m}}\cos m(\theta-\phi), & R\geq\rho\\ U^{E}_{\nabla^2,n}(s,x)=\dfrac{4}{\rho}+4\dfrac{R}{\rho^{2}}\cos(\theta-\phi)+\displaystyle\sum_{m=2}^{\infty}4\frac{R^{m}}{\rho^{m+1}}\cos m(\theta-\phi), & \rho>R\end{cases}$$

$$\Theta_{\nabla^2,n}(s,x)=\begin{cases}\Theta^{I}_{\nabla^2,n}(s,x)=\dfrac{4}{R^{2}}\cos(\theta-\phi)+\displaystyle\sum_{m=2}^{\infty}4m\frac{\rho^{m-1}}{R^{m+1}}\cos m(\theta-\phi), & R\geq\rho\\ \Theta^{E}_{\nabla^2,n}(s,x)=\dfrac{4}{\rho^{2}}\cos(\theta-\phi)+\displaystyle\sum_{m=2}^{\infty}4m\frac{R^{m-1}}{\rho^{m+1}}\cos m(\theta-\phi), & \rho>R\end{cases}$$

$$M_{\nabla^2,n}(s,x)=\begin{cases}M^{I}_{\nabla^2,n}(s,x)=\dfrac{8(\nu-1)}{R^{3}}\cos(\theta-\phi)+\displaystyle\sum_{m=2}^{\infty}4m(m+1)(\nu-1)\frac{\rho^{m-1}}{R^{m+2}}\cos m(\theta-\phi), & R\geq\rho\\ M^{E}_{\nabla^2,n}(s,x)=-\displaystyle\sum_{m=2}^{\infty}4m(m-1)(\nu-1)\frac{R^{m-2}}{\rho^{m+1}}\cos m(\theta-\phi), & \rho>R\end{cases}$$

$$V_{\nabla^2,n}(s,x)=\begin{cases}V^{I}_{\nabla^2,n}(s,x)=\dfrac{8(\nu-1)}{R^{4}}\cos(\theta-\phi)+\displaystyle\sum_{m=2}^{\infty}4m^{2}(m+1)(\nu-1)\frac{\rho^{m-1}}{R^{m+3}}\cos m(\theta-\phi), & R\geq\rho\\ V^{E}_{\nabla^2,n}(s,x)=\displaystyle\sum_{m=2}^{\infty}4m^{2}(m-1)(\nu-1)\frac{R^{m-3}}{\rho^{m+1}}\cos m(\theta-\phi), & \rho>R\end{cases}$$

Tangential derivative with respect to the field point

$$U_t(s,x)=\begin{cases} U_t^I(s,x)=-\left[R(1+2\ln R)+\frac{1}{2}\frac{\rho^2}{R}\right]\sin(\theta-\phi)-\sum_{m=2}^{\infty}\left[\frac{1}{m+1}\frac{\rho^{m+1}}{R^m}-\frac{1}{m-1}\frac{\rho^{m-1}}{R^{m-2}}\right]\sin m(\theta-\phi), & R\geq\rho \\ U_t^E(s,x)=-\left[R(1+2\ln\rho)+\frac{1}{2}\frac{R^3}{\rho^2}\right]\sin(\theta-\phi)-\sum_{m=2}^{\infty}\left[\frac{1}{m+1}\frac{R^{m+2}}{\rho^{m+1}}-\frac{1}{m-1}\frac{R^m}{\rho^{m-1}}\right]\sin m(\theta-\phi), & \rho>R \end{cases}$$

$$\Theta_t(s,x)=\begin{cases} \Theta_t^I(s,x)=-\left(3+2\ln R-\frac{1}{2}\frac{\rho^2}{R^2}\right)\sin(\theta-\phi)+\sum_{m=2}^{\infty}\left[\frac{m}{m+1}\frac{\rho^{m+1}}{R^{m+1}}-\frac{m-2}{m-1}\frac{\rho^{m-1}}{R^{m-1}}\right]\sin m(\theta-\phi), & R\geq\rho \\ \Theta_t^E(s,x)=-\left(1+2\ln\rho+\frac{3}{2}\frac{R^2}{\rho^2}\right)\sin(\theta-\phi)-\sum_{m=2}^{\infty}\left[\frac{m+2}{m+1}\frac{R^{m+1}}{\rho^{m+1}}-\frac{m}{m-1}\frac{R^{m-1}}{\rho^{m-1}}\right]\sin m(\theta-\phi), & \rho>R \end{cases}$$

$$M_t(s,x)=\begin{cases} M_t^I(s,x)=-\left[\frac{2(\nu+1)}{R}-(\nu-1)\frac{\rho^2}{R^3}\right]\sin(\theta-\phi)+\sum_{m=2}^{\infty}\left[m(\nu-1)\frac{\rho^{m+1}}{R^{m+2}}+\left(m(1-\nu)-2(1+\nu)\right)\frac{\rho^{m-1}}{R^m}\right]\sin m(\theta-\phi), & R\geq\rho \\ M_t^E(s,x)=-(\nu+3)\frac{R}{\rho^2}\sin(\theta-\phi)+\sum_{m=2}^{\infty}\left[\left(m(\nu-1)-2(\nu+1)\right)\frac{R^m}{\rho^{m+1}}+m(1-\nu)\frac{R^{m-2}}{\rho^{m-1}}\right]\sin m(\theta-\phi), & \rho>R \end{cases}$$

$$V_t(s,x)=\begin{cases} V_t^I(s,x)=\left[\frac{2(3-\nu)}{R^2}-\frac{\rho^2}{R^4}(1-\nu)\right]\sin(\theta-\phi)-\sum_{m=2}^{\infty}\left[m^2(1-\nu)\frac{\rho^{m+1}}{R^{m+3}}-m\left(4+m(1-\nu)\right)\frac{\rho^{m-1}}{R^{m+1}}\right]\sin m(\theta-\phi), & R\geq\rho \\ V_t^E(s,x)=-\frac{(3+\nu)}{\rho^2}\sin(\theta-\phi)+\sum_{m=2}^{\infty}\left[m\left(m(1-\nu)-4\right)\frac{R^{m-1}}{\rho^{m+1}}-m^2(1-\nu)\frac{R^{m-3}}{\rho^{m-1}}\right]\sin m(\theta-\phi), & \rho>R \end{cases}$$

Tangential-normal-tangential derivative with respect to the field point

$$U_{t,x,t}(s,x)=\begin{cases} U^{I}_{t,x,t}(s,x)=\dfrac{1}{R}\cos(\theta-\phi)+\sum\limits_{m=2}^{\infty}m\left(\dfrac{\rho^{m-1}}{R^{m}}-\dfrac{\rho^{m-3}}{R^{m-2}}\right)\cos m(\theta-\phi), & R\geq\rho \\ U^{E}_{t,x,t}(s,x)=\left(\dfrac{2R}{\rho^{2}}-\dfrac{R^{3}}{\rho^{4}}\right)\cos(\theta-\phi)-\sum\limits_{m=2}^{\infty}m\left(\dfrac{R^{m+2}}{\rho^{m+3}}-\dfrac{R^{m}}{\rho^{m+1}}\right)\cos m(\theta-\phi), & \rho>R \end{cases}$$

$$\Theta_{t,x,t}(s,x)=\begin{cases} \Theta^{I}_{t,x,t}(s,x)=-\dfrac{1}{R^{2}}\cos(\theta-\phi)-\sum\limits_{m=2}^{\infty}\left[m^{2}\dfrac{\rho^{m-1}}{R^{m+1}}-m(m-2)\dfrac{\rho^{m-3}}{R^{m-1}}\right]\cos m(\theta-\phi), & R\geq\rho \\ \Theta^{E}_{t,x,t}(s,x)=\left(\dfrac{2}{\rho^{2}}-\dfrac{3R^{2}}{\rho^{4}}\right)\cos(\theta-\phi)-\sum\limits_{m=2}^{\infty}\left[m(m+2)\dfrac{R^{m+1}}{\rho^{m+3}}-m^{2}\dfrac{R^{m-1}}{\rho^{m+1}}\right]\cos m(\theta-\phi), & \rho>R \end{cases}$$

$$M_{t,x,t}(s,x)=\begin{cases} M^{I}_{t,x,t}(s,x)=\dfrac{2(1-\nu)}{R^{3}}\cos(\theta-\phi)-\sum\limits_{m=2}^{\infty}\left[m^{2}(m+1)(\nu-1)\dfrac{\rho^{m-1}}{R^{m+2}}+\big(m(1-\nu)-2(1+\nu)\big)m(m-1)\dfrac{\rho^{m-3}}{R^{m}}\right]\cos m(\theta-\phi), & R\geq\rho \\ M^{E}_{t,x,t}(s,x)=-2(\nu+3)\dfrac{R}{\rho^{4}}\cos(\theta-\phi)+\sum\limits_{m=2}^{\infty}\left[\big(m(\nu-1)-2(\nu+1)\big)m(m+1)\dfrac{R^{m}}{\rho^{m+3}}+m^{2}(m-1)(1-\nu)\dfrac{R^{m-2}}{\rho^{m+1}}\right]\cos m(\theta-\phi), & \rho>R \end{cases}$$

$$V_{t,x,t}(s,x)=\begin{cases} V^{I}_{t,x,t}(s,x)=\dfrac{2(1-\nu)}{R^{4}}\cos(\theta-\phi)+\sum\limits_{m=2}^{\infty}\left[m^{3}(m+1)(1-\nu)\dfrac{\rho^{m-1}}{R^{m+3}}-m^{2}(m-1)\big(4+m(1-\nu)\big)\dfrac{\rho^{m-3}}{R^{m+1}}\right]\cos m(\theta-\phi), & R\geq\rho \\ V^{E}_{t,x,t}(s,x)=-\dfrac{2(3+\nu)}{\rho^{4}}\cos(\theta-\phi)+\sum\limits_{m=2}^{\infty}\left[m^{2}(m+1)\big(m(1-\nu)-4\big)\dfrac{R^{m-1}}{\rho^{m+3}}-m^{3}(m-1)(1-\nu)\dfrac{R^{m-3}}{\rho^{m+1}}\right]\cos m(\theta-\phi), & \rho>R \end{cases}$$

作者簡歷

中文姓名：廖奐禎
英文姓名：Huan-Zhen Liao
出生日期：民國 71 年 10 月 23 日
籍　　貫：台灣南投
聯絡地址：南投縣中寮鄉義和村永平路 446 之 27 號
聯絡電話：(049) 2232672
行動電話：0912385689
電子信箱：tashi0907@hotmail.com

學　　歷：

國立台灣海洋大學河海工程研究所碩士
國立台灣海洋大學河海工程系學士 (2001.09 ~ 2005.06)
省立台中一中 (1998.09 ~ 2001.06)
南投縣立水里國民中學 (1995.09 ~ 1998.06)
南投縣立水里國民小學 (1989.09 ~ 1995.06)

著作目錄：

(A) 期刊論文

1. Chen, J. T.; Ke, J. N.; Liao, H. Z. (2007): Construction of Green's function using null-field integral approach for Laplace problems with circular boundaries. Computers, Materials & Continua, **Accepted**.
2. Chen, J. T. ; Lee , W. M. ; Liao, H. Z. (2007): Discussion: "Isotropic Clamped -Free Thin Annular Circular Plate Subjected to a Concentrated Load" (Ajayi O. Adewale, 2006, ASME J. Appl. Mech., 73, pp. 658-663), **Submitted**.
3. Chen, J. T.; Liao, H. Z.; Lee, W. M. (2007): Analytical solutions for the Green's functions of biharmonic problems with circular and annular domains, **Submitted**.